THE Water Research FOUNDATION

PROJECT NO.
4953

Considerations and Blending Strategies for Drinking Water System Integration with Alternative Water Supplies

CALIFORNIA Water Boards
STATE WATER RESOURCES CONTROL BOARD
REGIONAL WATER QUALITY CONTROL BOARDS

THE METROPOLITAN WATER DISTRICT OF SOUTHERN CALIFORNIA

Considerations and Blending Strategies for Drinking Water System Integration with Alternative Water Supplies

Prepared by:

Nicole Blute, PhD, PE, Principal Investigator
Hazen and Sawyer

Daniel Giammar, PhD, PE
Washington University of St. Louis

Jacqueline Rhoades, PE
City of Arvada, Colorado

Janelle Junior
Hazen and Sawyer

Anushka Mishrra
Washington University of St. Louis

2023

THE
Water
Research
FOUNDATION

The Water Research Foundation (WRF) is the leading research organization advancing the science of all water to meet the evolving needs of its subscribers and the water sector. WRF is a 501(c)(3) nonprofit, educational organization that funds, manages, and publishes research on the technology, operation, and management of drinking water, wastewater, reuse, and stormwater systems—all in pursuit of ensuring water quality and improving water services to the public.

For more information, contact:
The Water Research Foundation

1199 North Fairfax Street, Suite 900
Alexandria, VA 22314-1445
P 571-384-2100

6666 West Quincy Avenue
Denver, Colorado 80235-3098
P 303-347-6100

www.waterrf.org
info@waterrf.org

WRF ISBN: 978-1-60573-661-7
WRF Project Number: 4953

Funding has been provided in full or in part through an agreement with the California State Water Resources Control Board. The California Water Quality, Supply, and Infrastructure Improvement Act of 2014 (Proposition 1) authorizes $7.545 billion in general obligation bonds to fund ecosystems and watershed protection and restoration, water supply infrastructure projects, including surface and groundwater storage, and drinking water protection. The contents of this document do not necessarily reflect the views and policies of the foregoing, nor does mention of trade names or commercial products constitute endorsement or recommendation for use.

This document was reviewed by a panel of independent experts selected by The Water Research Foundation. Mention of trade names or commercial products or services does not constitute endorsement or recommendations for use. Similarly, omission of products or trade names indicates nothing concerning The Water Research Foundation's positions regarding product effectiveness or applicability.

Acknowledgments

Research Team

Principal Investigators:

Nicole Blute, PhD, PE
Hazen and Sawyer

Daniel Giammar, PhD, PE
Washington University of St. Louis

Jacqueline Rhoades, PE
City of Arvada, Colorado

Project Team:

Anushka Mishrra
Washington University of St. Louis

Janelle Junior
Hazen and Sawyer

Ian Mackenzie, PE
Hazen and Sawyer

David Rodriguez
Hazen and Sawyer

Michelle Chebeir, PhD
Hazen and Sawyer

Ryan Gustafson, PhD, ENV SP
Metropolitan Water District of Southern California

WRF Project Subcommittee or Other Contributors

Clifton Herrmann
California State Water Resources Control Board

Quirien Muylwyk, MASc, PEng
AECOM

Caroline Russell, PhD, PE
Carollo Engineers

WRF Staff

John Albert, MPA
Chief Research Officer

Stephanie Fevig
Research Program Manager

Julie Minton
Research Unit Leader

Abstract and Benefits

Abstract:

Introduction of alternative water sources, such as direct potable reuse, into existing drinking water distribution systems offers resiliency in water supply but holds the potential for corrosion impacts to distribution system and premise plumbing materials. In this research project, re-circulating pipe loops were used to evaluate potential impacts of introducing advanced treated water into systems containing:

- Cast iron pipes with iron and manganese tuberculation
- Copper pipe with lead solder
- Brass rods inside PVC pipe to represent brass appurtenances

After a conditioning period with baseline water (i.e., groundwater), advanced treated water (ATW) was introduced into the pipe loops to evaluate the hypothesis that gradual introduction (i.e., adding 25%, then 50%, then 75% ATW to pipe loops over the course of the testing period) of a new water source coupled with stabilization of the ATW would mitigate negative impacts. The ATW used in this project was Full Advanced Treated (FAT) water produced at the Metropolitan Water District of Southern California's Regional Recycled Water Advanced Purification Center, treated by membrane bioreactor, reverse osmosis, and either UV/chlorine or UV/peroxide advanced oxidation. ATW was stabilized using calcite filters to add calcium and alkalinity and increase the pH of the water.

Results of the study demonstrated that effective stabilization of ATW minimized impacts to the water quality from cast iron pipes. Impacts on distribution plumbing were minor and were only observed once the groundwater was fully replaced with ATW during the abrupt introduction stage of testing. For copper pipe with lead solder, 100% ATW dramatically increased lead and decreased copper concentrations in the water, consistent with a mechanism of galvanic corrosion. The solids present in scales on the inner surface of the copper pipe and lead solder at the end of testing were different for the pipes that had been switched to ATW than for the pipes that remained with baseline water over the duration of the study, indicating that dissolution of sulfate minerals may occur with much lower sulfate water quality. Overall, the results of this testing highlighted that water quality stability for one type of material does not provide effective corrosion for all.

Benefits:

Critical benefits from this research project include the following:

- A literature review of corrosion mechanisms for iron, lead, and copper materials
- Methodologies for harvesting pipes, building, and running pipe loop test equipment, and analyzing scale
- Confirmation of treatment targets for stabilized advanced treated water
- Identification of conditions that cause corrosion and strategies to minimize corrosion when advanced treated water is introduced

This research will help subscribers and the water quality community by providing information on strategies to minimize corrosive conditions when using new sources. In addition, recommendations for future research studies are provided to supplement industry knowledge about the introduction of alternate water supplies such as advanced treated water.

Keywords: Corrosion, cast iron pipes, copper pipe with lead solder, brass, pipe loops, advanced treated water.

Contents

Tables

Figures

Acronyms and Abbreviations

AOC	Assimilable organic carbon
ATW	Advanced treated water
BLW	Baseline water
CSMR	Chloride to sulfate mass ratio
DIC	Dissolved inorganic carbon
DOC	Dissolved organic carbon
DPD	N,N diethyl-1,4 phenylenediamine sulfate
EBCT	Empty bed contact time
EDS	Energy dispersive x-ray spectroscopy
EPA	Environmental Protection Agency
ESEM	Environmental scanning electron microscope
FAT	Full advanced treated
HLR	Hydraulic loading rate
ICP-MS	Inductively coupled plasma mass spectrometry
IRB	Immunoreactive beads
Joint Plant	Joint Water Pollution Control Plant
LCR	Lead and Copper Rule
LCRR	Lead and Copper Rule Revisions
MCL	Maximum contaminant level
MDL	Minimum detection level
MRL	Method reporting limit
MWD	Metropolitan Water District of Southern California
ND	Non-detect
NOM	Natural organic matter
OPPP	Opportunistic premise plumbing pathogens
PVC	Polyvinyl chloride
RRWAPC	Regional Recycled Water Advanced Purification Center
SEM	Scanning electron microscope
SMCL	Secondary maximum contaminant level
SRB	Sulfate rebuilding bacteria
TOC	Total organic carbon
UCI	Unlined cast iron
WRF	The Water Research Foundation
WUStL	Washington University in St. Louis
XRD	X-Ray diffraction

Executive Summary

Water agencies across the United States as well as internationally are considering advanced water treatment, including treatment for indirect and direct potable reuse, desalination of seawater and brackish water, and impaired groundwater. Successful implementation of these alternative water supply projects depends on the ability to demonstrate that these waters are equivalent to existing drinking water supplies with respect to water quality (e.g., salinity, organic matter, nutrients, microconstituents, pathogens) and that they do not present an additional risk to public health compared to traditional water sources.

This research focused on the successful introduction of new supplies to maintain distribution system water quality. The work identifies methods (i.e., startup strategies, blending targets) to mitigate the potential issues (i.e., corrosion, biological regrowth, nitrification, premise plumbing pathogens, aesthetics) that may be associated with integrating these highly treated supplies into existing drinking water systems. The primary objectives of this research included the following:

- Identifying and evaluating impacts of alternative water supplies (in this project, advanced treated water [ATW] from a reverse osmosis/UV advanced oxidation process [RO/UVAOP] system was used) on the water quality of the end users' existing drinking water systems that have known issues with tuberculation (e.g., corrosion, biological regrowth, *Legionella*, aesthetics, and biofilm).
- Understanding impacts of blending ratios of advanced treated water from an RO/UVAOP potable reuse train on a variety of issues (e.g., nitrification, total chlorine residual, ammonia, nitrite, and nitrate).
- Developing management strategies and options to mitigate adverse impacts.

The testing approach focused on designing a pipe loop system to represent a full-scale system, determining a blending schedule, and conducting water quality testing informed by the literature review that was conducted prior to the testing and survey of utility partners. Two representative pipe loop systems were evaluated during the research: a distribution pipe system and a premise plumbing system.

Key findings from the distribution system included:

- Iron and manganese were released into the water during the conditioning period after pipe harvesting, as expected.
- ATW stabilization with calcite filters achieved the targets for alkalinity, calcium, and pH without need for additional chemical addition.
- Introduction of ATW, which varied significantly from baseline water (groundwater), did not result in higher release of iron and manganese either for gradual addition or abrupt addition of ATW.

Premise plumbing key findings included:

- Blending of 25–75% ATW with conventional treated water did not affect lead and copper release from lead solder in copper pipes and brass rods.
- Fully introducing ATW without conventional treated water in the copper pipes with lead solder increased lead release significantly and decreased copper release significantly. These observations can be correlated to the dramatic decrease in sulfate concentration, suggesting that galvanic corrosion was occurring.
- Introducing 100% ATW in brass pipes increased lead, copper, and zinc release.

Results of the study demonstrated that effective stabilization of ATW minimized impacts to the water quality from cast iron pipes. Impacts on premise plumbing were minor except for introduction of 100% ATW into the pipes. For copper pipe with lead solder, 100% ATW dramatically increased lead and decreased copper concentrations in the water, consistent with a mechanism of galvanic corrosion. The solids present in scales on the inner surface of the copper pipe and lead solder at the end of testing were different for the pipes that had been switched to ATW than for the pipes that remained with baseline water over the duration of the study, indicating that dissolution of sulfate minerals may occur with much lower sulfate water quality. Overall, the results of this testing highlighted that water quality stability for one type of material is not necessarily non-corrosive for all. Corrosion-related outcomes were assessed with regulatory standards in mind, including primary and secondary maximum contaminant levels (MCLs). Potential impacts of changes in water quality (including further stabilization of ATW and blends of water sources) were investigated through this project to identify potential strategies to minimize adverse consequences when ATW is introduced into the distribution system.

Critical benefits from this research project include the following:

- A literature review of corrosion mechanisms for iron, lead, and copper materials.
- Methodologies for harvesting pipes, building, and running pipe loop test equipment, and analyzing scale.
- Confirmation of treatment targets for stabilized advanced treated water.
- Identification of conditions that cause corrosion and strategies to minimize corrosion when advanced treated water is introduced.

This research will help WRF subscribers and the water quality community by providing information on strategies to minimize corrosive conditions when using new sources with existing water systems. In addition, recommendations for future research studies are provided to supplement industry knowledge about the introduction of alternate water supplies such as advanced treated water.

Related WRF Research

- Blending Requirements for Water from Direct Potable Reuse Treatment Facilities (4536)
- Public Health Benefits and Challenges for Blending of Advanced Treated Water with Raw Water Upstream of a Surface Water Treatment Plant in DPR (5049)
- Effects of Blending on Distribution System Water Quality (2702)

CHAPTER 1

Background and Objectives

Water agencies across the US are considering advanced treatment of water, including treatment for indirect and direct potable reuse, desalination of seawater and brackish water, and impaired groundwater. Successful implementation of these alternative water supply projects depends on the ability to demonstrate that these waters are equivalent to existing drinking water supplies with respect to water quality (e.g., salinity, organic matter, nutrients, microconstituents, pathogens) and that they do not present an additional risk to public health. This research focuses on the successful introduction of new supplies to maintain distribution system water quality. The work identifies methods (startup strategies, blending targets) to mitigate the potential issues (corrosion, biological regrowth, nitrification, premise plumbing pathogens, aesthetics) that may be associated with integrating these highly treated supplies into existing drinking water systems.

The scope included:

- Preparation of a literature review and research plan,
- Conducting loop testing of pipes extracted from a distribution system impacted by tuberculation,
- Evaluating corrosion and biofilms of premise plumbing materials containing copper and lead, and
- Benchmarking microbiological water quality prior to and after introduction of the advanced treated water.

The goal of the project was to provide guidance information for utilities considering integration of alternative water supplies into their systems. Introduction of alternative water sources into existing drinking water distribution systems offers resiliency in water supply but holds the potential for corrosion and biological growth impacts. Distribution system and premise plumbing scale and microbiology are complex, with many variables potentially impacting water quality as illustrated in Figure 1-1.

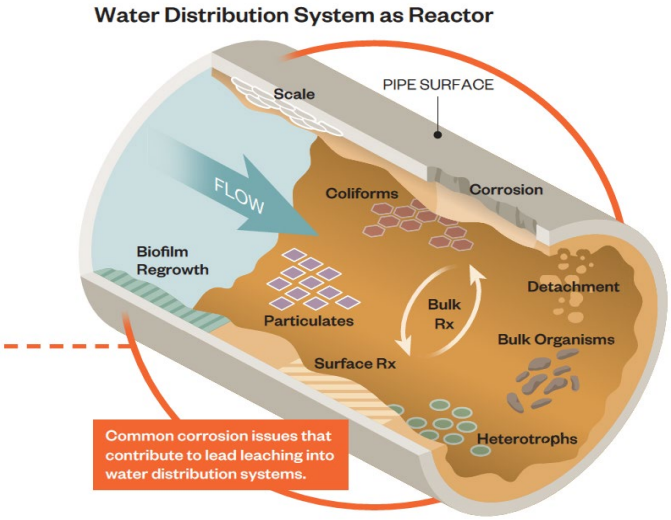

Figure 1-1. Distribution System Pipe Viewed as a Reactor to Depict Corrosion and Microbiological Factors Involved.

The primary drivers for this research were examples of negative outcomes when alternative water sources are used. Flint, Michigan and Washington, D.C. lead release are perhaps most well-known, but many other cases have been reported such as when agencies switch to alternative sources. Conversely, many agencies successfully switch supplies as a normal water supply strategy without negative impacts, indicating that mitigation strategies are available with planning. Only limited studies have been conducted to specifically evaluate the impacts of changing advanced treated water blends on distribution system water quality and metals release, necessitating this research.

The primary objectives of this research included the following:

- Identifying and evaluating impacts of alternative water supplies, (in this project, advanced treated water from a reverse osmosis/ UV advanced oxidation process (RO/UVAOP) system was used) on the water quality of the end users' existing drinking water systems that have known issues with tuberculation (e.g., corrosion, biological regrowth, *Legionella*, aesthetics, biofilm)
- Understanding impacts of blending ratios of advanced treated water from an RO/UVAOP potable reuse train on a variety of issues (e.g., nitrification, total chlorine residual, ammonia, nitrite, nitrate), and
- Developing management strategies and options to mitigate adverse impacts.

To achieve these objectives, the approach developed focused on field and laboratory testing and included pipe loop testing of tuberculated cast iron pipe harvested from a distribution system, copper pipe with lead solder, and brass components to represent a full-scale system. The output for the project is guidance material for utilities in need of strategies for alternative water supply integration.

Prior to running pipe loop testing of alternate water supplies, a literature review was performed to review factors that impact corrosion in drinking water distribution systems. This

review summarized relevant research, enabling the project to make the best use of past work. Three materials were selected for testing in the pipe loop study based on prevalence, potential for corrosion impacts to distribution system water quality, and outstanding research needs, and included cast iron pipe, lead (both solder and brass), and copper pipe. Cement mortar-lined pipe has been evaluated successfully in past studies and full-scale systems and was not identified to have outstanding research needs at this time since corrosion indices such as calcium carbonate precipitation potential (CCPP) can be effectively used to minimize corrosion to these materials. The literature review that follows focuses on the impact of source water quality and changes in source water quality on corrosion of the materials of interest.

1.1 Iron Corrosion

In a 2019 national utility survey, cast iron pipe was rated as the most challenging distribution system pipe material, and over half of utilities in the survey expressed concerns about corrosion of cast iron pipe (Arnold et al., 2020). Although corrosion control treatment often focuses on minimizing lead and copper release from building plumbing materials, control of iron corrosion in the distribution system is also a key objective for distribution system water quality. Evaluating the impacts of source water and treatment changes, such as blending of alternate water supplies, on iron corrosion is necessary for utilities to avoid impacts on water aesthetics, chlorine residuals, and even indirect effects on lead release.

Corrosion in the distribution system has implications for water quality as well as the physical condition of critical infrastructure that must be considered as utilities seek to maximize the life cycle of existing water distribution assets. Iron pipe corrosion is influenced by a variety of water quality, hydraulic, biological, and physical factors, and source water and treatment changes, especially those associated with advanced treatment. Iron pipe corrosion can result in several potential secondary impacts (McNeil and Edwards, 2001; Lytle et al., 2020), including:

- Pipe degradation increasing the potential for leaks and water main breaks
- Scale formation and tuberculation of cast iron water mains restricting the hydraulic capacity of the pipe and increasing pumping costs
- Corrosion by-product release from cast iron mains causing aesthetic concerns due to “red water” or “yellow water”

Iron release can mobilize particulate lead from downstream sources, such as lead service lines, increasing lead levels at the tap (Masters and Edwards, 2015; Trueman and Gagnon, 2016). Field and laboratory studies have demonstrated that the presence of an upstream unlined cast iron main can significantly increase lead release from downstream lead service lines (Camara et al., 2013; Trueman and Gagnon, 2016). Iron was of interest for this project in part because it has been found to influence lead release.

While cast iron pipe was the focus of the distribution pipe testing, aspects of relevant studies using new iron coupons or aged galvanized iron pipe were also considered in this review. The review covered the characteristics of iron pipe corrosion scales and how the characteristics of iron scales generally differ based on whether the pipe was historically exposed to groundwater, surface water, or a blend of the two. The impacts of water quality parameters on corrosion of

iron pipe were reviewed, including discussion of the impacts of alkalinity, sulfate, chloride, and oxidants. The impacts of biological growth on iron pipe corrosion were reviewed, including an assessment of the biological communities that affect iron pipe corrosion and interactions between biology, scale structure, and water quality. Iron corrosion associated with exposure to advanced treated water (ATW) is discussed and water quality characteristics of ATW were compared to that of surface water, groundwater, and blends of surface water and groundwater. The ATW used in this project was Full Advanced Treated (FAT) water produced at the Metropolitan Water District of Southern California's Regional Recycled Water Advanced Purification Center, treated by membrane bioreactor, reverse osmosis, and either UV/chlorine or UV/peroxide advanced oxidation. ATW was stabilized during testing using calcite filters to add calcium and alkalinity and increase the pH of the water.

The contents of this literature review were intended to help contextualize and interpret the data obtained during pilot pipe loop testing with unlined cast iron pipe.

1.1.1 Corrosion Scale Characteristics

The structure and characteristics of iron corrosion scales influence iron release, especially in response to changes in water source. Iron scales consist of layers of ferrous and ferric oxides that form tuberculation on the pipe's interior surface.

The morphology of iron corrosion scales tends to differ based on whether the pipe section was exposed to treated surface water or treated groundwater (Hu et al., 2018; Sun et al., 2014; Sun et al., 2017; Yang et al., 2012; and Yang et al., 2014). Pipes historically exposed to treated surface water tend to have thick-layered corrosion scales or densely distributed tubercles, and these types of scales have higher stability due to a higher proportion of stable constituents, mainly consisting of Fe_3O_4, in the top shell layer of the scale (Yang et al., 2012). Pipes historically exposed to treated groundwater tend to have thin and uniform non-layered corrosion scales, and these types of scales have lower stability due to higher proportion of less stable constituents such as β-FeOOH, $FeCO_3$, and green rust. A representation of these different types of scale is shown in Figure 1-2.

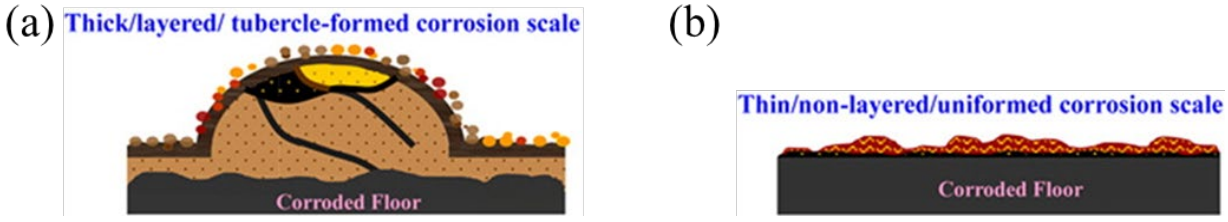

Figure 1-2. Typical Morphology of Iron Pipe Corrosion Scales in Pipes with Historical Exposure to (a) Treated Surface Water and (b) Treated Groundwater.

Source: Reprinted from Water Research 46(16); by F. Yang, B. Shi, J. Gu, D. Wang, and M. Yang; Morphological and Physicochemical Characteristics of Iron Corrosion Scales Formed Under Different Water Source Histories in a Drinking Water Distribution System; p. 11; Copyright (2012), with permission from Elsevier.

Figure 1-3 shows cross-sections of 20-year-old pipe cut from different areas of a drinking water distribution system, with one sample being exposed to treated surface water, one sample being exposed to treated groundwater, and two samples being exposed to a blend of surface water

and groundwater. The pipe sections exposed to surface water (Figure 1-3 a-c) demonstrated thick tuberculated layers of corrosion scales while the section exposed only to groundwater showed thinner and smoother layers of corrosion scale (Figure 1-3 d) (Sun et al., 2014), consistent with the findings of Hu et al. (2018), Sun et al. (2017), and Yang et al. (2012 and 2014).

Figure 1-3. Corrosion Scales in 20-Year-Old Cast Iron Pipe Sections from a Drinking Water Distribution System. Each section had a historical exposure to (a) treated surface water, (b) a blend of treated surface water and groundwater, (c) another blend of treated surface water and groundwater, and (d) treated groundwater Source: Sun et al. 2014. Reproduced with permission from the Royal Society of Chemistry.

The inner morphology of the thicker layers of tubercle-formed corrosion scale that are characteristic of pipes historically exposed to treated surface water have been shown to consist of layers of ferrous and ferric oxides, as depicted in Figure 1-4. The layer at the pipe wall typically has a porous structure consisting of ferric oxyhydroxide (goethite) and can be a source of soluble iron. The outer layer at the water-scale interface is typically a relatively insoluble layer of ferric scale. The outer scale layer is maintained by the presence of an oxidant in the bulk water, and interactions between scale layers and pores can influence iron release (Sarin et al., 2004b). Although this description applies generally to thick corrosion-scale tubercles, a large degree of morphological diversity has also been observed within a single distribution system, indicating that there is variability in internal and external morphology but also that factors in addition to water quality likely play an important role in corrosion scale formation (Gerke et al., 2008).

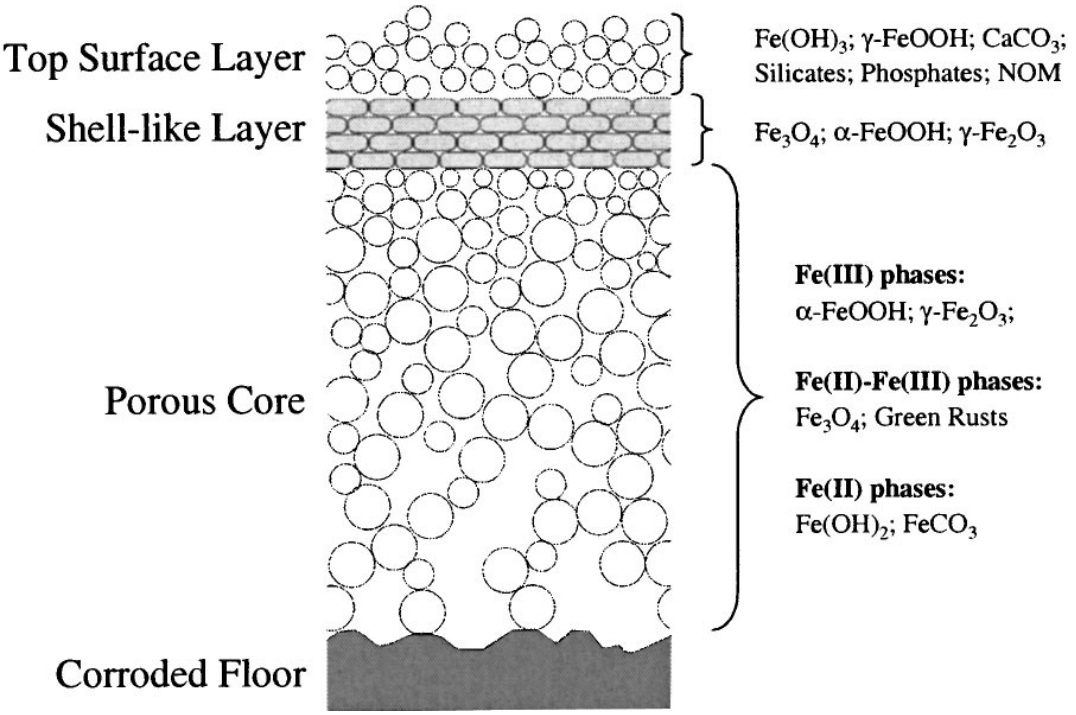

Figure 1-4. Schematic of Iron Pipe Scale and Corrosion Products Commonly Observed in Pipes Exposed to Treated Surface Water.

Source: Sarin et al. 2004b. Reproduced with permission from ASCE.

Corrosion products in iron pipes as a result of tuberculation build-up can often include co-occurring manganese deposits, resulting in mottled orange and black precipitate formation in pipes. Build-up of manganese "legacy" deposits can establish a reservoir of manganese that can be released into the water either by hydraulic or chemical pathways. In groundwater systems with even low concentrations of iron and manganese, build-up can be significant over time and release can cause customer complaints (Arnold et al., 2021). In addition, other inorganic contaminants can be released during these events, such as co-accumulated lead, barium, and cadmium (Hill and Lemieux, 2022).

1.1.2 Influence of Water Quality on Iron Corrosion

Iron corrosion and release are affected by physical, biological, and water quality factors, including pH, alkalinity/dissolved inorganic carbon (DIC), hardness, phosphate, chloride, and sulfate concentrations. Higher levels of alkalinity/DIC can decrease iron pipe degradation, corrosion by-product release, and potential for red water. Higher alkalinity levels also increase the buffer intensity, which provides further benefits for controlling iron corrosion. Factors influencing iron pipe degradation, tuberculation, and release are sometimes opposing; for example, iron corrosion by-product release typically decreases at higher pH levels, but pipe weight loss and tuberculation can increase at higher pH levels. Furthermore, sequestration treatment with polyphosphate or silicates may mask the appearance of discolored water but may not decrease the iron corrosion rate (McNeill and Edwards, 2001).

The presence and concentration of oxidants, including dissolved oxygen (DO) and disinfectant residual, are significant parameters affecting iron release. Oxidants enhance the structure of

the outer scale layers to decrease the release of soluble iron from porous inner layers (Benjamin et al., 1996, Sarin et al., 2004a, Sarin et al., 2004b). Stagnant conditions in pipelines can yield red water, due to depletion of oxidants at the pipe surface followed by reduction of iron scale and release of ferrous iron. When flowing conditions and higher oxidant levels return, oxidation of soluble ferrous iron to ferric iron occurs rapidly in the bulk water at typical pH levels in water systems, resulting in the appearance of oxidized iron (Sarin et al., 2004a, Sarin et al., 2004b). The type of disinfectant used also affects the density of the corrosion scale, with systems using chlorine resulting in loose corrosion products and systems using chloramine resulting in dense crystalized corrosion products (Li et al., 2014).

Chloride and sulfate can increase iron release (Figure 1-5) and are believed to diffuse through iron scale layers to the porous interior (Lytle et al., 2005; Lytle, 2017; Lytle et al., 2020). Iron release from unlined cast iron pipe has been shown to increase significantly when the concentrations of sulfate, chloride, or both are increased significantly and DIC concentration is low (blue, green, and pink). However, iron concentrations were reduced significantly when the DIC concentration was increased (yellow shading), and these changes in iron levels can occur rapidly (Lytle et al., 2020). When exposed to an abrupt increase in sulfate levels, pipe sections historically exposed to treated groundwater have been observed to demonstrate marked increases in iron release, resulting in red water. Pipe sections that have been historically exposed to treated surface water have been shown to demonstrate minimal changes in iron release when exposed to increased sulfate levels (Yang et al., 2014). However, other researchers have observed accelerated iron release after exposure to increased sulfates or chlorides in pipes historically exposed to either surface water, groundwater, or blended water (Hu et al., 2018).

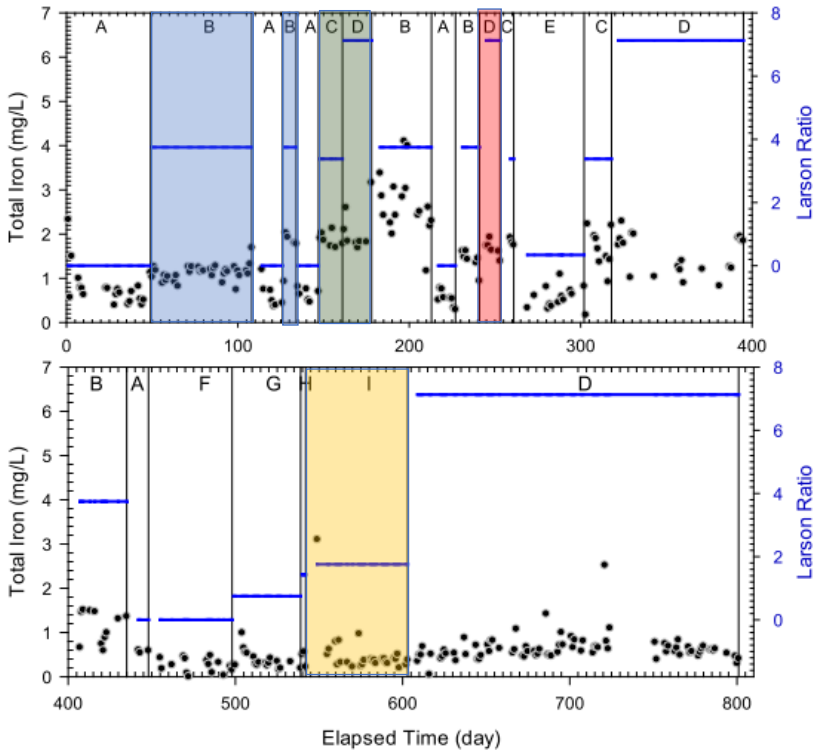

Summary of average water quality parameter values for 24 h of stagnation periods.

Water Condition	ET (day)	DIC (mg/L)	Chloride (mg/L)	Sulfate (mg/L)	Larson Ratio	Sample Size	pH_I		pH_F		DO_I (mg/L)		DO_F (mg/L)		Fe (II) (mg/L)		Total Fe (mg/L)	
							Ave	CI	Ave	CI	Ave	CI	Ave	CI	Ave	CI	Ave	CI
A	1–49	10	–	–	0	21	8.28	0.06	9.26	0.07	6.93	0.39	2.60	0.34	0.04	0.01	0.79	0.19
B	50–112	10	–	150	3.75	33	8.36	2.82	9.34	3.22	6.39	2.21	2.49	0.99	0.08	0.03	1.13	0.06
A	113–126	10	–	–	0	7	8.28	0.06	9.24	0.03	8.27	0.52	4.88	1.38	0.03	0.02	0.62	0.22
B	127–134	10	–	150	3.75	5	8.19	0.02	9.05	0.09	7.65	0.23	3.85	0.40	0.09	0.04	1.69	0.38
A	135–147	10	–	–	0	6	8.23	0.08	9.16	0.06	7.42	0.33	3.27	0.76	0.05	0.03	0.65	0.11
C	148–161	10	100	–	3.38	7	8.14	0.08	8.84	0.08	7.73	0.31	2.43	0.35	0.15	0.03	1.88	0.12
D	162–182	10	100	150	7.13	8	8.09	0.06	8.88	0.06	7.55	0.25	2.75	0.44	0.16	0.04	2.11	0.36
B	183–216	10	–	150	3.75	17	8.02	0.13	8.28	0.20	6.99	0.44	1.85	0.23	0.17	0.02	2.68	0.34
A	217–230	10	–	–	0	8	7.39	0.14	8.40	0.14	7.00	0.17	1.90	0.33	0.06	0.03	0.54	0.12
B	231–244	10	–	150	3.75	7	7.73	0.08	8.51	0.14	6.69	0.16	1.62	0.69	0.21	0.08	1.41	0.17
D	245–258	10	100	150	7.13	6	7.89	0.15	8.61	0.25	7.75	1.07	1.68	0.34	0.18	0.07	1.68	0.14
C	259–266	10	100	–	3.38	3	7.83	0.12	8.78	0.14	7.67	0.19	1.96	0.33	0.12	0.03	1.83	0.10
E	267–302	10	10	–	0.34	13	8.10	0.20	9.25	0.12	7.41	0.35	2.83	0.33	0.05	0.03	0.59	0.12
C	303–321	10	100	–	3.38	10	8.18	0.02	9.22	0.12	8.35	0.65	3.00	0.82	0.10	0.03	1.53	0.39
D	322–402	10	100	150	7.13	20	8.09	0.05	9.13	0.07	8.30	0.27	2.09	0.21	0.10	0.02	1.53	0.19
B	403–441	10	–	150	3.75	11	8.08	0.07	9.39	0.06	9.37	0.48	2.63	0.78	0.09	0.02	1.13	0.22
A	442–454	10	–	–	0	3	8.08	0.02	9.38	0.12	8.73	0.12	2.22	0.34	0.11	0.07	0.58	0.02
F	455–498	50	–	–	0	15	8.12	0.04	8.81	0.05	8.42	0.33	2.67	0.41	0.02	0.01	0.25	0.08
G	499–539	50	–	150	0.75	19	8.11	0.03	8.76	0.03	8.35	0.19	1.91	0.16	0.01	0.01	0.37	0.09
H	540–548	50	100	150	1.43	3	8.16	0.05	8.78	0.05	8.74	0.56	1.39	1.44	0.00	0.00	0.43	0.21
I	549–608	50	150	150	1.76	27	7.98	0.04	8.63	0.06	7.18	0.17	2.23	0.12	0.02	0.01	0.51	0.21
D	609–801	10	100	150	7.13	79	7.81	0.06	9.02	0.08	8.30	0.34	2.88	0.18	0.05	0.01	0.63	0.06

ET = elapsed time, DIC = dissolved inorganic carbon as C, pH_I = initial pH, pH_F = final pH, DO_I = initial dissolved oxygen, DO_F = final dissolved oxygen; Ave = average, CI = 95% confidence interval, Fe(II) = ferrous iron.

Figure 1-5. Impacts of Chloride, Sulfate, and DIC on Iron Release.

Source: Reprinted from Water Research 183; by D. A. Lytle, M. Tang, A. T. Francis, A. J. O'Donnell, and J. L. Newton; The Effect of Chloride, Sulfate, and Dissolved Inorganic Carbon on Iron Release from Cast Iron; p. 116037; Copyright (2020), with permission from Elsevier.

Silicates present in source water can lead to the formation of a protective iron scale and reduce the corrosion rate. Natural organic matter present in source water can decrease the iron corrosion rate but may increase corrosion byproduct release. Orthophosphate can significantly reduce iron release into drinking water through adsorption to iron scales or formation of iron phosphate scales, which may decrease iron solubility or decrease scale permeability (Lytle et al., 2005). Orthophosphate was shown to effectively reduce iron corrosion in samples of aged, galvanized iron pipe from a distribution system in Fresno, CA, which had a large proportion of exposed iron surface due to zinc layer deterioration (Tang et al., 2018). Polyphosphate can sequester iron to reduce the potential for discolored water; in addition, polyphosphate reverts to orthophosphate in the distribution system, and due to chemical interactions at the scale surface, can contribute to iron corrosion control by orthophosphate.

Although control of calcium carbonate saturation levels was conventionally viewed as a strategy for iron corrosion control, formation of a calcium carbonate scale has not been shown to provide benefits for iron corrosion control. Associated calcium saturation indices, such as Langelier Saturation Index (LSI) and CCPP, have shown limited usefulness in lead and copper corrosion control (McNeill and Edwards, 2001). The Larson Ratio, which considers the ratio of sulfate and chloride to bicarbonate, has been shown to be moderately predictive of changes in iron levels in water, with a potential dependance on whether the water started with high or low DIC (bicarbonate) (Lytle et al., 2020). A summary of the impacts of different water quality parameters on iron release from cast iron pipe is presented in Table 1-1.

Table 1-1. Summary of Water Quality Impacts on Iron Release from Cast Iron Pipe.

Parameter	Impacts
Oxidant (DO and chlorine)	Consistent oxidant levels maintain dense outer scale layer, minimizing soluble iron release
pH	Higher pH levels minimize soluble iron release by promoting formation of ferric iron oxides Lower pH levels increase formation of the porous ferrous iron layer
Alkalinity/DIC	Higher alkalinity maintains protective outer scale layer and increases buffer capacity to resist pH changes
Chloride	Higher levels of chloride increase iron release by increasing the formation of porous ferrous iron scale layers
Sulfate	Impacts of sulfate may depend on chloride and sulfate levels. Sulfate can affect presence of sulfate reducing bacteria, influencing iron release to water
Orthophosphate	Orthophosphate decreases iron release, potentially by forming an insoluble phosphate scale and decreasing scale permeability
Polyphosphate	Decreases appearance of red water through sequestration of dissolved iron
Silicates	Decrease iron corrosion rate; may form protective scale

1.1.3 Impact of Biological Growth on Iron Corrosion

Iron tuberculation can also create an environment that harbors biological growth. Cast iron pipes can stimulate biofilm formation due to the chlorine demand exerted by iron scale surfaces, which can protect bacteria from free chlorine, and increase organic accumulation on iron tubercles (LeChevallier et al., 1998; Volk et al., 1999). Changes in sulfate levels affect the biofilms present in distribution systems, which in turn affects corrosion in these systems (Yang et al., 2014; Li et al., 2014; Li et al., 2016; Wang et al., 2014). Introduction of high-sulfate water to stable corrosion scales (i.e., those typically found in surface water systems) was shown to

result in iron reducing bacteria maintaining dominance, but introduction of high-sulfate water to less-stable corrosion scales (i.e., those typically found in groundwater systems) results in increased sulfur oxidizing bacteria, sulfate reducing bacteria (SRB), and iron oxidizing bacteria populations. These results indicate that iron reducing bacteria inhibit iron release while sulfur oxidizing, sulfate reducing, and iron oxidizing bacteria promote iron release (Yang et al., 2014).

Biofilm formation is influenced by the concentration of biodegradable organic matter and assimilable organic carbon (AOC) entering the distribution system, and lower AOC concentrations can decrease biofilm densities (Volk et al., 1999). Some evidence exists that monochloramine may provide advantages due to better penetration of biofilms for microbial inactivation (LeChevallier et al., 1988), but other work has shown no significant difference in biofilm density on cast iron pipe between free chlorine and chloramines due to the impacts of corrosion by-products (LeChevallier et al., 1998). Effective corrosion control for iron can reduce the extent of tuberculation and increase the effectiveness of the disinfectant for biofilm control (LeChevallier et al., 1998). However, some biofilms, such as those containing high proportions of immunoreactive beads (IRB) or the nitrate reducing bacterium *Dechloromonas*, have been shown to inhibit iron release (Yang et al., 2014; Wang et al., 2014), so biofilms can also have a beneficial effect on iron pipe corrosion.

1.1.4 Literature Gaps on Iron Corrosion

Water treatment changes due to blending of membrane-treated advanced treated water (ATW) that decrease the alkalinity/DIC have the potential to significantly increase iron corrosion and release. This behavior has been observed in lab-scale corrosion loop experiments where exposure of iron coupons to nanofiltration-treated water resulted in severe iron corrosion, while blending with water only having undergone coagulation, sedimentation, and filtration decreased the extent of corrosion (Choi et al., 2015). High iron release has also been observed with the introduction of saline water treated with reverse osmosis to aged cast iron pipes historically exposed to groundwater (Taylor et al., 2005). A review of water quality data in the scientific literature indicates that ATW tends to have lower alkalinity and higher chloride content than surface water or groundwater, as shown in Table 1-2. The ratio of high chloride to low alkalinity (DIC) in ATW sources may partly explain the behavior observed by Choi et al. (2015) and Taylor et al. (2005). Few studies exist that assess differences in corrosion outcomes when switching to advanced treated water in systems that have historically used groundwater versus surface water or a blend of surface and groundwater.

Addition of orthophosphate or increasing the DIC of ATW may reduce iron release and counteract impacts of higher chloride and sulfate levels. Ozonation and resulting elevated DO levels were found in one study to have no impact on iron release (Sarin et al., 2003). Utilities have experienced unintended consequences affecting iron corrosion due to treatment changes; for example, one utility adjusting the pH value to optimize lead corrosion control triggered red water complaints due to increased iron corrosion (Masters et al., 2015). Water quality changes affecting distribution system iron corrosion can increase chlorine demand, requiring further adjustments to treatment and distribution system operational practices. Additional testing is necessary to evaluate if mitigation strategies such as gradual blending that have worked in other situations can be successful when water sources are integrated with ATW.

Table 1-2. Summary of Alkalinity, Sulfate, Chloride, and pH Data for NF-or RO-Advanced Treated Water, Surface Water, Groundwater, and Blends of Surface and Groundwater.

Water Type	Water Quality Indicator				Study
	Alkalinity (mg/L as $CaCO_3$)	Sulfate (mg/L)	Chloride (mg/L)	pH	
ATW (NF)	13.1	2	2.4	6.9	Choi et al., 2015
	50	30	50	8.3	Imran et al., 2006*
	4.1	5.5	157	6.43	Liu et al., 2010
ATW (RO)	69	5.8	91.7	8.06	Taylor et al., 2005*
	98	20	3.6	7.8	Hu et al., 2018
	255.1	302.4	111.9	7.6	Hu et al., 2018
	50	180	10	8.2	Imran et al., 2006*
	120	79	28	7.68	Liu et al., 2010
	60	190.2	37.1	7.92	Taylor et al., 2005*
	141	52.1	21	7.74	Yang et al., 2012
	155	50.7	15.7	7.84	Yang et al., 2012
	139	74.1	19.6	7.88	Yang et al., 2012
SW	155	50.8	15.8	7.84	Yang et al., 2014
	298.4	54.2	34.8	7.5	Hu et al., 2018
	225	10	15	7.9	Imran et al., 2006*
	207	26.1	28.9	7.87	Taylor et al., 2005*
	165.5	38	18.7	7.7	Yang et al., 2012
	241	99.1	57.7	7.46	Yang et al., 2012
	198.6	22.3	14.3	7.6	Yang et al., 2012
GW	187	20.1	24.4	7.16	Yang et al., 2014
BW (SW & GW)	134.3	17.1	22.7	7.43	Yang et al., 2014
	174.3	111.5	82.5	7.5	Hu et al., 2018

*Water source was synthetic for experiments or simulated for computer model.

1.2 Lead Corrosion

The most common sources of lead release to drinking water are lead-based premise plumbing materials and lead pipes used as service lines. The contributions of lead to tap water have been attributed to be in the range of 20-35% (by mass) from premise plumbing materials such as lead-soldered connections of copper tubing and leaded brass and 50-75% from lead service lines (Sandvig et al., 2008). Lead adsorbed onto iron deposits found in premise plumbing and lead service lines is another source of particulate lead release to tap water (Deshommes et al., 2010). Lead concentrations in tap water in the United States are regulated by the Lead and Copper Rule, which has a 15 µg/L action level for lead in tap water. This action level requires certain actions to be taken if the 90th percentile exceeds that level for homes sampled from a pool most likely to have lead sources. The Lead and Copper Rule Revisions (LCRR) include a new trigger level of 10 µg/L that will require introduction of corrosion control treatment if the 90th percentile value of tap water samples exceeds it.

Lead in the water can be present in dissolved and particulate forms (Figure 1-6). Elemental lead on lead metal surfaces is oxidized to Pb(II) and Pb(IV) in the presence of an oxidant. These oxidized forms of lead react with the solutes in the water to form lead complexes that can be soluble or remain as corrosion products in a scale that forms on the lead metal surface. Dissolved lead in the water is strongly influenced by pH, dissolved inorganic carbon (DIC) and

alkalinity, dissolved organic carbon (DOC), and free chlorine and phosphate that can result in the formation of Pb(II)- and Pb(IV)-based corrosion products (Schock and Lytle, 2010). Dissolved lead concentrations can be estimated based on equilibrium solubility calculations. Release of particulate lead resulting from surface erosion is more sporadic than the release of dissolved lead. Factors other than water chemistry also affect the lead measured in water including stagnation time, flowrate, and age of pipe material.

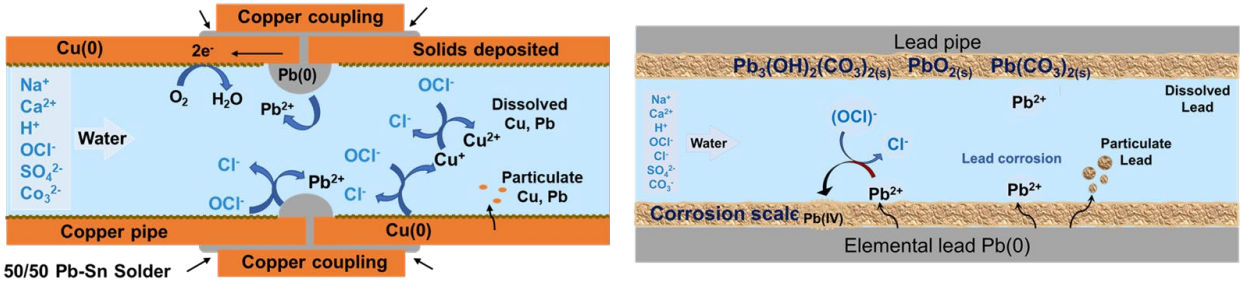

Figure 1-6. Corrosion Mechanism within a Copper Pipe Connection Made with a Lead-Containing Solder with Chlorine as Disinfectant (left). Lead Pipe with Corrosion Products (right).

1.2.1 Influence of Water Quality on Lead Release

Lead dissolved in water can be estimated by equilibrium solubility predictions in which dissolved lead in equilibrium with a particular lead-containing solid is a function of pH and concentrations of dissolved inorganic carbon and orthophosphate (Schock and Lytle, 2010). Studies by Kim et al. (2011) and Salveson et al. (2018) show that these solubility based estimations can also be used to interpret changes in lead concentrations with pH in real systems with lead pipes and brass rods respectively. The effect of pH and disinfectants on lead release from lead(V) oxides has also been studied. The rate of dissolution of Pb(IV) oxides increases with decreasing pH and with a switch from free chlorine to monochloramine (Lin and Valentine, 2009; 2010; Xie et al., 2010). The effect of alkalinity on lead release has often been studied in combination with pH (Arnold et al., 2011; Lytle and Schock, 2008; Tam and Elefsiniotis, 2009). At pH between 7.2 to 8.2, the change in lead concentration is independent of change in alkalinity within 15 to 100 mg C/L, but at higher pH, a decrease in lead is observed with increasing alkalinity (Schock and Lytle, 2010). Lead release from copper pipes and brass meters after being conditioned with desalinated water (with low alkalinity and high pH) and conventional treated water separately were found to be similar and below the action level (Blute et al., 2008). In blended water, increasing the ratio of desalinated water while maintaining a low alkalinity of 30 mg/L as $CaCO_3$ at pH 7.8 can be beneficial for limiting lead release (Liu et al., 2010). Similar conditions in chloraminated water can reduce nitrification induced corrosion as well (Zhang et al., 2009).

Other water quality parameters such as chloride, sulfate, dissolved organic carbon (DOC) or natural organic matter (NOM) and disinfectants like chlorine and chloramine can influence lead concentrations. The concentration and composition of dissolved organic carbon can vary as waters from different advanced treatment processes are blended. Lead released from Pb(IV) oxides in the presence of NOM increases with an increase in DOC concentration irrespective of the type of NOM (Dryer and Korshin, 2007). NOM also increases short- or long-term leaching of lead from pure lead, lead-containing solder, and leaded brass by inhibiting the formation of

crystalline lead corrosion products such as cerussite and alter the morphology of hydrocerussite (Korshin et al., 2000; 2005). The ability of NOM to chemically reduce Pb(IV) oxides that result in increased lead release is lower in the presence of free chlorine than in chloramine (Lin and Valentine, 2008; 2009). The use of coagulants such as $FeCl_3$ and $Al_2(SO_4)_3$ in water treatment can result in removal of certain fractions of NOM that are most potent at reductively dissolving Pb(IV) oxides. The use of granular activated carbon can also decrease DOC concentrations and alter the composition of the remaining DOC in ways that can affect reductive dissolution of Pb(IV) oxides.

The composition of anions in water, especially chloride and sulfate, can influence lead release. The concentrations of chloride and sulfate and their relative concentrations can vary as different water sources are used or treatment processes or treatment chemicals are changed. Chloride and sulfate tend to form different solids by migrating towards lead (acting as anodes) in aged pipes (Desantis et al., 2018). Several researchers have hypothesized that high chloride-to-sulfate mass ratio (CSMR) can be a factor increasing lead leaching through acceleration of galvanic corrosion of lead soldered copper pipes and brass (Edwards and Triantafyllidou, 2007; Triantafyllidou, 2006). However, other research has focused on the absolute changes in chloride and/or sulfate (Ng et al. 2015).

Increased lead leaching associated with higher CSMR was reported in a pilot-scale distribution study that tested groundwater, desalinated water, and surface water (Tang et al., 2006; Taylor et al., 2005). Bench-scale experiments with segments of copper pipe soldered with lead immersed completely in water showed increase in lead leaching at high CSMR (Nguyen et al., 2011). The effect of CSMR and NOM in different synthetic waters on lead and copper was studied by Willison and Boyer (2012), with findings showing that high lead concentrations were observed for higher chloride and sulfate concentrations than for lower concentrations for the same CSMR. In another study by Ng, et al. (2015), increasing either chloride or sulfate concentration resulted in an increased lead release which indicated that CSMR was not a good indicator of corrosivity. These studies together suggest that interpretation of the impact of chloride and sulfate on lead release needs to be studied individually with less stress on CSMR.

The impact of chloride and sulfate on lead release are particularly important for scenarios in which galvanic corrosion can occur. Galvanic corrosion can occur when two dissimilar metals are connected in a method that allows electrical conductivity between the two materials. This can occur with lead-containing solders connect copper pipe and when copper pipe is connected to lead pipe using brass couplings. In these situations, the lead is anodic relative to the copper, which results in greater corrosion of the lead than would occur for it in isolation (Figure 1-7). Lead within premise plumbing, especially at pipe connections, can act as anodic zones where galvanic corrosion can take place (Desantis et al., 2018). Galvanic corrosion in copper and lead connected pipe systems resulted in increased lead and decreased copper release to water (Arnold Jr et al., 2011; Cartier et al., 2013; Dore et al., 2019; Nguyen et al., 2010; Nguyen et al., 2011; Wang et al., 2012). High chloride concentrations in stagnating conditions can sustain high galvanic currents and prevent the formation of passivating layer and result in high lead release. Lead release is lower for lower chloride-to-sulfate mass ratios in stagnating conditions (Nguyen et al., 2010).

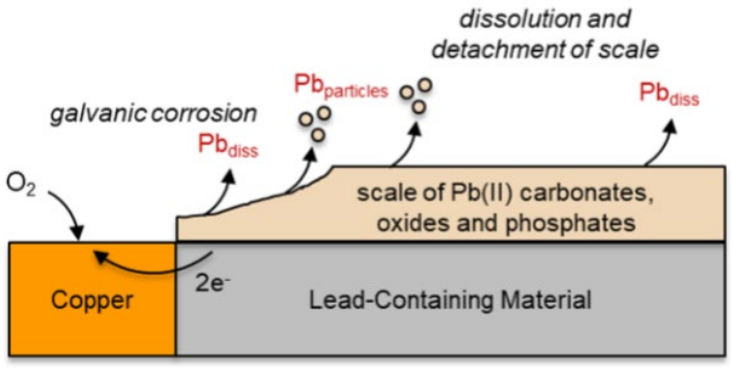

Figure 1-7. Processes Resulting in the Release of Dissolved and Particulate Lead from Scales on Lead-Containing Plumbing Materials.

The rate of lead release from both copper with lead solder and brass coupons was faster in the presence of combined chlorine (chloramine) than free chlorine (Dudi, 2004; Edwards and Dudi, 2004; Lin et al., 1997; Masters et al., 2015). In systems with chloramine, brass is more susceptible to lead/copper leaching due to low pH that may be induced by nitrification (Zhang et al., 2008).

1.2.2 Impact of Other Parameters on Lead Release

Factors other than water chemistry have also been studied with respect to lead release from brass and lead solder. Deshommes et al. (2010) and Doré et al. (2019) showed that particulate lead in water collected from taps increased with flowrate. Higher flowrates can decrease corrosion by enabling corrosion inhibitors to more efficiently reach the pipe surfaces to form passivating films; however a high flowrate can also detach the corrosion products from the scale (Salveson et al., 2018). In recent work, dissolved and particulate lead increased with stagnation time up to 16 hours and then remained constant for the next 320 hours (Doré et al., 2019). Lead concentrations from lead pipe gradually increased in the first 20 hours of stagnation and stabilized in a study by Lytle and Schock (2000). Longer stagnation in the pipe can deplete the disinfectant and result in increased microbial growth (Salveson et al., 2018; Schock and Lytle, 2010). Age of the pipe material is another parameter that can affect lead release. The inner surface of pipe materials in contact with water form corrosion products that accumulate over time. Relatively new materials, especially brass fixtures, are more susceptible to corrosion and can result in high level of lead (Elfland et al., 2010; Lei et al., 2018).

1.2.3 Impact of Corrosion Scales

Often, solubility calculations can predict dissolved lead in water flowing through lead pipes coated with a uniform layer of corrosion products (Kim and Herrera, 2010; Peng et al., 2010; Schock and Lytle, 2010). Lead-based corrosion products such as litharge (PbO), cerussite ($PbCO_3$), hydrocerussite ($Pb_3(OH)_2(CO_3)_2$), plattnerite (PbO_2), and hydroxylpyromorphite ($Pb_5(PO_4)_3(OH)$) can form based on the water chemistry and time of contact with lead surface. On brass surfaces, formation of malachite and hydrocerussite has been observed using X-ray absorption spectroscopy (Frenkel and Korshin, 1999). Research on galvanic corrosion shows solids such as lead sulfate and lead chloride formed at the junction of lead and copper or lead and brass joints (Desantis et al., 2018). Additionally, lead leaching due to galvanic corrosion

from solder or leaded brass in water was not seen in water chemistries favoring lead (IV) oxides.

1.2.4 Effect of Corrosion Inhibitors on Lead Release

Orthophosphate addition as a corrosion inhibitor at neutral and higher pH conditions can be effective in reducing lead concentrations in water to below the action level (Aghasadeghi et al., 2019; Bae et al., 2020; Chiodini, 1998; ; Lintereur et al., 2012; Lytle et al., 1996; McNeill and Edwards, 2002; ; Shuldener and Sussman, 1960; Stericker, 1938; Tam and Elefsiniotis, 2009; Thompson et al., 1997; Wehle, 1982). Silicate has also been added as a corrosion inhibitor in, although many studies of its use have not separately examined the effects of the increase in the concentration of dissolved silicate from the associated increase in pH when it is added. When pH and silicate concentration were separately examined, most studies found that there was no benefit for silicate addition (Li et al., 2021) in lead pipes, although one study did find that silicate had an effect for pipes with a thick aluminum-rich layer of scale that became an improved barrier to lead release upon silicate addition (Mishrra et al., 2021).

Lead released from brass and solder, rather than lead pipes, can be extremely high and sporadic mostly due to particulate lead. These spikes and sporadic lead release can be decreased to values below the action level by corrosion control methods such as pH adjustment, addition of zinc or calcium orthophosphate, and addition of sodium silicate at high pH (Lytle et al., 1996). Higher pH conditions are favorable for controlling lead by orthophosphate addition in lead-based premise plumbing materials for both conventional water supplies and blended desalinated water (Liu et al., 2010; Tam and Elefsiniotis, 2009).

1.2.5 Literature Gaps on Lead Corrosion

While much is known about the factors that influence lead concentrations in water, several knowledge gaps exist. Blending can affect more than one water quality parameter and while the effect of these parameters individually is understood, the combined effect is unknown. There are still uncertainties about situations when chloride and sulfate are key factors affecting galvanic corrosion. The effects of scale developed in copper pipes with solder and on brass materials have not been extensively studied. Effect of microbially enhanced corrosion on lead release from premise plumbing materials is also unknown.

1.3 Copper Corrosion

Copper is the most common material found in existing premise plumbing systems. While copper pipe provides a low-cost and relatively corrosion resistant alternative to other metals, copper corrosion can occur. Copper release into drinking water due to corrosion can result in blue/green water discoloration and health implications when high concentrations are consumed. The Lead and Copper Rule (LCR) established an action level for copper of 1.3 mg/L.

Two primary forms of copper corrosion include uniform corrosion (results in the release of copper to drinking water) and pitting (results in pinhole leaks). In either case, copper is oxidized into its cuprous and cupric states, resulting in the formation of insoluble precipitates and soluble complexes (AWWARF, 1996). The formation of precipitates can result in the formation of a passivating scale or may result in blue/green water discoloration when the precipitates

remain suspended (AWWARF, 1996). The formation of soluble complexes can impact the solubility of passivating solids and contribute to overall copper release (AWWARF, 1996).

1.3.1 Uniform Corrosion

Uniform corrosion and pitting of copper pipe are influenced by a variety of water quality factors including pH, alkalinity/DIC, chlorine, aluminum, chloride, sulfate, and NOM. Despite numerous studies, fully understanding the impacts of these water quality conditions on copper corrosion is challenging for researchers. Optimizing treatment to control both uniform and pitting corrosion presents another difficulty for utilities as the water quality conditions that decrease uniform corrosion and copper release may result in an increase in copper pitting.

Copper release, because of uniform corrosion of copper pipes, is typically associated with low pH and high alkalinity waters (Dodrill and Edwards, 1995; Edwards et al., 1996; AWWARF, 1996). Copper solubility decreases as pH increases (Dodrill and Edwards, 1995) and copper corrosion is almost always uniform at low pH values (AWWARF, 1996). Additionally, there is an approximate linear relationship between alkalinity and soluble copper release where the sensitivity of copper solubility to alkalinity is dependent on pH (Edwards et al., 1996). In general, an increase in alkalinity will increase soluble copper release; however, the impact of alkalinity is less significant at higher pH levels. Raising pH to above 7 has been found to be a simple and effective method to mitigate high copper release for utilities with low pH/low alkalinity waters and above 7.8 for low pH and slightly higher alkalinity waters (Dodrill and Edwards, 1995).

1.3.2 Non-Uniform Corrosion

Corrosion of copper at higher pH levels (e.g., pH > 8.0), is generally associated with non-uniform corrosion processes. Localized corrosion of copper pipe can lead to pitting and pinhole leaks, which can cause significant property damage. Several types of copper pitting have been identified and are associated with a variety of different water quality parameters. Cold-water pitting is almost always associated with cold, high hardness well waters with pH in the range of 7 to 8.2 and hot-water pitting is typically associated with hot waters having a pH of less than 7.2 (Edwards et al., 1994; AWWARF, 1996). Soft-water pitting is most common in chlorinated waters with high pH and low alkalinity in the presence of free chlorine, especially with moderate levels of chloride and sulfate (Sarver et al., 2011; Lytle and Schock, 2008). Forensic investigation techniques can be used to determine the type and cause of copper pitting by identifying the formation of particular scales within the pits and observing the physical characteristics of the pits themselves (AWWARF, 1996; Sarver et al., 2011; Edwards et al., 1994).

In addition to pH and alkalinity, several other water quality parameters have been found to influence pitting in copper pipes. Aluminum solids have been found to have a synergistic interaction with chlorine, increasing the likelihood of pitting when aluminum solids are present in chlorinated, high pH waters (Rushing and Edwards, 2004; Marshall, 2004). Additionally, copper pitting in the presence of high pH/low alkalinity waters can be further influenced by the presence of low DIC and significant levels of chloride and potentially sulfate (Lytle and Schock, 2008). While sulfate has been found to impact the composition of corrosion by-products,

research has found that sulfate may not be necessary for the initiation of pitting itself (Lytle and Schock, 2008). One study suggests that chloride, in the short-term, may be aggressive towards copper pipe; however, it can result in the formation of a protective scale in the long-term, passivating copper corrosion and pitting (Edwards et al., 1994). In contrast, this study found that sulfate, often thought to be less aggressive towards copper than chloride, can result in the formation of a scale that promotes copper corrosion in the long-term.

Based on the water quality parameters typically associated with copper pitting, advanced treatment processes resulting in low alkalinity, low hardness, and high pH water (e.g., RO treatment with pH adjustment) could create conditions promoting copper pitting corrosion. In these cases, utilities may evaluate the use of orthophosphate corrosion inhibitors to reduce lead and copper corrosion. Copper pitting can be inhibited by phosphate, and copper pitting is also less common with chloramine than with free chlorine (Sarver et al., 2011). The impacts of corrosion control treatment on both uniform and pitting corrosion must be evaluated when selecting an optimal strategy for controlling the corrosion of copper pipe.

1.3.3 Impact of Natural Organic Matter on Copper Corrosion

NOM, even at trace levels, has been found to result in increased water copper concentrations by inhibiting the formation of a low-solubility scale on the pipe interior (Edwards and Sprague, 2001; Arnold et al., 2012). NOM impedes the natural aging and passivation of copper pipe, ultimately resulting in increased copper release. This can be especially troublesome when dealing with newly installed copper pipe. One study found that the temporary use of GAC treatment to remove NOM after the installation of new copper pipe, could allow for the formation of a low-solubility scale, providing a long-term mitigation strategy for copper release (Arnold et al., 2012). The impact of NOM on copper release has also been found to be more detrimental at higher alkalinities (Arnold et al., 2012). Additionally, the presence of NOM has been found to decrease the effectiveness of orthophosphate, requiring a higher orthophosphate dose for equivalent corrosion control (Arnold et al., 2012; Li et al., 2004). At low levels of NOM, accelerated pipe passivation and formation of a low-solubility scale such as malachite or tenorite (Figure 1-8) can result in low copper concentrations (Edwards and Sprague, 2001; Arnold et al., 2012).

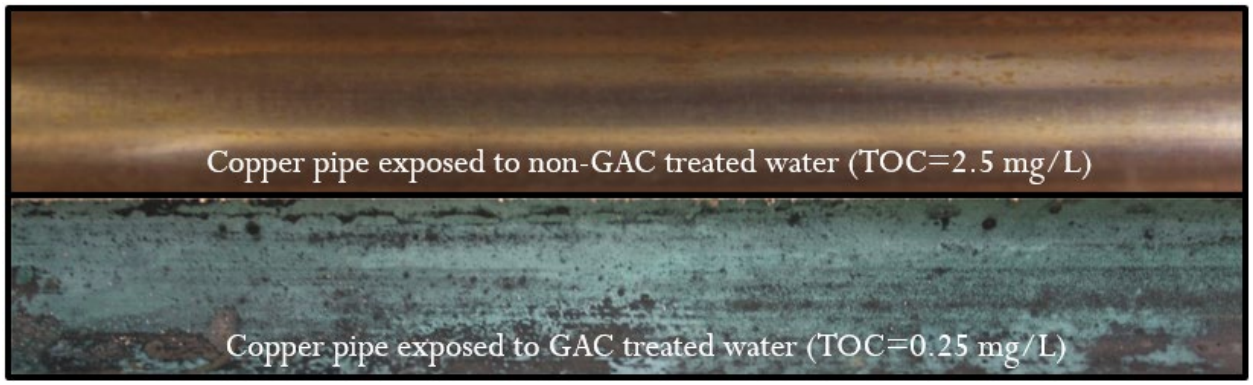

Figure 1-8. Illustration of Scale Differences in Low-NOM Water on Copper Pipe.
Source: Arnold et al. 2011.

1.3.4 Effect of Corrosion Inhibitors on Copper Corrosion

Orthophosphate is generally effective for reducing overall copper concentrations at the tap. Performance of orthophosphate is dependent on pH and alkalinity, and optimizing the pH is beneficial to maximize inhibitor effectiveness (Dodrill and Edwards, 1995; Cantor et al., 2000; Edwards et al., 2002). Phosphate-based inhibitors are very effective corrosion control strategies in waters with low pH, especially when raising the pH for corrosion control is not feasible due to increased precipitation of calcium carbonate (Marshall, 2004; Dodrill and Edwards, 1995). While some benefit from phosphates is anticipated at pH levels as high as pH 10 (Marshall, 2004), the performance of phosphate-based inhibitors at pH levels greater than 7.8 has been reported to be variable (Dodrill and Edwards, 1995). High levels of both orthophosphates and silicates have been found to greatly reduce instances of copper pitting (Sarver and Edwards, 2012), as shown in Figure 1-9.

Polyphosphates, typically added as a sequestering agent for iron, can increase soluble copper concentrations (Cantor et al., 2000; Edwards et al., 2002). The performance of polyphosphate inhibitors is more unpredictable than orthophosphate (Cantor et al., 2000) and typically do not reduce metal levels as much as orthophosphate (Edwards, 2002).

Copper solubility is initially controlled by cupric hydroxide, and copper pipe passivation can lead to the natural formation of a low solubility internal scale, such as malachite or tenorite. The duration of this transition is dependent on water quality (pH, alkalinity, total organic carbon, and orthophosphate). The presence of orthophosphate inhibits the formation of an insoluble copper oxide scale on the pipe interior. Therefore, in some cases, phosphate can increase copper solubility in the long term compared to natural pipe passivation (Edwards et al., 2002; Arnold et al., 2012). In most cases, moderate doses of phosphates have been found to generally decrease copper release in the long-term; however, in at least one case the use of phosphate- based inhibitors decreased copper release in the short-term but significantly increased copper release after several years (Edwards, 2002).

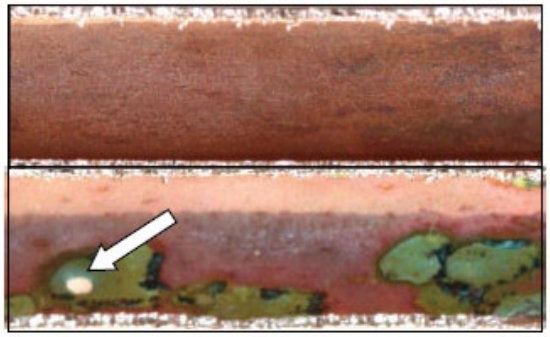

Figure 1-9. Copper Samples after Scale Removal.
Top is 1 mg/L phosphate as P; Bottom is 0.015 mg/L phosphate as P. Arrow indicates pinhole leak.
Source: Sarver and Edwards 2012. CC BY 3.0 DEED.

1.3.5 Additional Factors Impacting Copper Corrosion

Several other factors have been identified that have the potential to impact copper corrosion. In several circumstances, pitting corrosion has been found to increase with higher flow velocity and frequency (Marshall, 2004; AWWARF, 1996; Sarver et al., 2011). Additionally, pipe bends

and polished pipe have been found to result in favorable conditions for pitting corrosion (Marshall, 2004). Temperature is also influential, with hot water typically increasing copper corrosion (AWWARF, 1996).

1.3.6 Corrosion Scales

Forensic investigative techniques such as X-ray diffraction (XRD), scanning electron microscopy (SEM), and energy dispersive spectroscopy (EDS) can be utilized to determine the mechanisms associated with the initiation and propagation of pitting corrosion. Physical characteristics of the pits and scales can be evaluated with these techniques.

Cold-water and hot-water pitting are both typically associated with deep, narrow pits and the formation of malachite/calcite for cold-water or bronchanite/malachite for hot-water pitting (Edwards et al., 1994; AWWARF, 1996). Soft water pitting is typically associated with wider, more shallow pits and the formation of bronchanite (Edwards et al., 1994; Lytle and Nadagouda, 2010). Three distinct internal structural features are associated with pitting, including the pit cap, a perforated pit membrane, and the pit itself (Figure 1-10), (Lytle and Nadagouda, 2010).

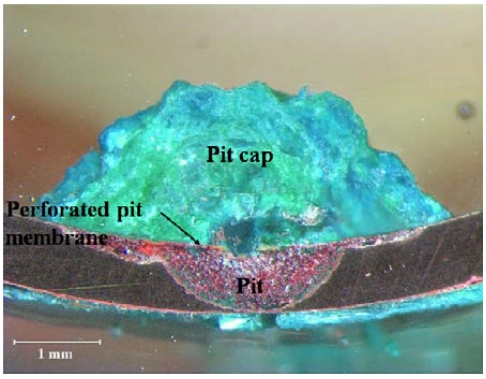

Figure 1-10. Illustration of the Structural Components of a Copper Pit.
Source: Reprinted from Corrosion Science 52(6); by D. A. Lytle and M. N. Nadagouda; A Comprehensive Investigation of Copper Pitting Corrosion in a Drinking Water Distribution System; p. 1927; Copyright (2010), with permission from Elsevier.

Forensic techniques have been further utilized to identify scale formation within each of the structural features. In one study, the individual structural components of pipes that had failed due to soft-water pitting were examined (Lytle and Nadagouda, 2010). The relatively porous cap was found to be primarily composed of brochantite and characterized by a blue-green color. The thin, porous pit membrane was found to be composed of cuprite and the pit itself was typically bowl-shaped and filled with cuprite crystals. When pits did form pinhole leaks, a blue-green corrosion deposit was often present at the pit/pipe interface. This deposit can also form on the exterior of the pipe, and when present may serve as a sealing mechanism and decrease overall leaking.

1.3.7 Literature Gaps on Copper Corrosion

Prior research has certainly provided an expansive amount of information regarding copper corrosion; however, several inconsistencies and knowledge gaps remain. Blending can have significant impacts on the stability of water quality within ranges of blending. While the impact

of variations in individual water quality parameters has been studied, the combined effect of these water quality variations on copper corrosion is not well understood. Also, balancing water quality conditions and best practices for mitigating both uniform and pitting corrosion in copper pipe are not well understood. Finally, inconsistencies are found within the literature regarding the effectiveness of corrosion inhibitors in preventing galvanic corrosion of lead soldered copper pipe. Despite past research, pitting corrosion continues to be poorly understood, unpredictable, and difficult to remediate (Lytle and Nadagouda, 2010).

CHAPTER 2

Research Approach and Test Plan

This section describes the testing approach, blending schedule, sampling locations, water quality parameters of interest, and sampling frequency of the project test. The testing approach focused on a blending schedule and water quality testing informed by the literature review. The reasons for evaluating the selected water quality parameters are provided below:

1. Water quality parameters indicative of water stability for corrosion control used to calculate LSI, CCPP, and Larson Ratio (LR) (alkalinity, calcium, pH, temperature, TDS, chloride, and sulfate)
2. Metals release into the water as they relate to regulatory standards (for unlined cast iron (UCI) pipe – iron and manganese; for copper pipe with lead solder and brass components – copper, lead, and zinc),
3. Other water quality parameters that may impact corrosion or DBP formation (conductivity, dissolved oxygen, turbidity, oxidation-reduction potential (ORP) and TOC)
4. Disinfectant concentrations (total chlorine, total ammonia) and nitrite (by-product from nitrification)

Corrosion-related outcomes were assessed with regulatory standards in mind, including primary and secondary maximum contaminant levels (MCLs) and Action Levels (ALs). However, loop results provided a "worst-case" scenario by circulating the water for 6 days and did not directly indicate that regulatory limits would be exceeded. The results are intended for relative comparison between conditions only and not assessing levels at the tap. Potential impacts of changes in water quality (including further stabilization of ATW and blends of water sources) were investigated to identify potential mitigation strategies when ATW is introduced into the distribution system.

The primary objectives of this research included the following:

- Identifying and evaluating impacts of alternative water supplies, (in this project, advanced treated water was used), on the water quality of the end users' existing drinking water systems that have known issues with tuberculation (e.g., corrosion, biological regrowth, *Legionella*, aesthetics, biofilm)
- Understanding impacts of blending ratios of alternative water supplies, including potable reuse, at a full-scale system into existing treated water on a variety of issues (e.g., nitrification, total chlorine residual, ammonia, nitrite, nitrate)
- Developing management strategies and options to mitigate adverse impacts

To achieve these objectives, an approach focused on testing mitigation strategies was used. The test plan included the development of the study design, specific procedures that were carried out in preparing test waters (including blends), on-site monitoring, collection of laboratory samples, and operating procedures for the pipe loops. Both pipe loop design and water quality

test plans for distribution system pipes and premise plumbing are described in the following sections.

2.1 Water Sources

Source waters included baseline water obtained from the Joint Water Pollution Control Plant (Joint Plant) site and ATW obtained from Metropolitan Water District Regional Recycled Water Advanced Purification Center (MWD RRWAPC). Baseline water was a groundwater-based tap supply. The baseline water and ATW were blended in different proportions and recirculated through pipe loops during the study to assess any adverse impacts of blending on water quality. All pipe loops were conditioned first with baseline water. After baseline conditioning, two gradual change pipe loops were operated with an increasing proportion of ATW blended with baseline water until 100% ATW was achieved. Two "Abrupt Change" pipe loops were operated with 100% ATW, when 100% ATW was introduced to the gradual change pipe loops. The exact blending schedules for each pipe loop are in Section 2.2.3 and 2.3.5.

Following testing with 100% ATW, baseline water (100%) was reintroduced to the pipe loops to assess the impact of a loss of the ATW source. For blended waters, a totalizer flow meter was used to monitor the water volumes added to the pipe loop tanks. Both baseline water and ATW were shipped to the Aquatic Chemistry Lab at WUStL, where it was added to the copper pipe with lead solder and brass rod pipe loops. The disinfectant and pH of the water shipped was adjusted once it was transferred to the recirculation reservoir. The ATW was blended with MWD water in the reservoirs for the stages requiring blending of these two waters.

2.1.1 Advanced Treated Water Source

The ATW used in this project was Full Advanced Treated (FAT) water produced at the Metropolitan Water District of Southern California's Regional Recycled Water Advanced Purification Center, treated by membrane bioreactor, reverse osmosis, and either UV/chlorine or UV/peroxide advanced oxidation.

Unstabilized ATW (MF/RO/UV AOP treated water) is by nature low in calcium and alkalinity, which can cause the water to be corrosive to pipes and plumbing materials. ATW was stabilized using calcite contactors with chlorine and ammonia addition to the stabilization tank. Excess peroxide from the advanced oxidation process in the demonstration study was quenched with chlorine. Figure 2-1 shows a schematic of the stabilization approach. ATW was produced at MWD's RRWAPC and piped to the integration testing area, which was located onsite at the RRWAPC. ATW was piped from the RRWAPC to a break tank, where it was pumped into a calcite contactor. The pump was necessary due to the low pressure of the RO permeate and the head loss in the calcite contactor resulting from small particle sizes.

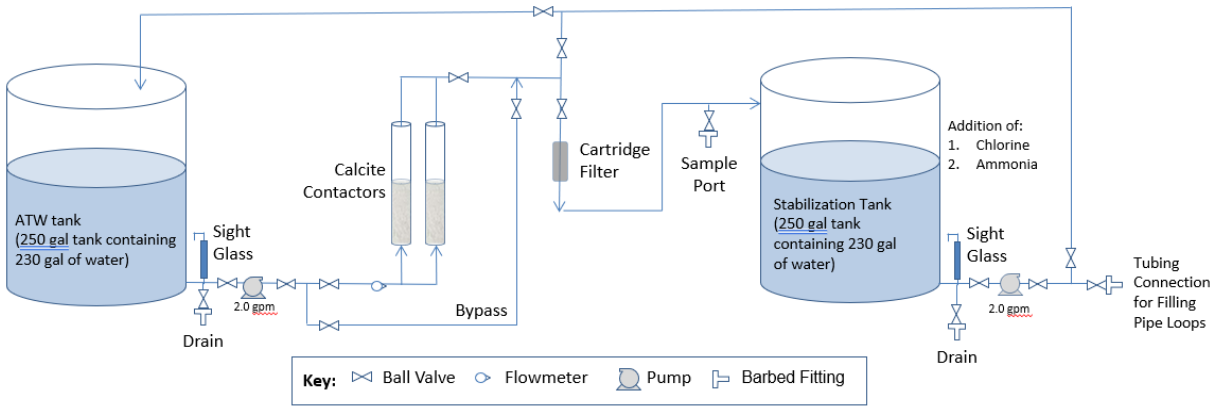

Figure 2-1. Advanced Treated Water Stabilization Process.

The calcite contactor consisted of granular calcium carbonate ($CaCO_3$), which dissolves into the water. Water quality targets were developed in a previous corrosion pipe loop study conducted by West Basin Municipal Water District in collaboration with Metropolitan (Blute et al., 2014). Based on this prior work, it was hypothesized that if stabilized water quality achieved the targets shown in Table 2-1, then introduction of ATW would be acceptable. This study further evaluated the introduction strategy of gradual versus abrupt introduction of ATW.

Stabilization targets were set irrespective of the baseline water quality, as the ATW might be introduced into a wide variety of systems in the future. Initial targets were set based on Metropolitan's treated water goals, which were confirmed in the pipe loop study at West Basin (Blute et al., 2014). Additional testing may be beneficial for other systems prior to introduction of ATW if the baseline water quality or desired targets vary from those tested.

Table 2-1. Stabilized Water Quality Targets.

Constituent	Concentration
Alkalinity	65 – 80 mg/L as $CaCO_3$
Calcium	> 65 mg/L as $CaCO_3$
pH	8.2 ± 0.2
CCPP	> 0
LSI	> 0
Total Chlorine Residual	2.5 mg/L
Total Ammonia	0.5 mg/L as N

Table 2-2 presents the design criteria for the pilot calcite contactor. An empty bed contact time (EBCT) of 5 minutes at a hydraulic loading rate (HLR) of 5 gpm/sf was expected to provide sufficient calcite dissolution to increase alkalinity – to 65 - 80 mg/L as $CaCO_3$. As the pH-adjusted desalinated water flowed through the calcite contactors, the calcite dissolved and increased calcium, alkalinity, and pH. After the calcite contactor, the water was filtered using a 20–30-micron bag filter to capture any calcite that may be carried over. This water then flowed into the 250-gallon tank. Water from the stabilized water tank was recirculated at a rate of approximately 17.5 gpm back into the tank, allowing for mixing and chemical addition directly into the tank.

Chloramines were formed in the stabilization tank by first adding chlorine, mixing for the amount of time necessary to achieve CT for 0.5-log Giardia and 4-log virus inactivation (i.e., approximately 7 minutes at 3 mg/L and pH 7.5). Due to early inconsistencies in stabilization, it was found that the water needed to be stabilized the day before use and dosed with the disinfectant residual of 2.5 mg/L total chlorine and 0.5 mg/L ammonia as N. Additional information is provided in Section 3.1.6.

Design criteria for ATW stabilization are provided in Table 2-2.

Table 2-2. ATW Water Quality Stabilization Design Criteria for a Single Contractor.

Constituent	Concentration
Flow rate (gpm)	1
Influent water pH	5.5
Calcite product	Puri-Cal™ C from Columbia River Carbonates[2]
Calcite particle size (mm)	1
Calcite contactor diameter (inch)	6
Calcite contactor bed depth (feet)	3.3
Calcite contactor volume (cf)	0.66
Hydraulic loading rate (gpm/sf)	5
Empty bed contact time (minutes)	5
Bag filter size (micron)	20-30
Chloramine concentration[1]	2.5 mg/L as Cl_2, 4.5:1 Ratio of Cl_2:NH_3-N
Final pH after caustic soda	8.2 ± 0.2

1 Chloramines were formed by adding chlorine to water, mixing, then adding ammonia.
2 Product data sheet attached in Appendix B

2.1.2 Baseline Water Source

Baseline water was supplied from a line installed by MWD terminating in a hose bib at the perimeter of the pilot site. Baseline water was supplied to pipe loop tanks by connecting a flexible hose section with a flow totalized connector, allowing the volume of water supplied to each tank to be measured. The potable water source at the RRWAPC was supplied by a local agency that uses various combinations of groundwater wells. Typical water quality is provided in Table 2-3. Initial startup testing determined that the water line required flushing prior to use to ensure that the water was fresh and characterized by typical residuals (i.e., at least 2.0 mg/L total chlorine). Baseline water was tested for ammonia and nitrite concentrations to check for nitrification in the source water.

Table 2-3 provides a summary of expected water quality, including the stabilized ATW and baseline water. Baseline water and stabilized ATW were fairly similar with respect to the key parameters impacting corrosion control for most distribution system materials, including alkalinity, pH, and calcium. The different source waters were expected to vary in chloride and sulfate concentrations based on historical data, with chloride and sulfate being lower for the stabilized ATW compared with baseline water. Baseline water showed a more significant range compared with ATW water in historical data, likely due to the use of different combinations of groundwater wells.

Table 2-3. Expected Baseline Water Quality Compared with Stabilized ATW.

Parameter	Stabilized ATW	Baseline Water[1]
Alkalinity (mg/L as $CaCO_3$)	65 – 80	67 – 180
Calcium (mg/L as $CaCO_3$)	> 65	17 – 330
CCPP (mg/L as $CaCO_3$)	> 0	TBD
Chloride (mg/L)	62	20 – 80
Chlorine, Total (mg/L)	2.5[2]	84
Conductivity (µS/cm)	TBD	880
Copper (mg/L)	ND	0.13[3]
Iron (µg/L)	ND	ND
Lead (µg/L)	ND	ND[3]
LSI	> 0	0.68
Manganese (µg/L)	ND	ND – 24
pH	8.2 ± 0.2	6.4 – 8.7
Sulfate (mg/L)	0.3	ND – 350
Total Organic Carbon (mg/L)	0.2	1.7 – 2.6
Total Dissolved Solids (mg/L)	96	ND – 490
Turbidity (NTU)	TBD	ND – 0.54

TBD – to be determined during testing.
ND – non-detect.
[1] 2019 Water Quality Report. Additional information was requested from the water system on the sources that feed the Joint Plant site to narrow the concentration ranges, as the values in the Water Quality report reflect both groundwater and MWD surface water supplies.
[2] Initial chlorine target of 3.0 mg/L was tested to account for chlorine demand/decay.
[3] Lead and Copper Rule 90th percentile values.

2.2 Distribution System Pipe Loop Testing

2.2.1 Pipe Loop Design and Operations

To evaluate the effects of ATW introduction on existing distribution system piping, four harvested 4-foot long, 6-inch diameter unlined cast iron (UCI) distribution pipe segments were used during this study.

The UCI pipe loops were tested with continuously recirculated water for 6 days with water replacement at the end of the week. This recirculation approach was selected to result in the accumulation of metals for easier detection of corrosion should it arise, with a detention time typical of distribution system detention times in this area (i.e., typically, they range from 2 days to one week).

UCI pipe loops were constructed at MWD's RRWAPC in Carson, California. The pipe loops were placed onto racks to maximize access for staff activities and to avoid disturbance of the pipe. The racks were approximately 5 feet long (with pipes and end caps), 5 feet high and 4 feet wide. Figure 2-2 shows the configuration of the pipe loops used for gradual introduction of ATW and abrupt introduction of ATW; both of these loops were operated in duplicate for a total of four pipe loops. Each UCI pipe loop was sampled from a sample tap on the PVC recirculation line after 6 days of recirculation. The isolation valve was closed after sampling to keep water in the pipe during changeout of the recirculation tank water, and the return PVC

line was built to an elevation greater than the tank to avoid draining the tank during the changeout. The volume of water held in the pipe was sent to waste, then the valve to waste was closed and the fresh water recirculated for the next 6 days.

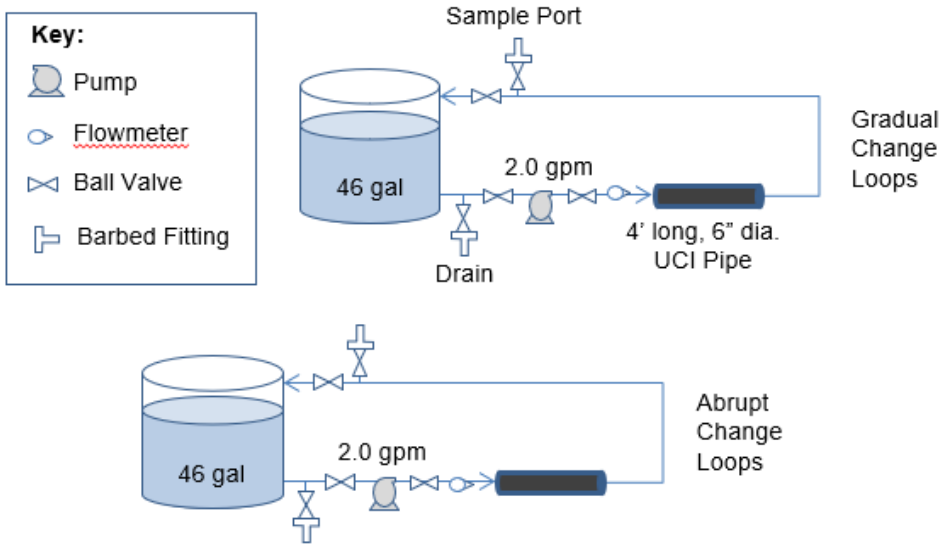

Figure 2-2. UCI Pipe Loop Schematic.

Cast iron pipes (circa 1920s) were harvested from the City of Pasadena's distribution system (Figure 2-3). Selection of materials and detailed harvesting procedures are provided in the Unlined Cast Iron Pipe Harvesting Plan (Appendix A). Measurements of the pipe outer diameter were taken in advance of the pipe harvesting to determine the proper size fittings for the pipe ends to have the fittings available during harvesting. The fittings for each pipe end were comprised of a mechanical joint with restraining gland and a blind flange that was tapped and threaded to receive 1" PVC pipe. Exposed fitting surfaces were coated with bituminous tar lining, as they ordinarily are available from the manufacturer for use in drinking water distribution systems.

Figure 2-3. Unlined Iron Pipe Harvesting from the City of Pasadena with Visible Tuberculation and Deposits (left); Pipes Installed in the Pipe Loops at the MWD Demonstration Facility in Carson, CA (right).

Hazen and Sawyer staff ensured that the pipes were properly plugged and sealed during pipe harvesting to contain existing moisture in the pipes during the time of removal. Pipes were carefully delivered to the site to minimize potential damage to the existing scale formation. The pipes were placed onto racks and baseline water was introduced into the pipes on the same day as harvesting.

Figure 2-4 shows a plan view layout of system components at the site. The rack for the UCI pipes contained two rows with two pipes vertically stacked. The recirculation pumps were placed on a shelf located at the front of the rack. 60-gallon capacity, black, food-grade polyethylene tanks were placed next to the rack. One-inch Schedule 40 piping was used to connect piping throughout the system and provide the return from the pipe to the recirculation tank. All glue was NSF-certified for use in potable systems. The pumps, tanks, and circulation piping were ordered and set up before the pipe harvesting so that assembly of the pipe loops was completed on the pipe harvesting day.

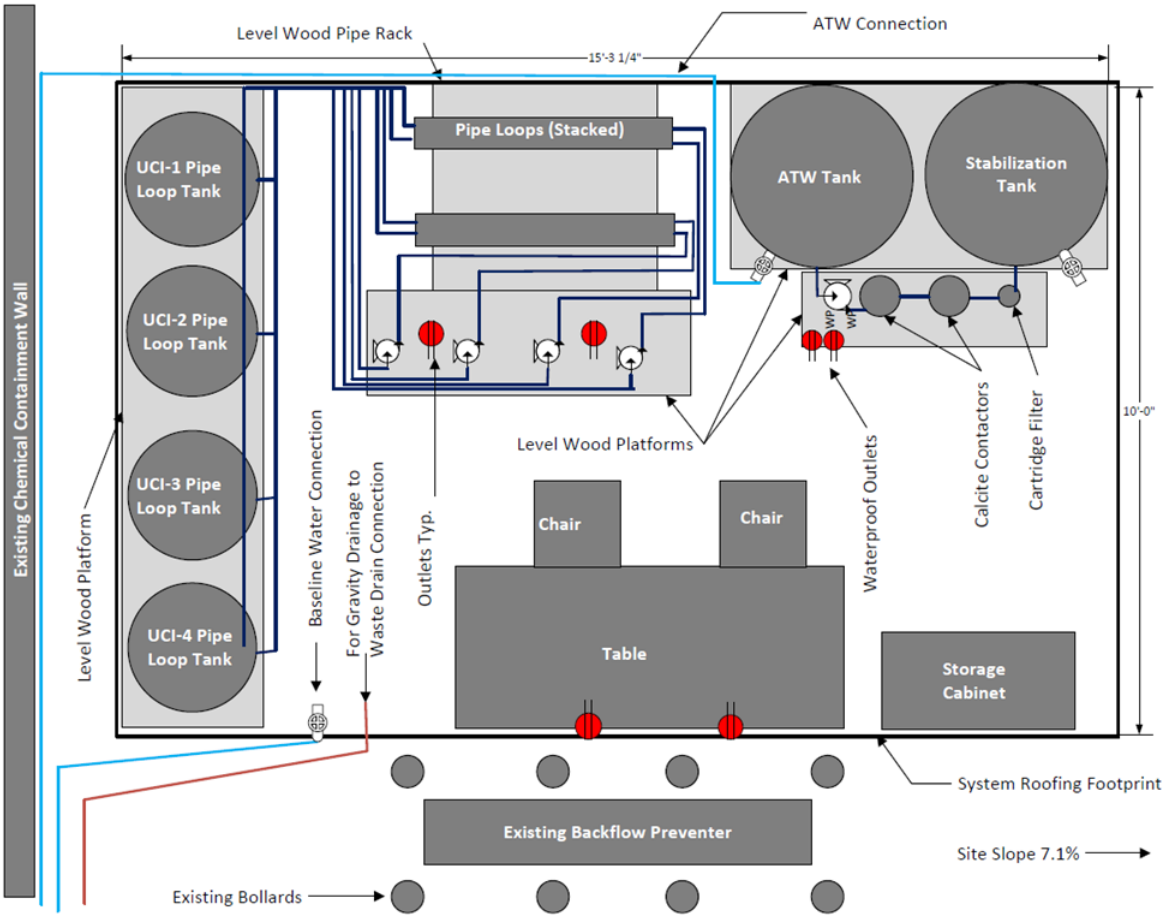

Figure 2-4. Plan View Layout of UCI Pipe Loop Pilot Testing System.

UCI pipe loops were operated continuously at a velocity of approximately 0.05 fps, corresponding to a recirculation pump rate of 2.0 gpm. The selected velocity was unlikely to induce physical erosion of pipe deposits.

Table 2-4 provides design criteria for the UCI pipe loops.

Table 2-4. Design Criteria for UCI Pipe Loops.

Design Parameter	Design Value
Pipe Diameter	6 in.
Length	4 ft.
PVC Diameter for Return and Connecting Pipe	1 in.
Velocity	0.05 ft/sec
Flow rate	2.0 gpm
Volume of UCI Pipe	0.7 ft^3
Volume of PVC	0.04 ft^3
Total Volume in Pipe	6 gal
Recirculation Tank	46 gal
Pipe Surface Area to Water Volume	0.11 cf surface area/ cf volume

2.2.2 Testing Approach and Analytical Methods

The distribution pipe loop pilot system was designed to evaluate the difference in impacts between abrupt and gradual introduction of ATW into typical pipe materials found in distribution systems. Testing to evaluate differences in impacts between abrupt and gradual ATW introduction was conducted for a period of eight months. A period of two months was used for stabilization of the pipes with baseline water, based on previous studies of a similar nature (Blute et al., 2008; Zhang et al., 2010). Following stabilization, the remaining six months allowed for collection of data on the differences in impacts between abrupt and gradual introduction of ATW. After testing to compare differences in impacts between abrupt and gradual introduction of ATW, further testing was conducted to evaluate reintroduction of baseline water. Pipe lengths, flow velocities, recirculation/stagnation periods, and exposure times were selected to represent typical operating conditions in distribution systems while allowing enough time to observe potential corrosion caused by introduction of ATW.

2.2.2.1 Analytical Methods

Table 2-5 and Table 2-6 summarize the field and lab analytical methods, including sample volumes, method reporting level (MRL), minimum detection level (MDL), and required preservatives. For field analyses (Table 2-5), the MRL equals the MDL. Field and laboratory measurements conformed to accepted drinking water test methods, including EPA approved methods, methods described in Standard Methods for the Examination of Water and Wastewater (2012), and Hach field test methods. Laboratory analyses except pathogens were performed at the Aquatic Chemistry Lab at WUStL.

The occurrence of the opportunistic premise plumbing pathogens (OPPPs) *Legionella* spp. and nontuberculous mycobacteria (NTM) in each harvested pipe loop were assessed during testing as well. *Legionella* samples were analyzed using the Legiolert method and NTM samples were analyzed by culture. These OPPPs were selected based on research showing that, in building water systems and distribution systems, *Legionella* and NTM are the most frequently isolated OPPPs of concern (which include P. aeruginosa, free-living amoebae, and thermophilic amoebae). Both of these OPPPs were expected in the biofilms. *Legionella* and NTM were analyzed by Aerobiology Laboratories.

Table 2-5. Field Analytical Methods.

Analyte	Analytical Method/ Instrument	Sample Volume Required (mL)	Method Reporting Limit
Alkalinity, Total	Hach 8203 (Digital Titration)	100	10 mg/L as $CaCO_3$
Ammonia, Total	Hach 8155 (Salicylate Method)	10	0.02 mg/L as N
Calcium	Hach 8204 (Digital Titration)	100	10 mg/L as $CaCO_3$
Chlorine, Total	Hach 8167 (DPD Method)	10	0.02 mg/L
Conductivity	SM 2510B (Conductance) / DO610: ExStik® II DO/pH/Conductivity Kit	30	N/A
Dissolved Oxygen	DO Probe / DO610: ExStik® II DO/pH/Conductivity Kit	100	0.1 mg/L
Nitrite	Hach 8507 (Diazotization Method)	30	0.005 mg/L as N
ORP	ORP Probe / RE300: ExStik® ORP	10	-2000 mV

Analyte	Analytical Method/ Instrument	Sample Volume Required (mL)	Method Reporting Limit
pH/Temperature	SM 2550 (Thermometric)/ SM 4500H-B (Electrometric) DO610: ExStik® II DO/pH/Conductivity Kit	30	N/A
Turbidity	SM 2130B (Nephelometric) / Hach 2100Q	30	0.02 NTU

N/A – Not Applicable

Table 2-6. Laboratory Analytical Methods at Aerobiology Laboratories.

Analyte	Analytical Method	Sample Volume (mL)	Preservatives	Method Reporting Limit	Method Detection Limit	Holding Time (hours)
Legionella	Legiolert	100	Sodium thiosulfate	N/A	<10.0 MPN/100mL	48
Nontuberculous mycobacteria (NTM)	Cell Culture	100	Sodium thiosulfate	N/A	<0.4 cfu/mL	24

N/A – Not Applicable; MPN – most probable number; cfu – colony forming unit

2.2.2.2 Water Quality Testing Parameters and Frequency

Table 2-7 summarizes the water quality parameters and testing frequencies for field analysis. Key parameters indicating corrosion or contributing to corrosion index stability were analyzed once a week to characterize the initial and final water qualities from the pipe loops. A weekly frequency for metals and key stability indicators matched the operational strategy of changing out water sources and water in contact with the pipe loops each week. This approach also allowed for the development of a reasonable number of data points during the testing period to enable conclusions to be drawn. Table 2-8 shows the sample collection frequency for laboratory analyses.

Table 2-7. Field Testing for UCI Pipe Loops.

Analyte	Stabilized ATW	Baseline Water	Freshly Filled Pipe Loop Tanks	Recirculated Water
Alkalinity, Total	1/W	1/W	1/W	1/W
Ammonia, Total	1/W	1/W	1/W	1/W
Calcium	1/W	1/W	1/W	1/W
Chlorine, Total	1/W	1/W	1/W	1/W
Conductivity	1/W	1/W	1/W	1/W
Nitrite	1/W	1/W	1/W	1/W
ORP	1/W	1/W	1/W	1/W
pH/Temperature	1/W	1/W	1/W	1/W
Turbidity	1/W	1/W	1/W	1/W

1/W – Once per week; ORP – Oxidation Reduction Potential

Table 2-8. Laboratory Testing for UCI Pipe Loops.

Analyte	Stabilized ATW	Baseline Water	Freshly Filled Pipe Loop Tanks	Recirculated Water
Iron – Dissolved and Total	1/M	1/W	1/W	1/W
Manganese – Dissolved and Total	1/M	1/W	1/W	1/W
Chloride	1/W	1/W	-	-
Sulfate	1/W	1/W	-	-
Total Organic Carbon (TOC)	1/M	1/M	-	-
Legionella pneumophilia	1/M	1/M	-	1/M
Nontuberculous Mycobacteria (NTM)	1/M	1/M	-	1/M

2.2.3 Stages of Distribution Piping Tests

The distribution piping evaluation progressed through four stages from conditioning to evaluating the impact of large changes in water quality.

- **Stage 1 – Conditioning.** The plumbing materials were operated with the baseline water chemistry for two months, based on findings from West Basin (Blute et al., 2014) and Carlsbad testing (Blute et al., 2008).
- **Stage 2 – Gradual Blending Compared with Baseline.** In this stage, two of the pipe loops were maintained at the baseline water chemistry while two received water that was gradually blended with ATW. The gradual blending progressed through a series of steps starting with 25% ATW and ending with 100% ATW over the course of three months.
- **Stage 3 –Gradual Blending Compared with Abrupt Transition.** In this stage, water in pipe loops for the first two stages was abruptly switched to ATW for one month. This stage overlapped with Stage 2 such that all of the pipes (abrupt transition and gradual blending) were brought to 100% ATW at the same time.
- **Stage 4 – Switch Back to Baseline Conditions.** In this stage, the pipe loops were all switched back to baseline water for two weeks to observe impacts of switching abruptly between water sources.

As previously noted, baseline water was used to condition the pipe materials and then ATW was introduced. Beginning in Stage 2, water from advanced treatment was introduced into the system. Pipe loop testing occurred on a schedule that allowed for the observance of differences in water quality outcomes between gradual and abrupt introduction of ATW to be investigated, as shown in Table 2-9. Two pipe loops were exposed to an abrupt introduction of ATW and the other two pipe loops were exposed to a gradual introduction of ATW. All pipe loops were first conditioned with 100% baseline water for a period of two months and the two “Abrupt Change” loops were exposed to 100% baseline water for an additional three months. After the two-month baseline water conditioning period, the two “Gradual Change” loops were exposed to a blend of 25% ATW for one month. The proportion of ATW used in the Gradual Change loops was increased by 25% each month until 100% ATW was achieved. When 100% ATW was introduced in the Gradual Change loops, 100% ATW was also introduced to the Abrupt Change loops and all four loops were exposed to 100% ATW for three months.

Table 2-9. Blending Schedule for Unlined Cast Iron Pipe Loops.

Start Date	Timeline	Unlined Cast Iron Pipes			
		Gradual	Duplicate – Gradual	Abrupt	Duplicate – Abrupt
3/17/2021	2 Months	Baseline	Baseline		
5/27/2021	1 Month	25% ATW	25% ATW		
6/23/2021	1 Month	50% ATW	50% ATW		
7/27/2021	1 Month	75% ATW	75% ATW	Baseline	Baseline
8/25/2021	3 Months	100% ATW	100% ATW	100% ATW	100% ATW
11/4/2021	1 Month	Baseline	Baseline	Baseline	Baseline

2.2.4 Pipe Scale Analysis

A 3-inch in length and 6-inches in diameter pipe section was cut and shipped to WUStL for the analysis (Figure 2-5). The pipe wall was 0.5-inches thick. The scale thickness was non-uniform and varied from 2.5 to 10 mm. The pipe scales were tuberculated in some regions and flatter in others as seen in the top view of the pipe in Figure 2-5. Scales were collected from the tuberculated region using a spatula, and these materials are referred to as outer scales. Scales underneath the tuberculated scales are referred to as inner scales that resembled the scales in the flatter regions of the inner pipe surface. The outer scales were dark red and the inner scales were brown-black. To prepare a cross-section of the scale for electron microscopy imaging, approximately half inch of the bottom of the pipe (as seen in Figure 2-5) was embedded in epoxy. A slice of the embedded pipe scales was cut out for further analysis. The outer scales were flaky and therefore did not maintain the structure when the pipe was cut for SEM-EDS analysis as seen in Figure 2-5.

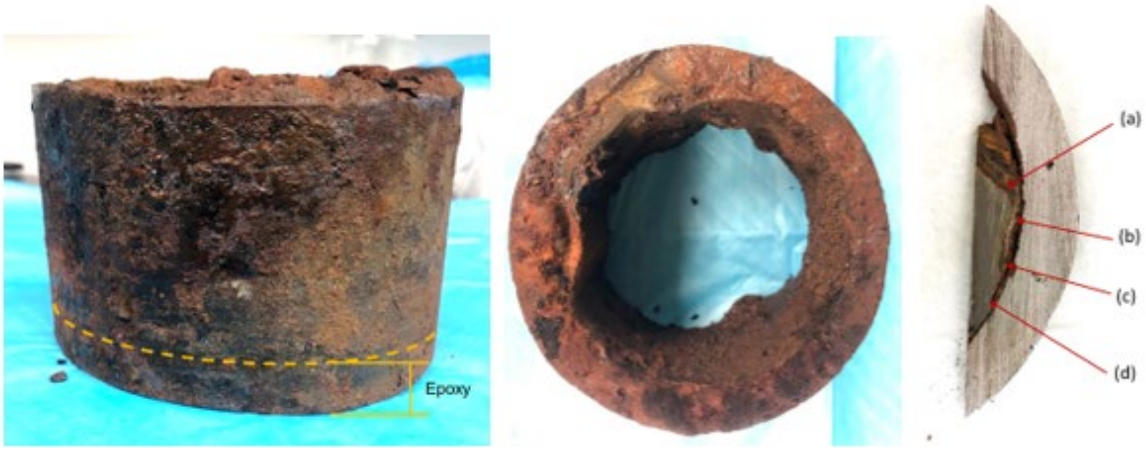

Figure 2-5. Images of (left) Side View of the As-Received Cast Iron Pipe with Dashed Line Indicating the Region Embedded in Epoxy, (middle) Top View of the As-Received Cast Iron Pipe, and (right) Part of a Cross-Section of the Cast Iron Pipe Embedded in Epoxy with Labels Indicating the Areas Analyzed by SEM.

2.3 Premise Plumbing Pipe Loop Testing

2.3.1 Pipe Loop Design and Operations

To represent lead-containing premise plumbing materials, two kinds of plumbing materials were selected (Figure 2-6). The first was 50:50 lead/tin solder, which was applied along the length of 1-foot of Type M copper pipe (0.65-inch inner diameter). A strip of lead/tin solder that

was 11.5” long with flux core weighing 88 g was melted along the length of the copper pipe at 300 °C by heating the pipe segment using heating tape wrapped around the exterior of the pipe.

Figure 2-6. Pipe Materials Used for the Premise Plumbing Study.
(Top) 1-foot copper pipe with cross-sectional view on the right. Lead solder was applied along the length of the pipe as seen through the cross-section; (Bottom) 1-foot C360 brass rods placed in a PVC pipe with the cross-sectional view on the right.

The second material was C360 brass that contained 3% lead by weight. The percentages of Cu, Fe, Pb, Zn are 61.5%, 0.35%, 3.0%, 35.5%. The brass was incorporated into the pipe loops using 1-foot-long brass rods (0.84-inch diameter) placed within 1-foot-long PVC pipes with 1.06-inch inner diameters. The dimensions of the brass rods and the copper pipes with Pb/Sn solder were selected such that the ratio of the metal surface area to the volume of water in the pipe loop is very similar for the brass rods (0.38 sq. inches/mL) and the copper pipes with Pb/Sn solder (0.49 sq. inches/mL).

Nine brass and nine copper pipes with lead solder assemblies (Figure 2-7) were tested in long-term pipe loop experiments. Each pipe loop setup (Figure 2-8) consisted of a 4-L water tank closed with respect to exchange with the atmosphere, clear PVC pipes and tubing, two two-way valves and one three-way valve, a flowmeter, a pump, and a timer.

Figure 2-7. Laboratory Setup with Nine Loops of Copper Pipes Containing Lead Solder (left) and Nine Loops of Brass Rods within PVC Pipes (right).

At the beginning of each week, each tank was filled with 4 L of water. The pipes were filled with water with the help of the pump. The water sat stagnant for 8 hours and then recirculated for 16 hours at a flowrate of 4.5 L/min. For lead and copper materials, stagnant conditions provide the most significant opportunity for leaching because a steady-state concentration is accumulated in the water. Cycles of water flow and stagnation are typical of corrosion studies for copper and lead release (AWWA, 1996). This daily pattern of 8 hours of stagnation and 16 hours of recirculating flow was repeated for the rest of the week. At the end of each week, the water in the pipe loop was replaced with new water. During each day of recirculation, the disinfectant was measured and readjusted, and the pH of the water was noted.

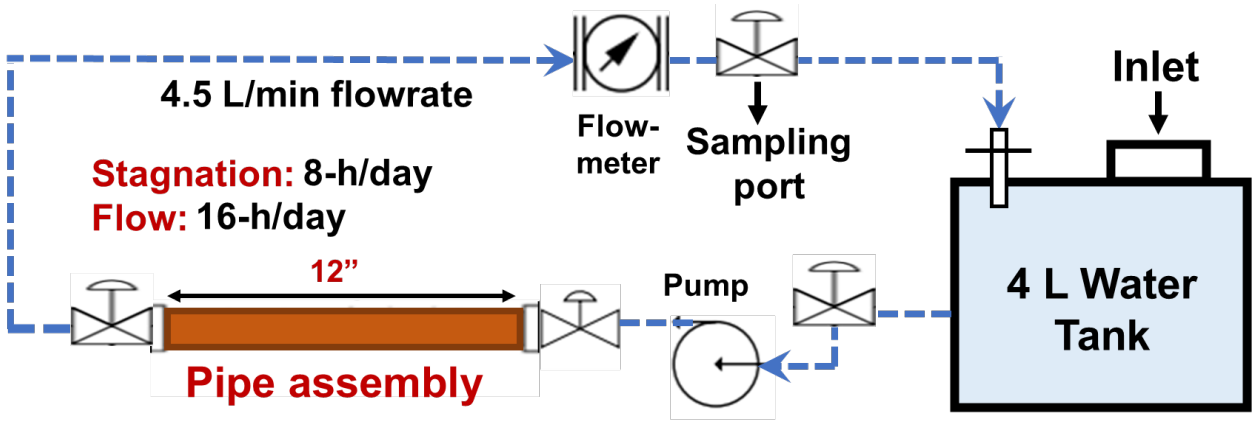

Figure 2-8. Recirculating Pipe Loop Setup.
Including a 1-ft pipe assembly connected to a 4-L water closed tank with clear PVC pipes and tubing, two two-way and one three-way valves, a flowmeter and a pump designed to stagnate water for 8 hours and then circulate water at 4.5 L/min for 16 hours each day.

The effect of gradual and abrupt blending of ATW was studied with recirculating pipe loops. To compare the gradual and abrupt blending with baseline water for each of the materials studied, three pipe loops were maintained as control pipes that received only baseline water through the entire duration of project, three pipes were conditioned to then receive ATW in increasing percentages (25%, 50%,75%, 100% ATW) referred to as “gradual ATW” and three were conditioned to then receive an abrupt switch in water source from baseline to 100% ATW referred to “abrupt ATW”.

2.3.2 Testing Approach and Analytical Methods

The water collected after the end of one week of recirculation was used for sampling metal concentrations. Water samples were collected for residual disinfectant, pH, major anion concentrations, alkalinity, and dissolved metal concentrations (Table 2-10 and Table 2-11). The remaining volume in the 4-L tank was then acidified to 1% nitric acid in preparation for analysis of total metal concentrations.

Table 2-10. Field Analytical Methods, including Sample Volumes and Minimum Detection Limit (MDL).

Analyte	Analytical Method/ Instrument	Sample Volume Required (mL)	Minimum Detection Limit
Alkalinity, Total	2320 B. Titration	100	5 mg/L as $CaCO_3$
Ammonia, Total	4500-NH3 F (Phenate method)	10	0.1 mg/L as N
Chlorine, Total	4500-Cl G (DPD Method)	10	0.1 mg/L
pH	Accumet pH meter and electrode	10	N/A

Table 2-11. Lab Analytical Methods, including Sample Volumes, Preservatives, Method Reporting Level (MRL), MDL, Holding Time, and MCL.

Analyte	Analytical Method	Sample Volume (mL)	Preservatives	MRL	MDL	Holding Time (days)	MCL	California SMCL (or Notification Level*)
Copper	EPA 200.8	10	HNO_3	0.1 µg/L	0.01 µg/L	180	1.3 mg/L^	1.0 mg/L
Zinc	EPA 200.8	10	HNO_3	0.1 µg/L	0.01 µg/L	185	N/A	5 mg/L
Lead	EPA 200.8	10	HNO_3	0.1 µg/L	0.01 µg/L	185	0.015 mg/L^	N/A
Iron	EPA 200.7	10	HNO_3#	1 µg/L	0.1 µg/L	180	N/A	0.3 mg/L
Manganese	EPA 200.8	10	HNO_3#	0.1 µg/L	0.01 µg/L	180	N/A	50 µg/L
Chloride	EPA 300.0	10	None	0.5 mg/L	0.10 mg/L	28	N/A	250 mg/L*
Sulfate	EPA 300.0	10	None	0.5 mg/L	0.10 mg/L	28	N/A	250 mg/L*
Nitrate	EPA 300.0	10	None	0.5 mg/L	0.10 mg/L	28	10 mg/L as N	N/A
TOC	SM 5310B	80	HCl#	0.10 mg/L	0.016 mg/L	28	N/A	N/A

"*" indicates the secondary MCL
"^" indicates the action level
"#" indicates that the samples were acidified after they were shipped to the laboratory from the distribution system.

2.3.3 Pipe Scale Analysis

Scale analysis involved the examination of cross sections and half cylinders of pipes (Figure 2-9). For the copper pipes, two shorter sections of pipe (2" in length) were cut from each 12" segment. A cross section was prepared by immersing a 2" section in a mixture of epoxy resin and hardener. Once the epoxy was cured, a disc (1 to 2 cm in thickness) was cut from the rest of the segment and then polished using sandpapers of increasingly fine grit (up to 1200 grit). The polishing was done with mineral oil on the sandpaper to minimize the generation of airborne particles. The polished sample was sonicated in ethanol for 5 minutes to removal residual mineral oil and pipe particles prior to analysis. For the brass rods, a short piece of 1 cm thickness was cut from one end of the brass rod. The cross-section was polished directly with sandpaper and mineral oil. No epoxy was used for preparing cross sections of the brass. The cross section was sonicated in ethanol similar to the copper pipes. The cross sections were analyzed using a Thermofisher Quattro S environmental scanning electron microscope (ESEM). Energy dispersive X-ray (EDX) spectroscopy with the SEM was used to semi-quantitatively determine the elemental composition of the pipe scales.

For copper pipes, solids were collected from the remaining section of the pipe (8” in length) that had been cut lengthwise into two half cylinders (Figure 2-9). For brass rods, solids were collected from the exterior surface of the midpoint of the length of the rod. A stainless-steel spatula or 1200 grit sandpaper was used to remove solids from the surfaces of the pipes and rods. Portions of the removed solid were powdered using a mortar and pestle and were analyzed by X-Ray powder diffraction (XRD) on a Bruker d8 Advance X-ray diffractometer with Cu Ka radiation. Another portion of the solids weighing about 0.05 g was digested in a 12 mL mixture of concentrated hydrochloric acid and concentrated nitric acid in a volumetric ratio of 3:1, respectively, and then analyzed for their elemental compositions using inductively coupled plasma mass spectrometry (ICP -MS).

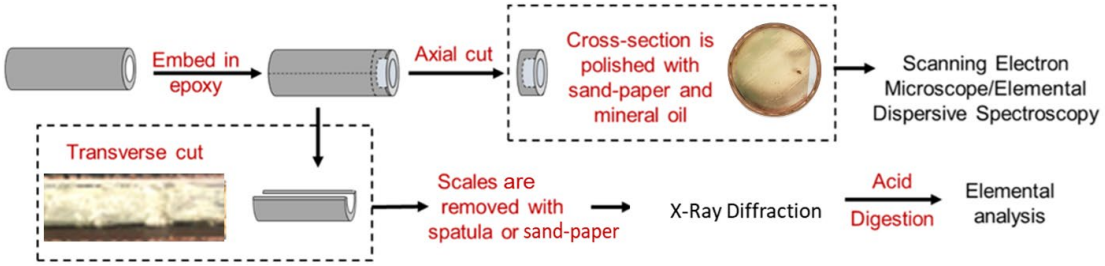

Figure 2-9. Scale Analysis Procedure for Copper Pipes with Lead Solder (top) and Brass Rods (bottom).

2.3.4 Advanced Treated Water Stabilization

The ATW shipped to WUStL was stabilized with calcite at Washington University. An in-lab flow-through reactor (Figure 2-10) was built for ATW stabilization. The starting pH of the ATW was 6.0 to 6.5. The water flowed through the calcite at rate of 200 mL/min for a contact time of 5 min. The water after passing through the calcite contactor flowed through a filter with pore size 10 µm for the removal of any suspended calcite particles leaving the contactor.

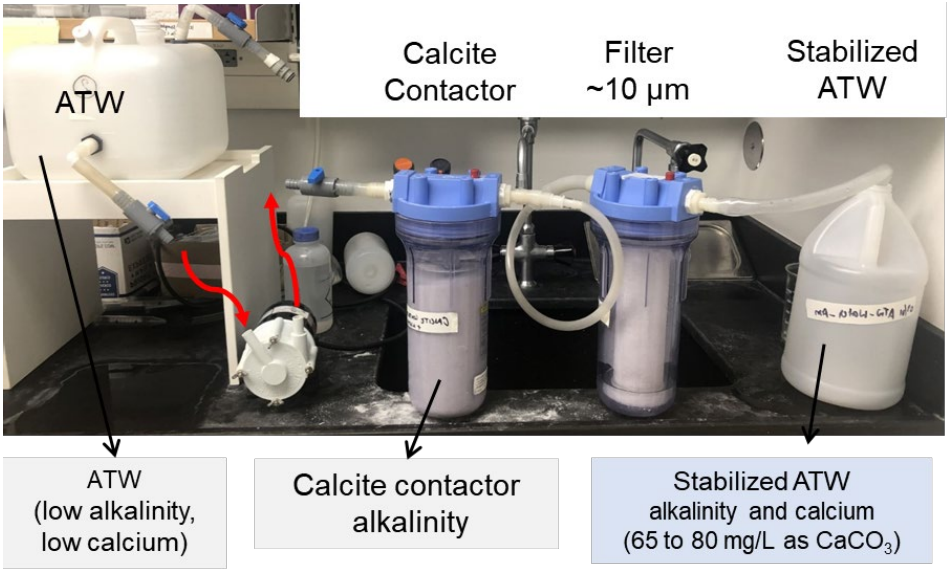

Figure 2-10. Calcite Contactor Setup for Calcite Stabilization of Advanced Treated Water.

2.3.5 Stages of Premise Piping Tests

Overall, the premise plumbing tests were conducted for 54 weeks including 22 weeks of conditioning (Stage 1) and test stages that were each 8 weeks long (Table 2-12). In the four test stages, ATW was gradually increased from 25 to 100% in steps of 25% for the pipes receiving gradual blending (C1-C3 and B1, B3, B5). The rest of the pipes continued to receive baseline water. During the last test stage, the water was switched to 100% ATW in both the set of pipes for which ATW was gradually introduced and for the set of pipes that were switched abruptly to 100% ATW, while the three control pipes continued to receive baseline water.

Table 2-12. Timeline for Premise Plumbing Pipe Loop Testing.

Timeline	Copper Pipes			Brass Rods		
	Gradual (C1 – C3)	Abrupt (C4 – C6)	Baseline (C7 – C9)	Gradual (B1, B3, B5)	Abrupt (B4, B6, B7)	Baseline (B2, B8, B9)
5 months	Baseline		Baseline	Baseline		Baseline
2 months	25% ATW		Baseline	25% ATW		Baseline
2 months	50% ATW		Baseline	50% ATW		Baseline
2 months	75% ATW	Baseline	Baseline	75% ATW	Baseline	Baseline
2 months	100% ATW stabilized	100% ATW stabilized	Baseline	100% ATW stabilized	100% ATW stabilized	Baseline
1 month	100% unstabilized	100% unstabilized	Baseline	100% unstabilized	100% unstabilized	Baseline
5 weeks	100% stabilized	Baseline	Baseline	100% stabilized	Baseline	Baseline
4 weeks	100% ATW unstabilized	100% ATW unstabilized	Baseline	100% ATW unstabilized	100% ATW unstabilized	Baseline
3 weeks	100% ATW stabilized	Baseline	Baseline	-	-	-

2.3.6 Additional Stages of Premise Piping Tests

After the completion of the four test stages, additional tests with the copper pipes continued for nine more weeks, and experiments with the brass rods continued for four more weeks. The purpose of this additional testing was to compare unstabilized ATW with stabilized ATW corrosivity. In this extended testing period, Pipes C1 – C6 were tested with unstabilized ATW for four weeks. After four weeks of exposure to unstabilized ATW, C1 – C3 were brought back to stabilized ATW and C4 – C6 were brought back to baseline water. Pipes C7 to C9 remained with baseline water throughout. For the brass rods, pipe loops B1, B3-B7 were tested with unstabilized ATW for four weeks while B2, B8, and B9 stayed at the baseline. The testing with brass was stopped after this four-week stage.

2.3.7 Equilibrium Solubility Estimation

Solubility calculations were performed in Visual MINTEQ 3.1. Calculation of lead and copper solubility was performed using information on pH, alkalinity, chloride, and sulfate. Dissolved inorganic carbon (DIC) was calculated from the pH and alkalinity. Ionic strength was set at 1 mM. The solid phase with the lowest solubility was used to calculate equilibrium lead and copper concentrations. Hydrocerussite ($Pb_3(CO_3)_2(OH)_2$) was used for estimating equilibrium solubility for lead. Brochantite ($Cu_4(SO_4)(OH)_6$) and cuprite (Cu_2O) were used for estimating copper solubility for baseline water, blended water (25%, 50%, 75%) and stabilized ATW (100%).

CHAPTER 3

Results

This section presents the results for the pipe loops for both the distribution system and the premise pipe loop system. Results reported include field data and laboratory data. Corrosion-related outcomes were assessed by observing water chemistry over time.

3.1 Distribution Systems Pipe Loops

Distribution pipe loops were labeled UCI-1, UCI-2, UCI-3, and UCI-4, with a classification of "F" for freshly filled and "R" for recirculated. Freshly filled corresponds to the initial time when the pipe loops were filled with water (after approximately 30 minutes of mixing). Recirculated water was collected after 6 days. ATW-3 represents the stabilized ATW in the results. Pipe loops were tested by gradual introduction of advanced treated water and abrupt introduction. As stated in Section 2.1 all pipe loops were conditioned first with baseline water. After baseline conditioning, two gradual change pipe loops were operated with an increasing proportion of ATW blended with baseline water until 100% ATW was achieved. Two "Abrupt Change" pipe loops were operated with 100% ATW, when 100% ATW was introduced to the gradual change pipe loops. Table 3-1 shows which pipe loops were used for gradual and abrupt change.

Table 3-1. Pipe Loop Treatment Classification for Abrupt vs. Gradual.

Distribution Pipe Loop	Water Change
UCI-1	Abrupt Change
UCI-2	Abrupt Change
UCI-3	Gradual Change
UCI-4	Gradual Change

3.1.1 Water Chemistry

For the distribution pipe, the baseline period was conducted from March 17 through May 27, 2021. Table 3-2 includes the water chemistry ranges and average during the baseline period and ATW period.

Table 3-2. Water Chemistry Ranges and Averages for Baseline Water and Advanced Treated Water.

Parameter	BLW Range	BLW Avg.	ATW Range	ATW Avg.
Alkalinity (mg/L as $CaCO_3$)	76 – 279	131	60 – 117	82
Calcium (mg/L as $CaCO_3$)	64 – 282	169	68 – 158	79
Chloride (mg/L)	77 – 105	82	5.7 – 13.7	9.9
Conductivity (µS/cm)	578 – 1012	880	163 – 663	250
ORP (mV)	280 – 406	346	278 – 409	357
pH	7.99– 8.4	8.12	7.63 – 8.37	8.10
Sulfate (mg/L)	102 – 238	178	0.1 – 0.42	0.31
Temperature (deg. C)	19.5 – 31.6	24.9	25 – 33.8	28.6
TOC (mg/L)	0.5 – 6.2	4.5	0.1 – 1.1	0.76
Total Chlorine (mg/L)	0.06 – 3.88	1.8	0.45 – 2.74	1.9
Total Ammonia (mg/L as N)	0.14 – 0.59	0.44	0.31 – 0.56	0.44
Nitrite (mg/L as N)	0 – 0.057	0.025	0.017 – 0.080	0.030
Turbidity (NTU)	0.16 – 0.39	0.27	0.31 – 23.6	6

3.1.1.1 Turbidity

Figures 3-1 and 3-2 show the differences between the turbidity in the baseline (BLW) and ATW over the course of the testing periods. During the conditioning period with baseline water in the pipe loops, the turbidity was on average 0.27 mg/L. Figure 3-1 displays the UCI loops for the recirculated water where the turbidity stabilized in the pipes after the two-month baseline conditioning period. At the onset of stabilized ATW introduction, ATW had a turbidity of 23.6 mg/L. Introducing 25% stabilized ATW into UCI-3 and UCI-4, resulted in an increase in the turbidity from an average of 0.94 mg/L to 3.18 mg/L for UCI-3 and 0.75 to 2.89 mg/L for UCI-4 after freshly filling the loops. After recirculating for a week, the turbidity decreased to an average of 0.81 mg/L (UCI-3) and 0.60 mg/L (UCI-4). The turbidity of the stabilized ATW in the pipe loops showed a trend of increasing turbidity when a greater amount of stabilized ATW was introduced into the system due to calcite fines; after recirculation, the turbidity decreased and stabilized in the pipe loops. At 100% ATW in the pipe loops, UCI-1 and UCI-2 were abruptly changed to stabilized ATW from 100% BLW. During this period, the turbidity in the water did not change and turbidity was stable across all pipe loops.

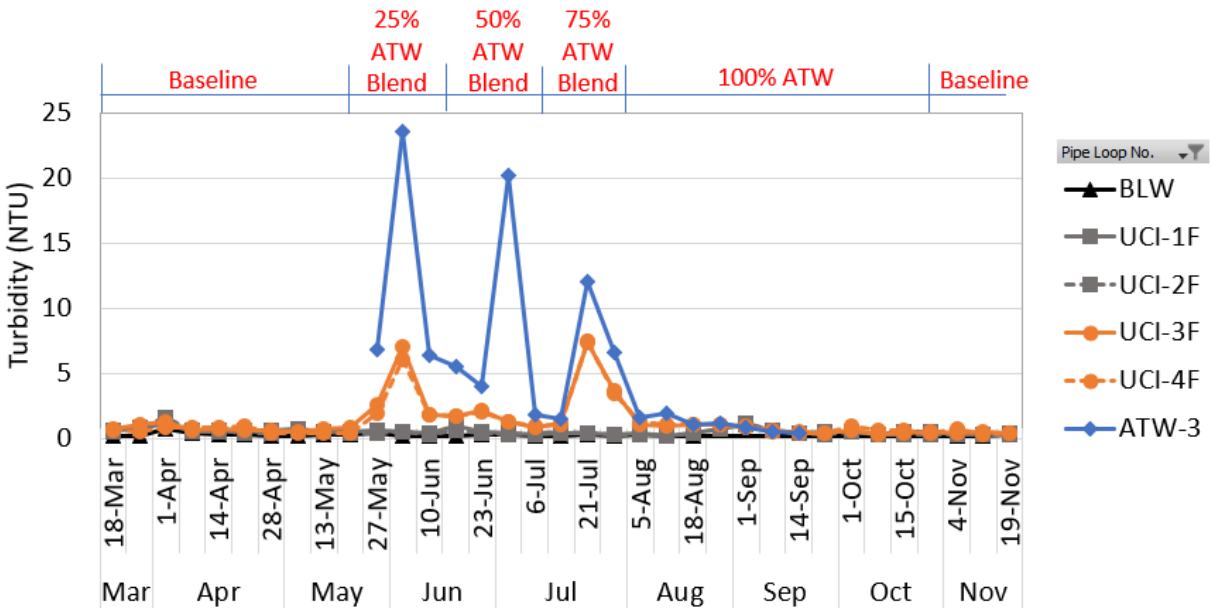

Figure 3-1. Weekly Turbidity Concentration in Freshly Filled UCI Pipe Loops, Baseline Water, and ATW.

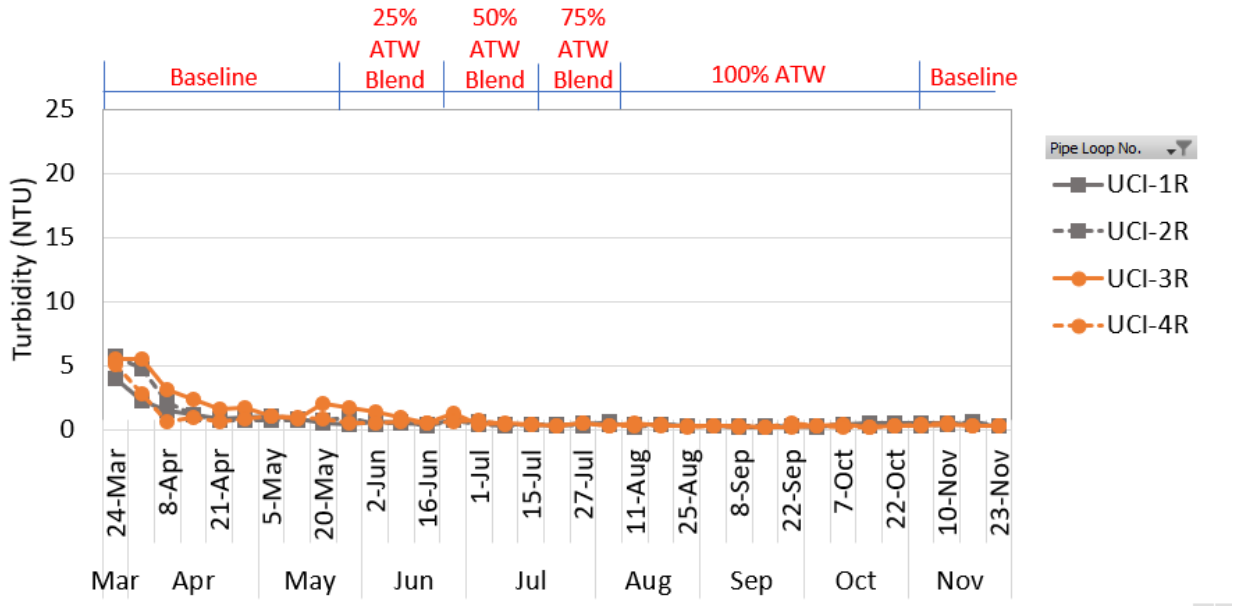

Figure 3-2. Weekly Turbidity Concentration in Recirculated UCI Pipe Loops.

3.1.2 Iron Impacts

3.1.2.1 Total Iron

Figures 3-3 and 3-4 show the differences between total iron in pipe loops over the course of the testing periods. Figure 3-4 displays the UCI loops for the recirculated water where total iron increased and then stabilized in the pipes after the two-month baseline conditioning period. The introduction of 25% ATW into UCI-3 and UCI-4 did not cause total iron to increase and the concentration remained relatively stable. After recirculating for a week, total iron decreased by roughly 50% in both UCI-3 and UCI-4. Total iron continued to decrease in UCI-3 and UCI-4 after the addition of 75% and 100% ATW. In Stage 3, UCI-1 and UCI-2 were abruptly changed to 100%

ATW from 100% BLW. During this period, the total iron in the water did not change and the total iron remained under the MCL of 300 µg/L. ATW had a lower concentration in total iron compared to BLW which explains the trend of the decreased iron in the pipe loops.

At the end of the testing (Stage 4), pipe loops were switched from 100% ATW to 100% BLW. An increase in iron was observed, which reflected the iron concentrations in the 100% BLW rather than iron released from the pipe loops.

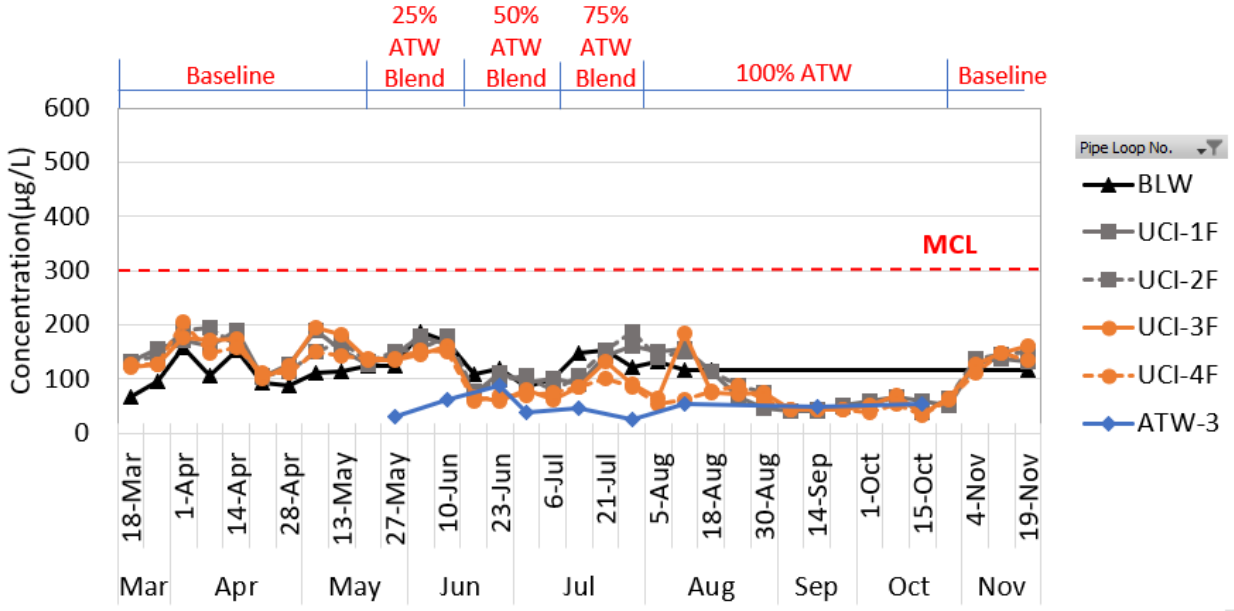

Figure 3-3. Weekly Total Iron Concentration in Freshly Filled UCI Pipe Loops, Baseline Water, and ATW.

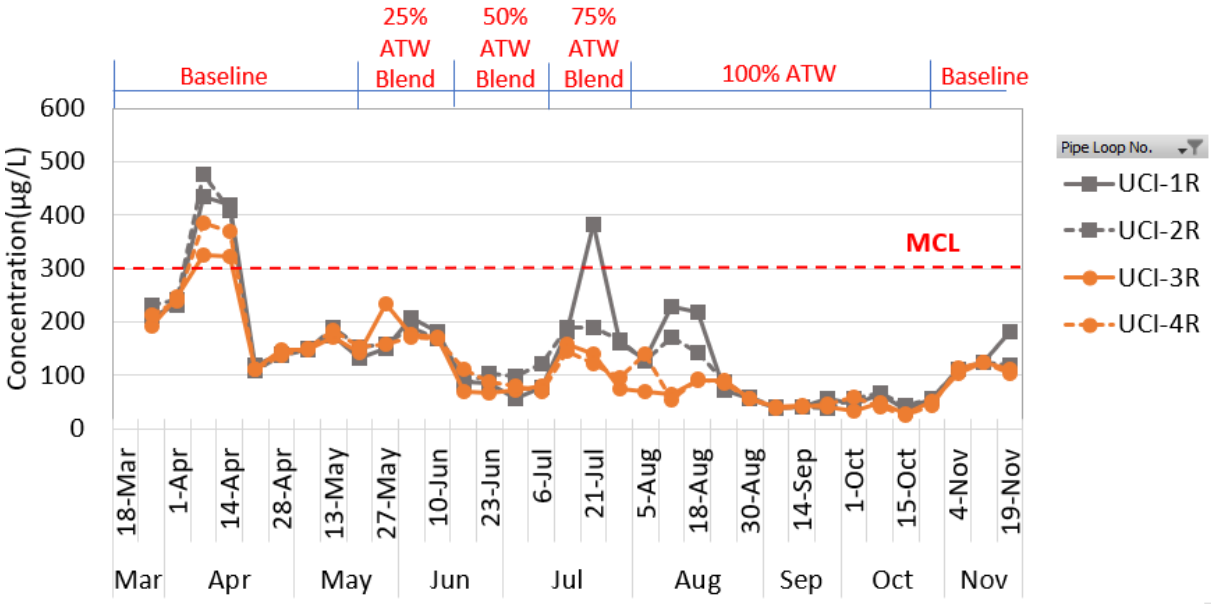

Figure 3-4. Weekly Total Iron Concentration in Recirculated UCI Pipe Loops.

3.1.2.2 Dissolved Iron

Figures 3-5 and 3-6 show the differences between dissolved iron in the pipe loops over the course of the testing periods. Dissolved iron stabilized in the UCI pipe after a month with baseline water, as shown in Figure 3-6. The introduction of ATW did not significantly impact concentration of dissolved iron in the UCI-3 and UCI-4 pipe loops compared with UCI-1 and UCI-2 pipe loops that continued to receive baseline water. Dissolved iron concentrations decreased in all pipes with the addition of 100% ATW. Similar to total iron, an increase in dissolved iron was observed at the end when 100% ATW was switched to 100% BLW, which reflected the iron concentrations in the 100% BLW rather than iron released from the pipe loops.

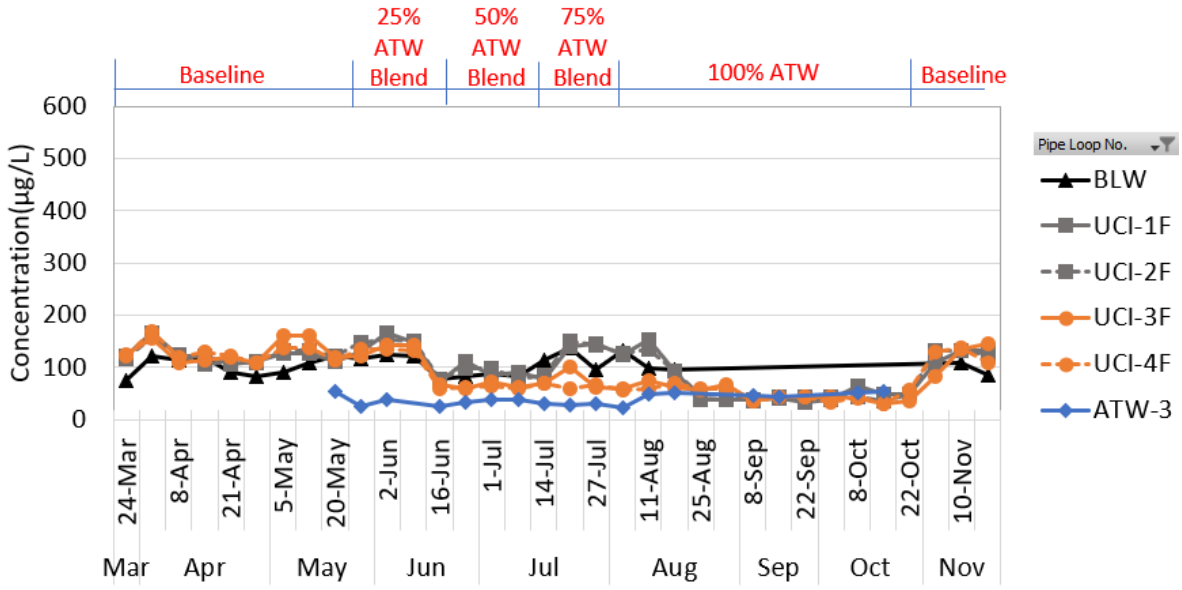

Figure 3-5. Weekly Dissolved Iron Concentration in Freshly Filled UCI Pipe Loops, Baseline Water, and ATW.

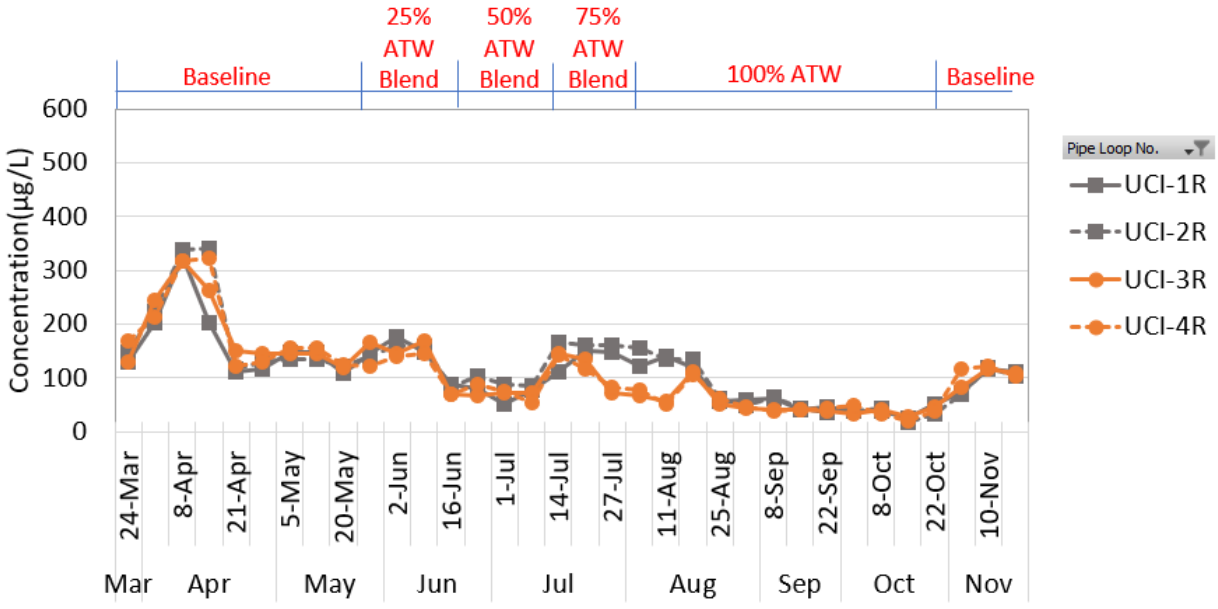

Figure 3-6. Weekly Dissolved Iron Concentration in Recirculated UCI Pipe Loops.

3.1.3 Manganese Impacts

3.1.3.1 Total Manganese

Figures 3-7 and 3-8 show the differences between total manganese in the pipe loops over the course of the testing periods. Total manganese decreased in the UCI pipe after a month with baseline water, as shown in Figure 3-8. This manganese release was from the UCI pipe loop and not from the source water. The introduction of 25% ATW caused a slight increase in manganese concentration in the UCI-3 after recirculation, but not the UCI-4 pipe loop. Similarly, a similar increasing trend observed in UCI-1 that continued to receive baseline water. As the blend percentage of ATW increased, total manganese concentrations decreased in all pipes. A return to baseline water following 100% ATW caused a slight increase in manganese concentration. Overall, manganese remained under the secondary maximum contaminant level (SMCL) of 50 µg/L.

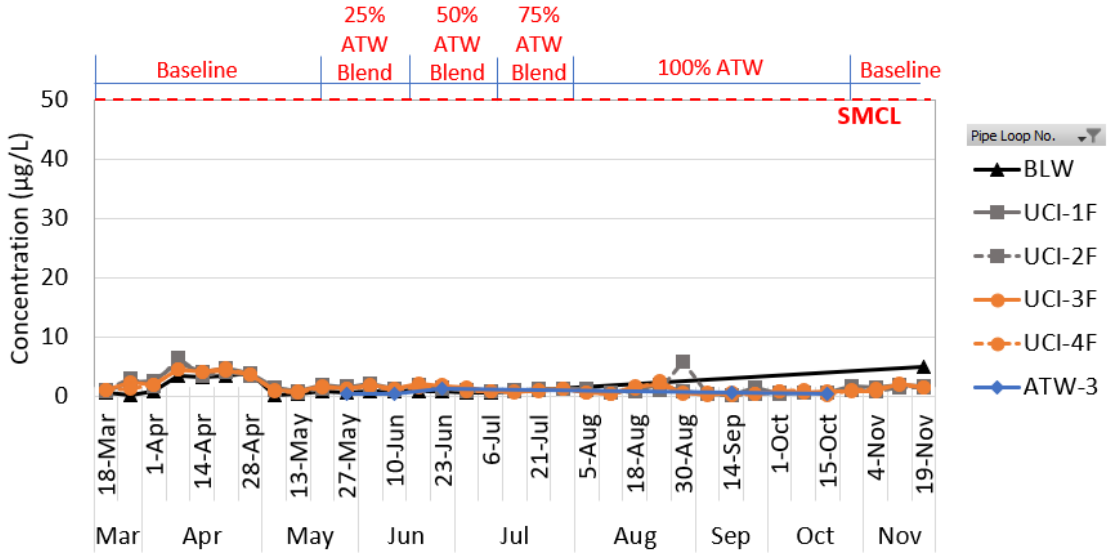

Figure 3-7. Weekly Total Manganese Concentration in Freshly Filled UCI Pipe Loops, Baseline Water, and ATW.

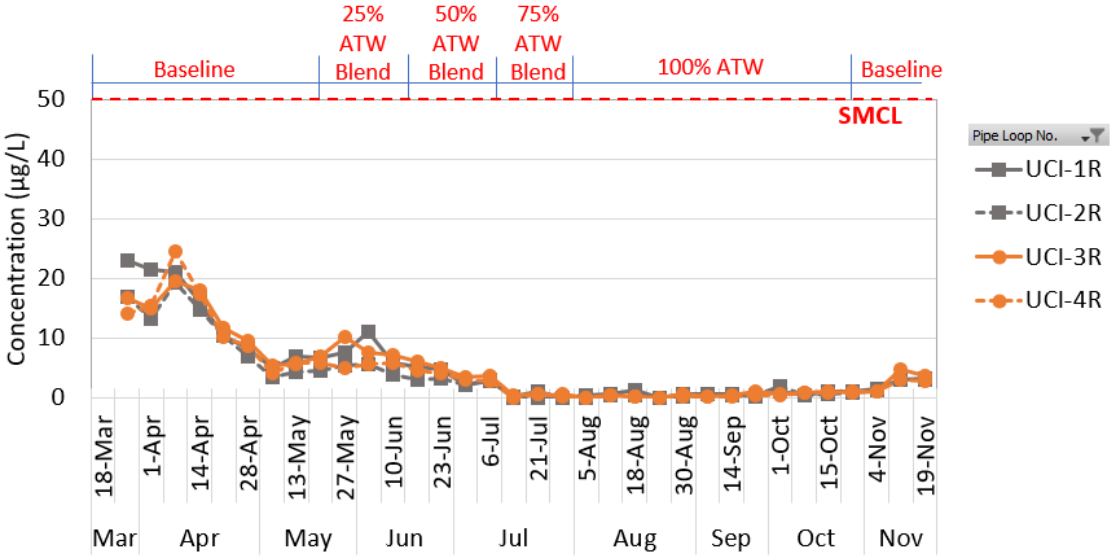

Figure 3-8. Weekly Total Manganese Concentration in Recirculated UCI Pipe Loops.

3.1.3.2 Dissolved Manganese

Figures 3-9 and 3-10 show the differences between dissolved manganese in the pipe loops over the course of the testing periods. Dissolved manganese stabilized in the UCI pipe after a month with baseline water, as shown in Figure 3-9. The increase in blend percentage ATW from 25% to 100% resulted in the decrease of dissolved manganese in all pipe loops. The return to baseline water after 100% ATW did not result in any increase in manganese concentrations.

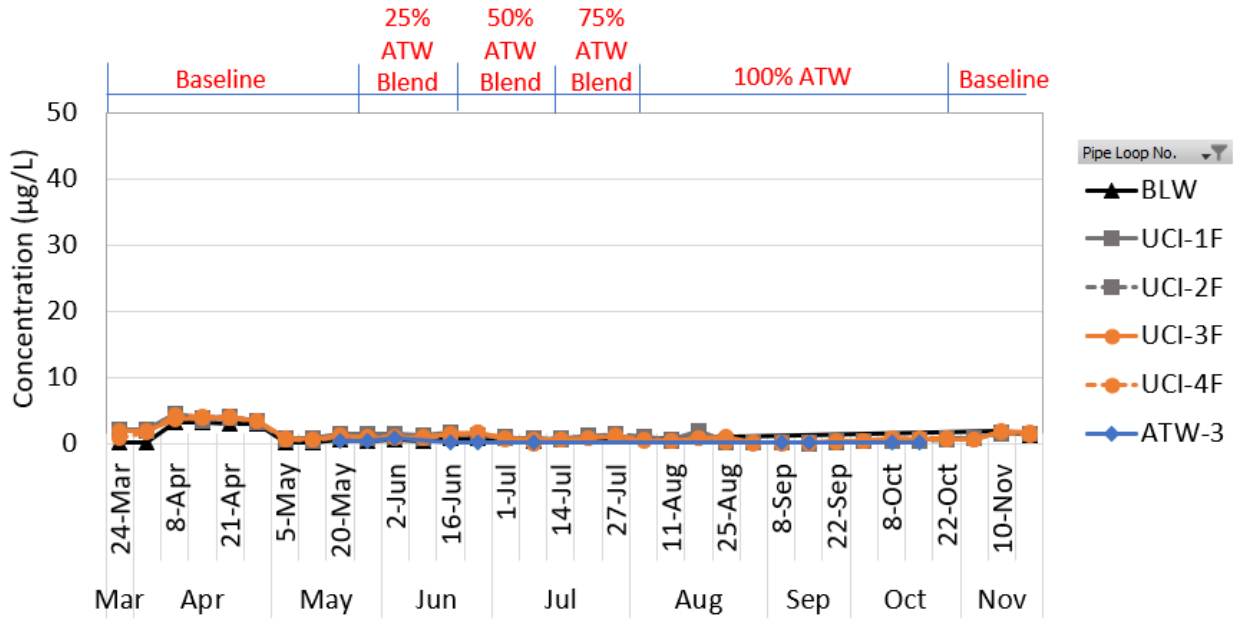

Figure 3-9. Weekly Dissolved Manganese Concentration in Freshly Filled UCI Pipe Loops, Baseline Water, and ATW.

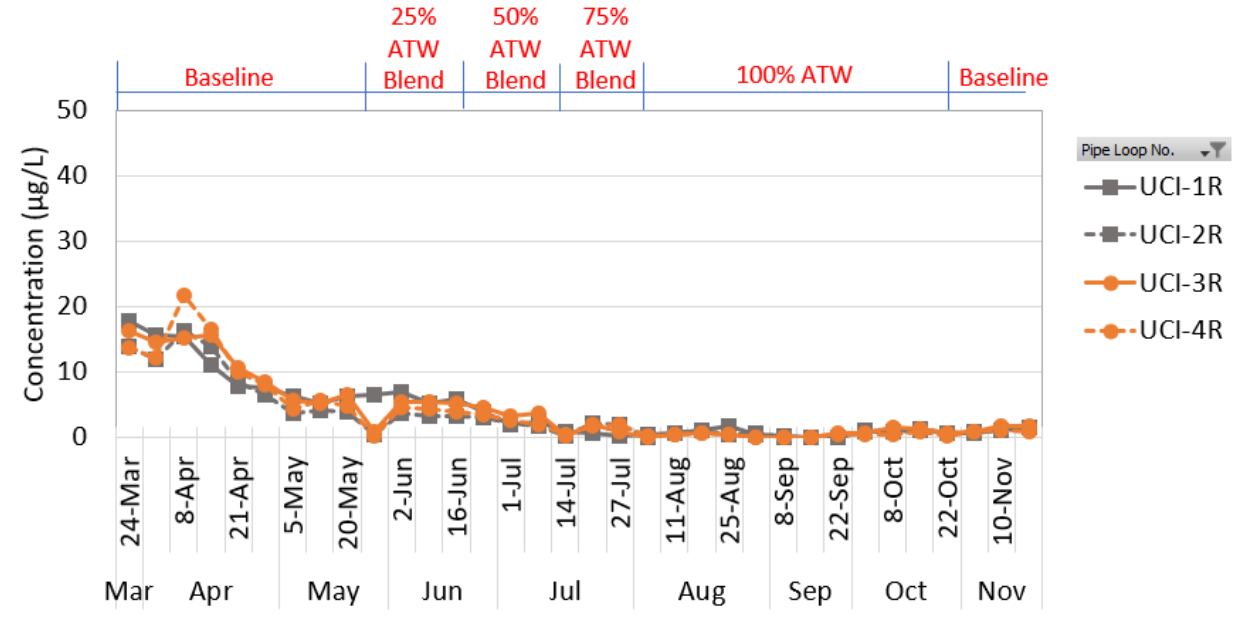

Figure 3-10. Weekly Dissolved Manganese Concentration in Recirculated UCI Pipe Loops.

3.1.4 Corrosion Indices

3.1.4.1 Factors that Impact Corrosivity

In addition to evaluation of corrosion indices, individual parameters such as alkalinity, chloride, sulfate, temperature, pH, calcium, and conductivity/TDS were used to evaluate corrosivity. Alkalinity and calcium were inversely proportional to each other in both ATW and baseline water. Figure 3-11 shows the correlation between alkalinity and calcium as well as pH for the baseline water.

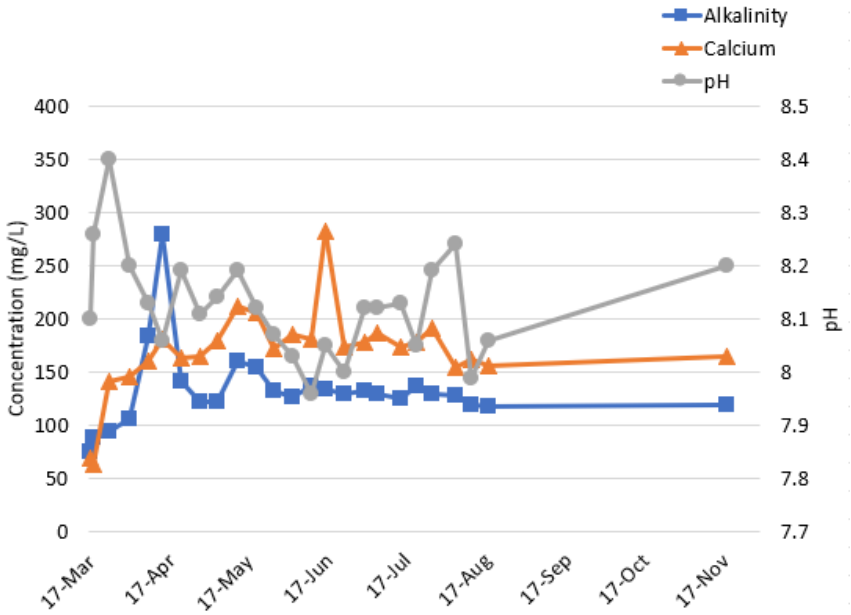

Figure 3-11. Alkalinity, Calcium, and pH Observed in Baseline Water.

The target concentration for alkalinity was 65-80 mg/L as $CaCO_3$ and greater than 65 mg/L as $CaCO_3$ for calcium. As shown in Figure 3-12, calcium remained in the target range until the last month in which calcium spiked to a 158 mg/L $CaCO_3$. During the same time period, alkalinity spiked to 117 mg/L as $CaCO_3$ before decreasing back to the target range. These two spikes could have been due to additional dissolution of calcite in the advanced treated water, due to increase in the amount of water being processed for stabilization.

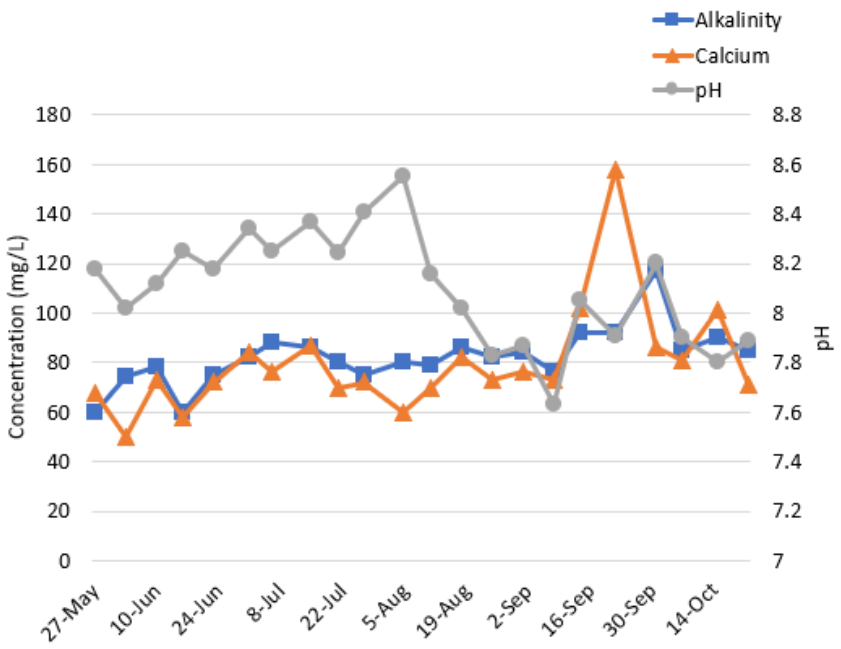

Figure 3-12. Alkalinity, Calcium, and pH Observed in Advanced Treated Water.

The pH of the baseline water on average was 8.12 and the pH for ATW was 8.09. The average pH in the pipe loops ranged from 8.12 to 8.15 over the period of testing. Figure 3-13 shows a visual representation of the pH in the pipe loops, and it is observed that for the freshly filled pipe loops the pH was steady during the testing period. Figure 3-14 shows the pH for the pipe loops after recirculating for one week. It was observed that the recirculated pipe loops had slightly higher pH averages than the freshly filled pipe loops. The pH average ranged from 8.21 to 8.26. There were no significant differences seen between the gradual blend of ATW and abrupt introduction of ATW.

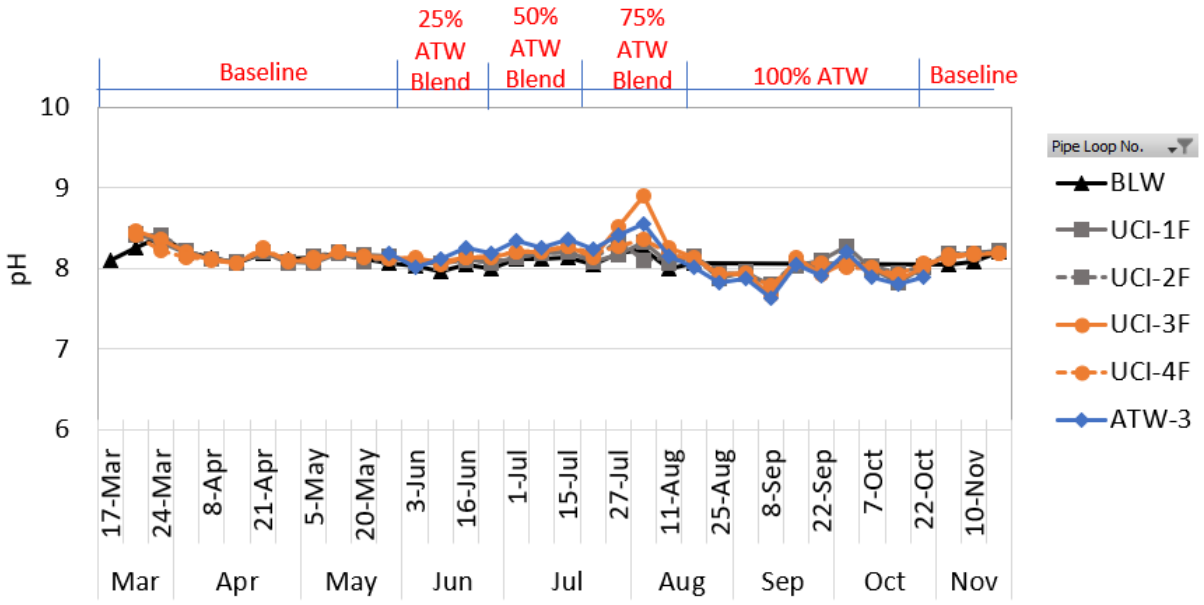

Figure 3-13. Weekly pH Measurements in Freshly Filled Pipe Loops, Baseline Water, and ATW.

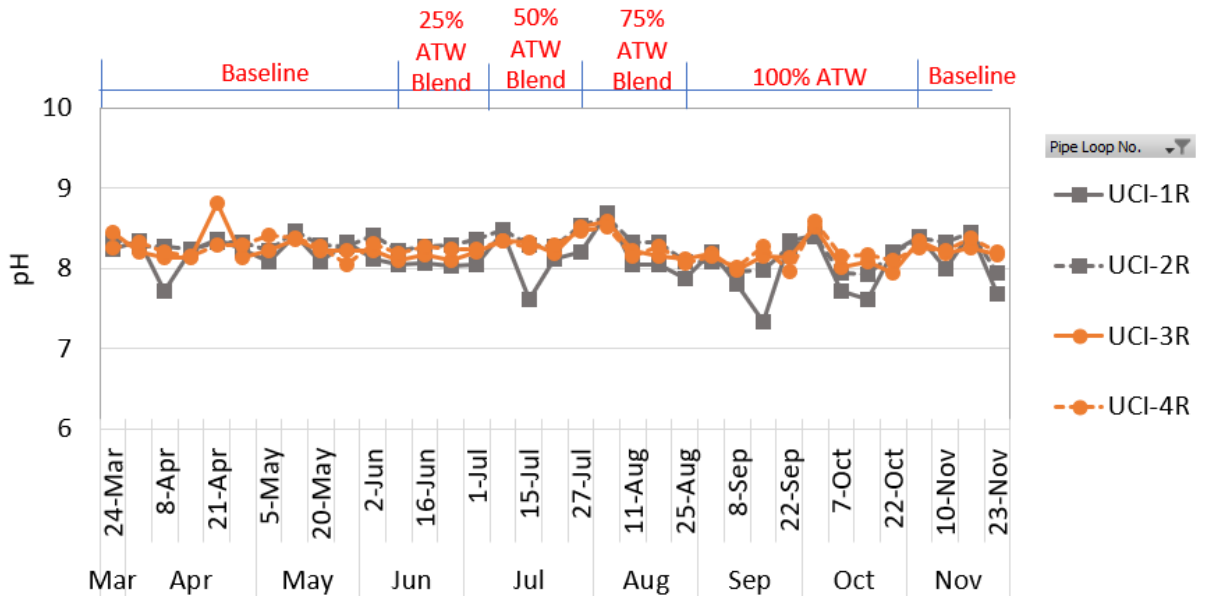

Figure 3-14. Weekly pH Measurements in Recirculated Pipe Loops.

Figures 3-15 and 3-16 illustrate conductivity for the freshly filled and recirculated pipe loops. Conductivity declined in the pipe loops over time as the ATW percentage increases in the pipe loops. The abrupt change from BLW to ATW in the pipe loops also shows a sudden decrease in conductivity. Similar conductivity trends were observed for both freshly filled water and recirculated water during the testing.

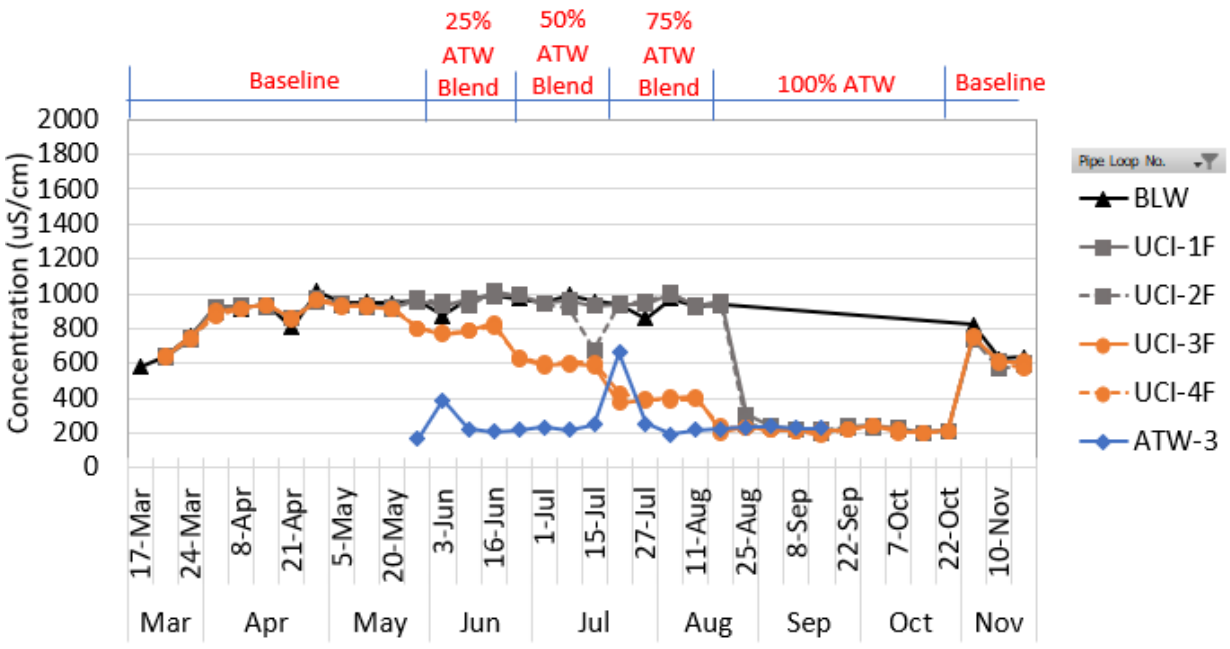

Figure 3-15. Weekly Conductivity Measurements in Freshly Filled Pipe Loops, Baseline Water, and ATW.

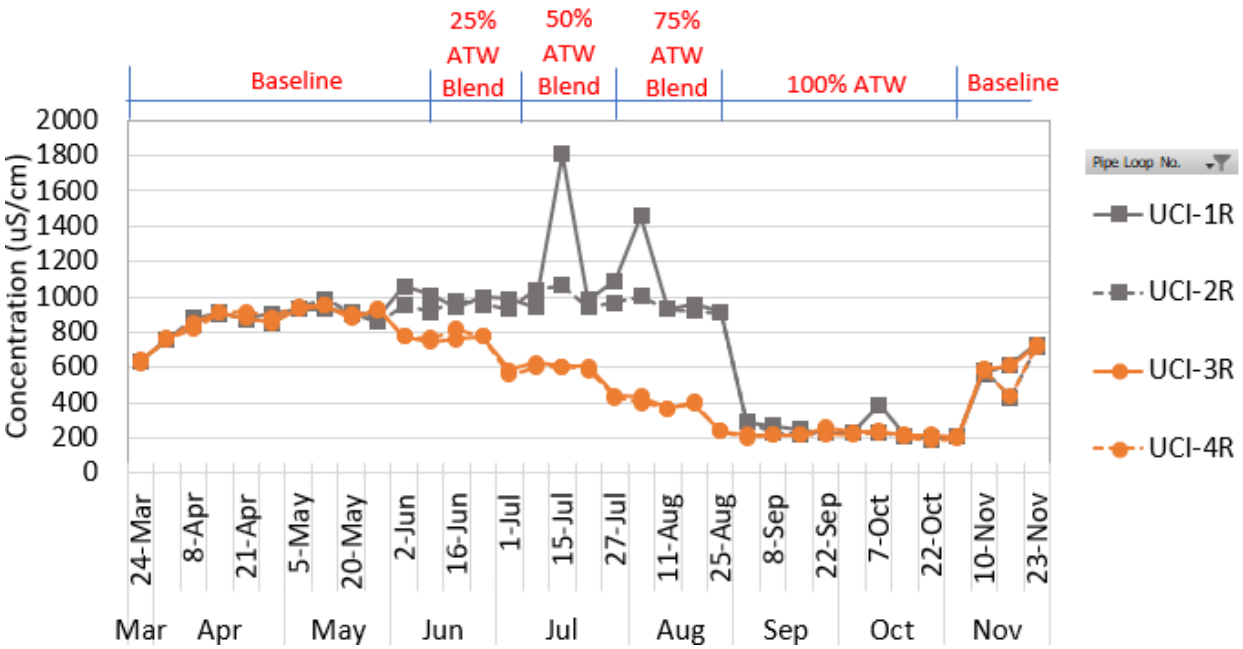

Figure 3-16. Weekly Conductivity Measurements in Recirculated Pipe Loops.

Figure 3-17 shows the variations in the chloride concentrations in the BLW and ATW. The chloride in the baseline water ranged between 72 and 108 mg/L. The stabilized ATW ranged from 6 to 14 mg/L chloride.

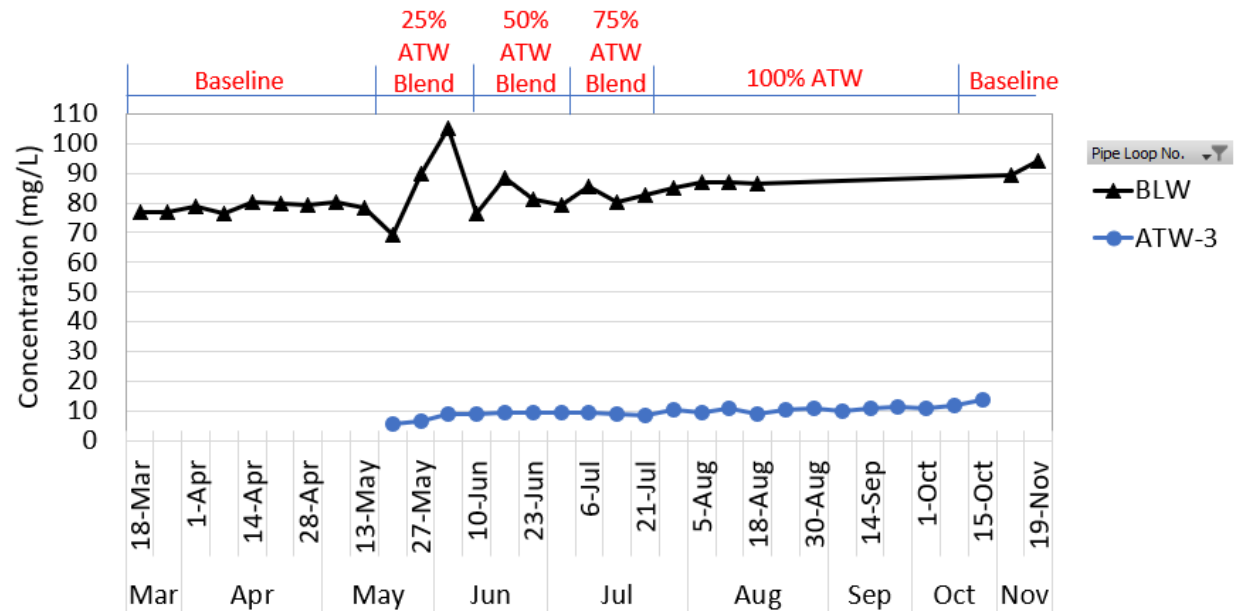

Figure 3-17. Weekly Chloride Measurements for Baseline Water and Advanced Treated Water.

Sulfate concentrations in the baseline water varied significantly from the start of the testing to the end. An increase in BLW sulfate was observed, ranging from 102 to 245 mg/L (Figure 3-18). The ATW sulfate concentrations ranged from 0.1 to 0.38 mg/L.

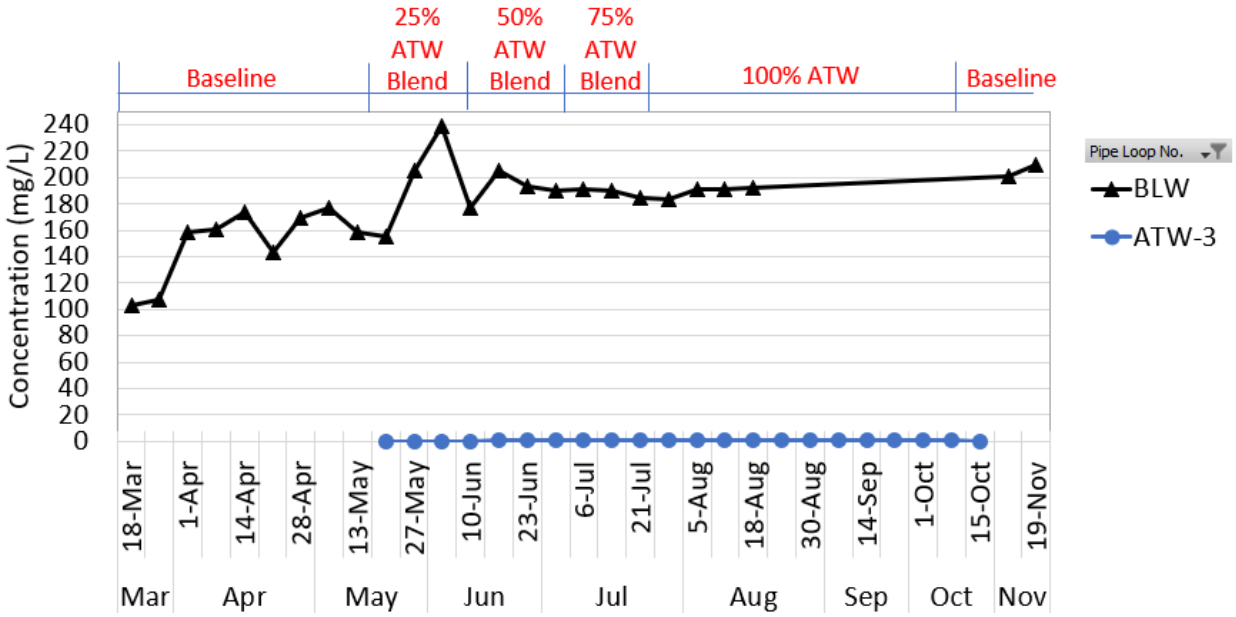

Figure 3-18. Weekly Sulfate Measurements for Baseline Water and Advanced Treated Water.

The magnitude of variation in chloride and sulfate has the potential to increase iron corrosivity/release, as observed by Lytle et al. (2020). The lack of significant iron release after the baseline conditioning period suggests that the relatively high DIC in the BLW mitigates this potential impact. Re-introduction of BLW after an extended period of ATW similarly did not see an increase in iron (that is, greater than the iron in the BLW introduced).

3.4.1.2 Calcium Carbonate Precipitation Potential, Langelier Saturation Index, and Larson Ratio

To further investigate the potential of corrosion potential in the pipe loops, the calcium carbonate precipitation potential (CCPP) and Langelier Saturation Index (LSI) were evaluated using the Tetra Tech Rothberg Tamburini and Windsor Model (RTW). EPA recommends a range of 4-10 mg/L for CCPP and an LSI that is greater than zero (US EPA 2004). A positive CCPP indicates that the water is oversaturated with respect to calcium carbonate and tends to precipitate $CaCO_3$ onto the pipes. A negative CCPP indicates that the water is under-saturated with respect to calcium carbonate, and the water may dissolve the $CaCO_3$ in the water. LSI calculates saturation with calcium carbonate as a function of pH, resulting in positive LSI corresponding to oversaturation and negative LSI corresponding to undersaturation.

The parameters used to calculate CCPP and LSI are alkalinity, calcium, pH, TDS, and temperature. Figures 3-19 and 3-20 show the CCPP and LSI for both BLW and ATW. The CCPP and LSI for the BLW and ATW were both positive and greater than zero. These findings indicate the waters used were non-corrosive conditions toward cement-mortar lined pipes and potential positive scale formation that could minimize other corrosion impacts.

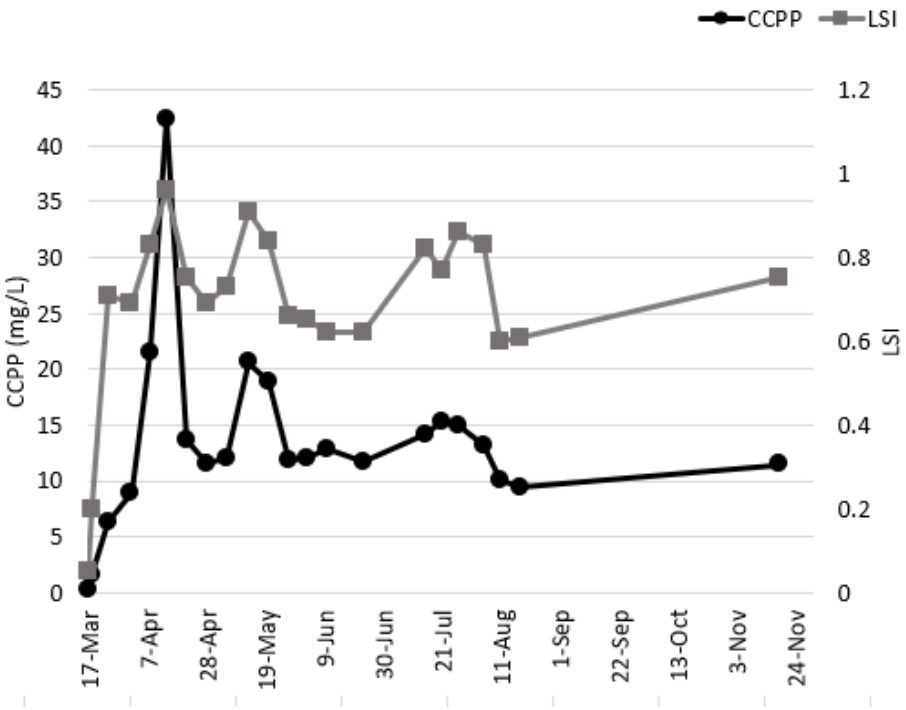

Figure 3-19. Baseline Water CCPP and LSI Comparison.

ATW achieved positive LSI and CCPPs using the calcite filters on the majority of days. ATW LSI and CCPPs were negative twice during the testing period. The first instance was during the initial introduction of ATW into the pipe loop systems and the second instance was during the 100% ATW period of testing. During the gradual introduction of ATW into the pipe loop system, both the CCPP and LSI gradually increased. Once 100% ATW was introduced into the pipe loops, the CCPP and LSI both trended downward. During this period, a decline in the pH of the water was observed while all other parameters were steady.

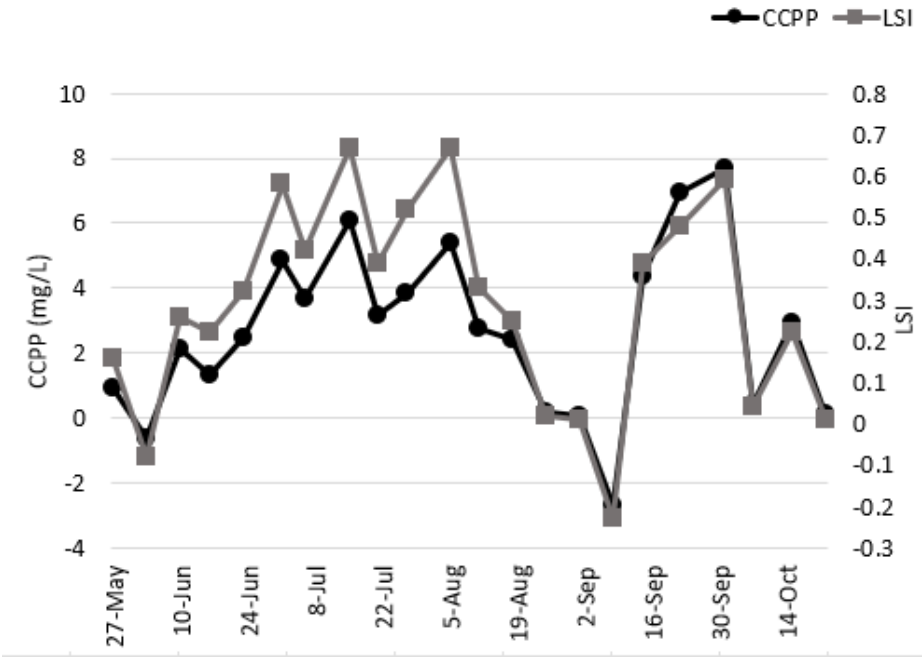

Figure 3-20. Advanced Treated Water CCPP and LSI Comparison.

The Larson Ratio (LR) describes the corrosivity of water towards low carbon steel and iron. It is the sum of the equivalents of chloride and sulfate divided by the equivalents of bicarbonate. In general, lower LR values are meant to indicate that the water is non-corrosive. Figure 3-21 shows the LRs for BLW and ATW during the testing period. LR data showed that BLW was higher than ATW, due to higher chloride and sulfate, despite a similar to higher alkalinity. As discussed in Section 1, absolute changes in chloride, sulfate, and alkalinity can impact corrosivity toward iron materials.

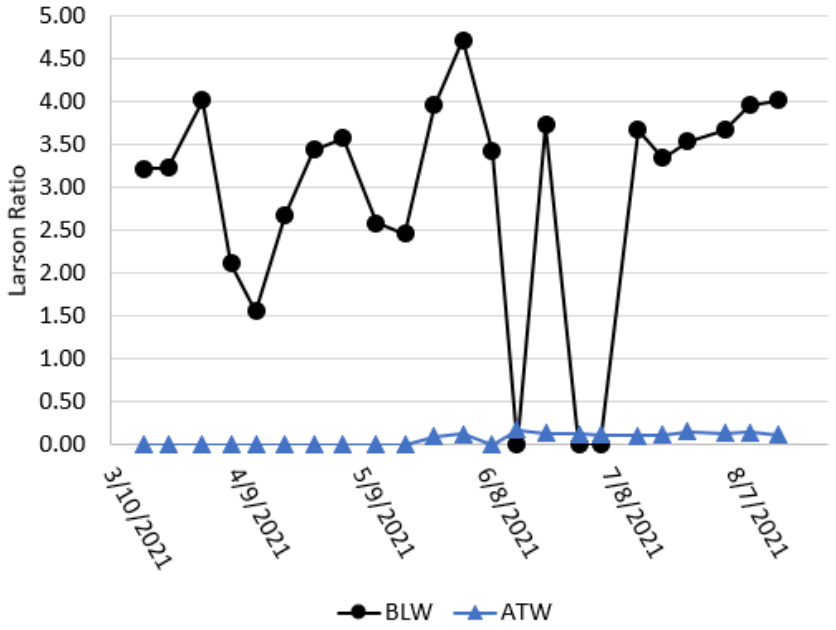

Figure 3-21. Larson Ratio Comparison of Baseline Water and Advanced Treated Water.

3.1.5 Total Organic Carbon

Total organic carbon (TOC) was measured biweekly in BLW and ATW. The concentration of TOC prior to testing was 1.7 to 2.6 mg/L for BLW. BLW TOC during testing ranged from 2.3 to 6.2 mg/L with an average of 3.7 mg/L. ATW TOC concentration ranged from 0.1 to 1.1 mg/L. Figure 3-22 shows the TOC comparison of baseline water to ATW.

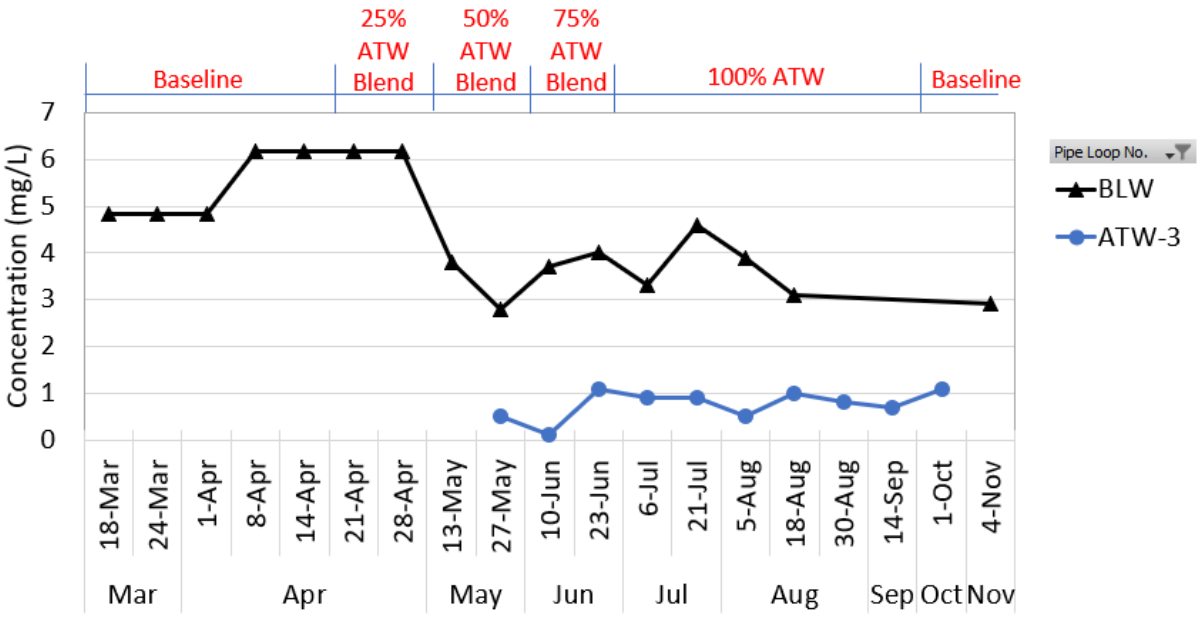

Figure 3-22. Biweekly TOC Concentrations in the Baseline Water and ATW.

3.1.6 Disinfection Dosing and Residual

Chlorine and ammonia were used for disinfection of the stabilized advanced treated water. The process of disinfection included adding 6% sodium hypochlorite solution into the stabilized ATW, mixing the water, confirming the dose, and then adding in ammonium chloride and mixing again. The target total chlorine residual concentration was 2.5 mg/L as Cl_2 and the total ammonia target concentration was 0.5 mg/L as N.

3.1.3.1 Chloramine Formation

Challenges were unexpectedly observed in the formation of chloramines in the stabilized ATW. After chlorine was added to stabilized ATW, residuals significantly dropped, requiring approximately 2.3 times the dose required in distilled water. Initial bench testing confirmed a rapid degradation of chlorine concentrations, ruling out causes from potential incomplete mixing. For the testing, a strategy to add 2.3 times the dose and hold the chlorinated water overnight was instituted, resulting in a more stable water quality for the addition of ammonia to form chloramines. The cause of this higher demand in ATW (which has little TOC and other constituents due to reverse osmosis) was unknown, prompting additional study (Section 5).

3.1.3.2 Residuals in Pipe Loops

Figure 3-23 shows the residual total chlorine in the freshly filled pipe loops, baseline water, and ATW. The chlorine residual in the baseline water on average was 1.77 mg/L. During the conditioning period, the chlorine residual in the pipe loops was 1.52 mg/L across all loops. As ATW was introduced into the pipe loops, an increase in chlorine demand occurred across the

blends. At 100% ATW, the total chlorine residual dropped significantly in all pipe loops that were freshly filled with ATW. It was observed that the chlorine residual decreased on average of 1 mg/L through the first month of 100% ATW testing.

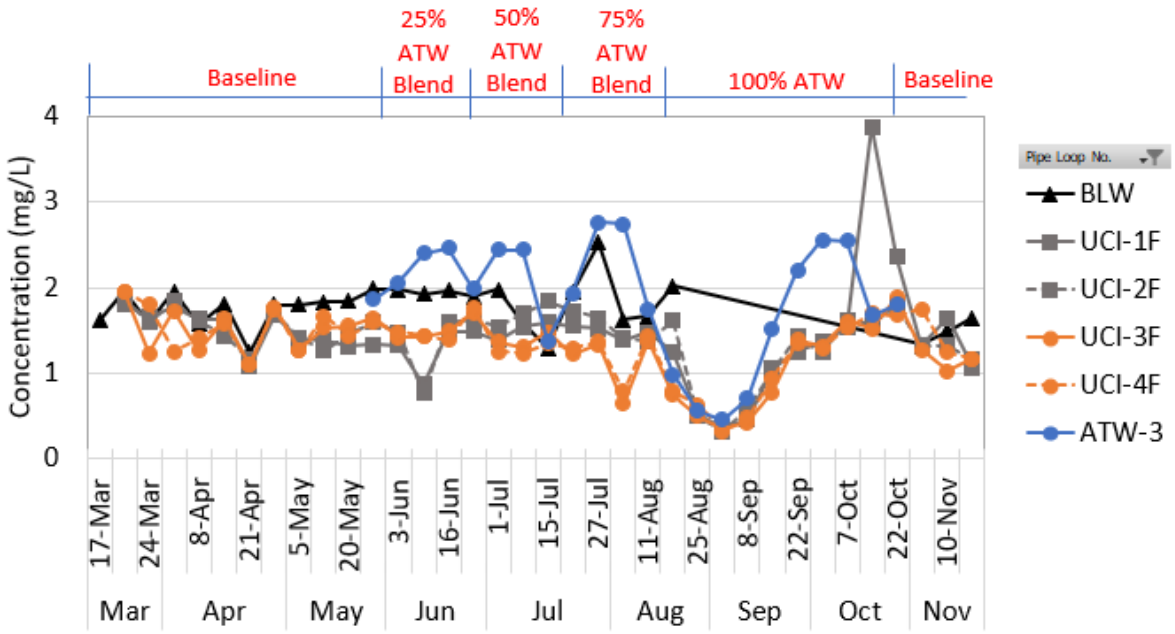

Figure 3-23. Weekly Total Chlorine Measurements in Freshly Filled Pipe Loops, Baseline Water, and ATW.

Figure 3-24 shows the total chlorine residual after one week of recirculation in the pipe loops. Similar chlorine residuals were observed for all four pipe loops. The average residual was 0.15 mg/L after recirculating for 6 days, which indicated chlorine demand in the iron pipes. Chloramine boosting was not part of this study but should be considered as part of an ATW introduction strategy if found to be necessary.

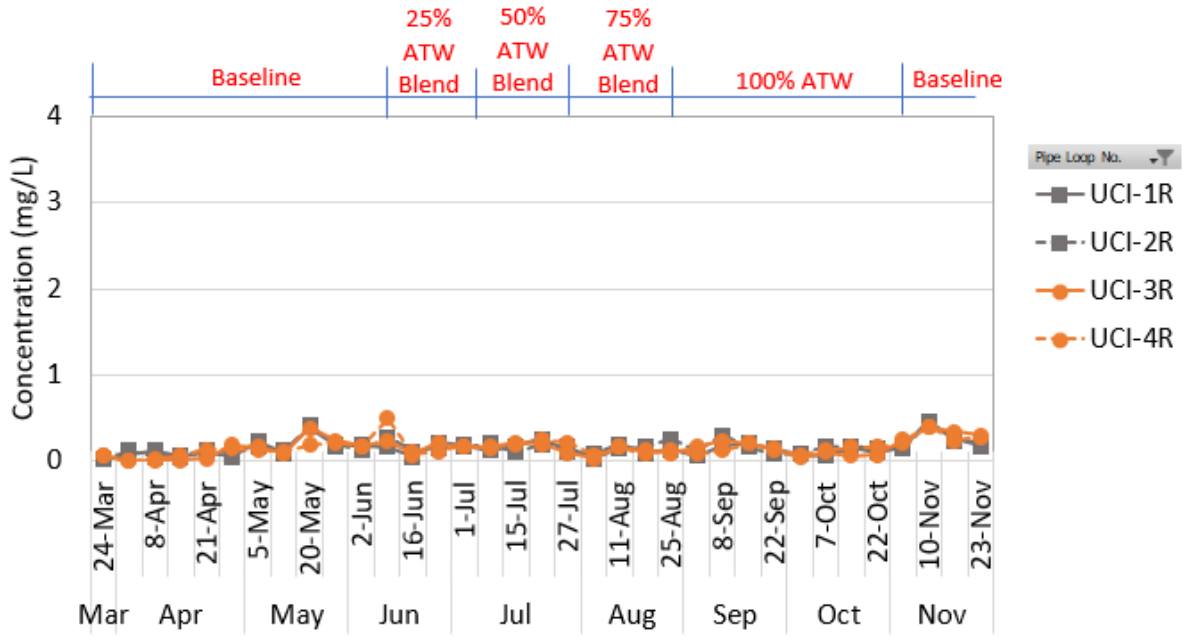

Figure 3-24. Weekly Total Chlorine Measurements in Recirculated Pipe Loops, Baseline Water, and ATW.

3.1.7 Microbiological Results

Table 3-3 shows the results for *Legionella* in the water sources and after recirculation in the pipe loops. Baseline water was not found to have detectable *Legionella*, whereas stabilized ATW had elevated concentrations on three sampling occasions. In the initial testing with 100% BLW, *Legionella* was not present in the water or pipe loops. As stabilized ATW was introduced into UCI-4R, *Legionella* was found to be present. While *Legionella* was present in UCI-4R for 25% and 100% ATW, it was not found to be present in UCI-3R, which were duplicates of each other. *Legionella* was not detected in UCI-1R until the 100% stabilized ATW water source was introduced. UCI-2R had three dates of elevated *Legionella* when 100% stabilized ATW was introduced to the pipe loops.

Table 3-3. *Legionella* Tests Results.

		4/28/21	6/10/21	8/11/21	9/8/21	10/7/21	11/4/21
Sample	**Units**	**100% BLW**	**25% ATW**	**75% ATW**	**100% ATW**	**100% ATW**	**100% ATW**
BLW	MPN/mL	ND	ND	ND	—	—	—
ATW-3	MPN/mL	—	ND	2,487	2,580	6,801	—
UCI-1R	MPN/mL	ND	ND	ND	ND	ND	84
UCI-2R	MPN/mL	ND	ND	ND	ND	3,501	7,855
UCI-3R	MPN/mL	ND	ND	ND	ND	ND	ND
UCI-4R	MPN/mL	ND	854	ND	ND	58	ND

"—" = not tested, ND = non-detect, MRL = 10 MPN/100 mL

Table 3-4 shows the test results for NTM in the pipe loops, BLW water, and ATW. NTM was non-detect or was found in low quantities in both BLW and ATW, with values of either non-detect or less than 1 with a method reporting limit (MRL) of 0.2 CFU/mL. In the first month of testing, during 100% BLW, NTM was found in three loops. The NTM significantly decreased during the introduction of 25% stabilized ATW and but was present in all four pipe loops. For pipe loop UCI-3R, the NTM increased every month before decreasing to non-detect at the end of the testing with 100% ATW. More testing is needed in order to draw a clear conclusion on the results from the NTM testing.

Table 3-4. NTM Test Results.

		4/28/21	6/10/21	8/11/21	9/8/21	10/7/21	11/4/21
Sample	**Units**	**100% BLW**	**25% ATW**	**75% ATW**	**100% ATW**	**100% ATW**	**100% ATW**
BLW	CFU/mL	ND	<1	ND	—	—	—
ATW-3	CFU/mL	—	ND	ND	<1	ND	—
UCI1R	CFU/mL	ND	6	<1	<1	ND	ND
UCI2R	CFU/mL	60	1	100	<1	ND	ND
UCI3R	CFU/mL	<1	2	ND	20	80	ND
UCI4R	CFU/mL	400	<1	12	<1	1	ND

"—" = not tested, ND = non-detect, MRL = 0.2 CFU/mL

Although *Legionella* and NTM both appeared in the pipe loops, no clear correlations in OPPP growth could be identified. Further investigation would be necessary and may be warranted particularly due to the elevated *Legionella* observed in ATW.

3.1.8 Scale Analysis

The entire length of the scale cut out from the pipe was analyzed using SEM and with images at four points shown Figure 3-25.

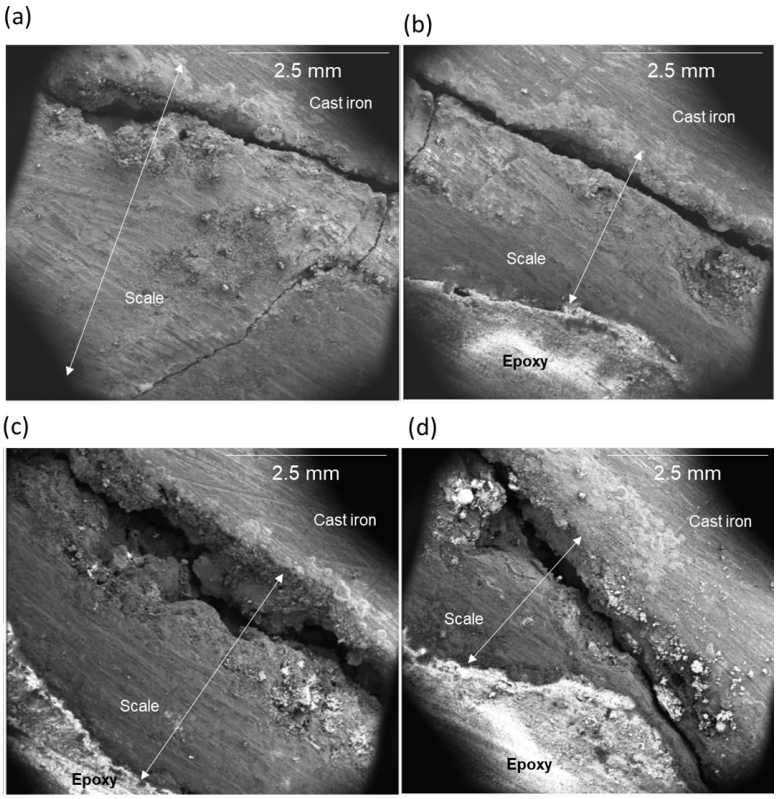

Figure 3-25. SEM Images of the Slice of Cast Iron Pipe and the Scale Embedded in Epoxy.
The Entire Slice of the Pipe was Viewed In 4 Parts – Panels A, B, C, and D Follow the Scale from One End to Another.

The EDS mapping of an area of the cross-section indicated presence of Fe, O, Ca, C and Si (Figure 3-26). The EDS map also shows a localized layer of carbon next to the cast iron pipe which is considered as the inner layer and a localized layer of calcium and silicon in the outer layer. Elemental analysis from ICP-MS indicated the presence of Fe and Ca in abundance. No other metal was detected above detection limit of 5 mg/g of scale (Table 3-5). The digestion approach used for elemental analysis would not fully dissolve Si, so no quantitative information for the Si content of the scale is reported. The thickness of the inner layer varied from 0.7 to 1.3 mm while the outer layer thickness ranged from 1 to 15 mm.

Both the inner and the outer scale were composed of magnetite (Fe_3O_4), goethite (α-$Fe^{3+}O(OH)$) and magnesium-containing calcite (Figure 3-26, Table 3-6). The inner layer also consisted of siderite ($FeCO_3$). The outer layer is rich in both calcium and silicon; however, no Si-containing minerals could be identified by XRD. One peak in the inner layer also remained unidentified. The peak seen at 12° in the XRD pattern of inner layer has been previously seen for green rust consisting of chloride or sulfate.[1-3] Green rusts are mixed Fe(II)/Fe(III) solids that can form in anoxic corrosion contexts. The exact mineral composition of green rust could not be identified and is therefore not added to the XRD patterns (Figure 3-27).

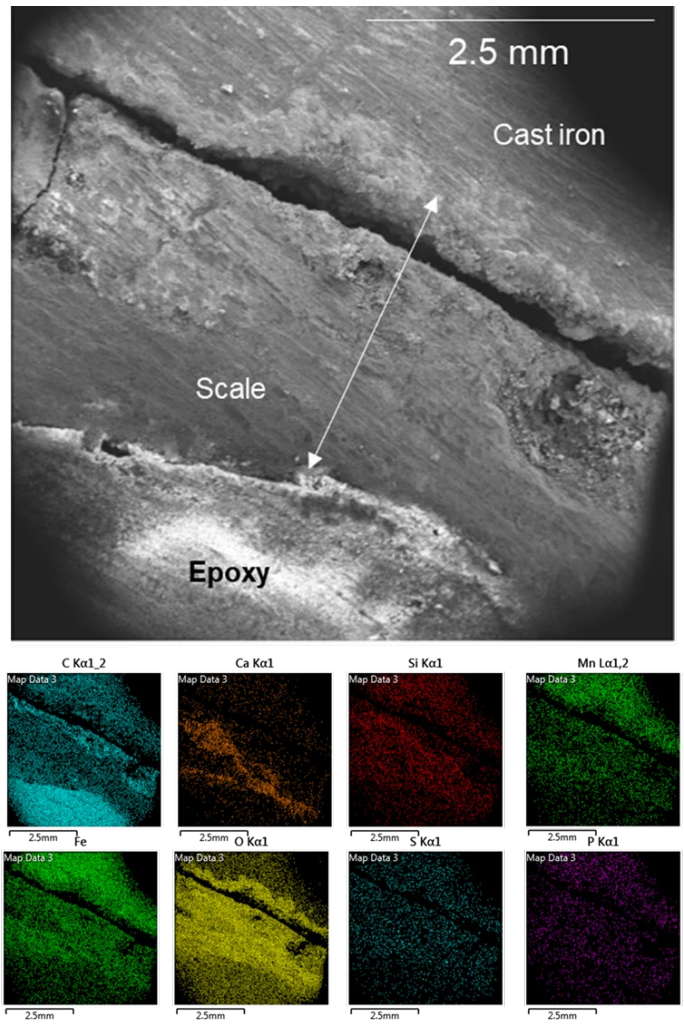

Figure 3-26. XRD Patterns of Cast Iron Pipe.
Each Set of Images includes the Original SEM Image (Top), and EDS Maps (Bottom) of Different Elements in the Selected Area of EDS.

Table 3-5. Solids Present on the Cast Iron Pipe Surface.

	Iron	Magnetite	Goethite	Siderite	Magnesium Containing Calcite
Inner	+	+	+	+	++
Outer		+	+		++

+++ indicates the relative intensity of the solids in the pipe surface

Table 3-6. Elemental Composition Reported In mg/g of Scales Collected from the Cast Iron Pipe.

	Ca (mg/g)	Fe (mg/g)
Inner	208	358
Outer	464	278

Detection limit: 5 mg/g for 0.1 g of solid digested (for all elements except Ca and Fe)
Detection limit: 25 mg/g for 0.1 g of solid digested (for Ca and Fe)
Silicon, carbon, hydrogen, and oxygen are not accounted for in the elemental analysis.

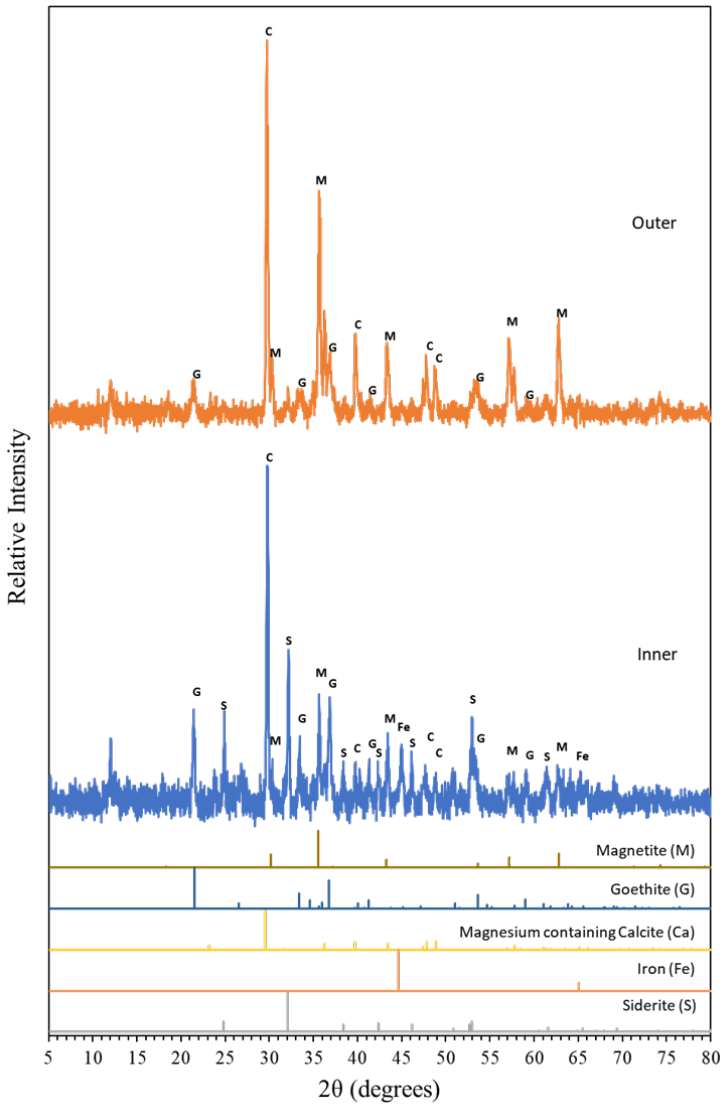

Figure 3-27. XRD Pattern of Scales Collected from the Cast Iron Pipe Surface.
Reference Peaks from Magnetite (Fe3O4 ICDD 04-013-2098), Goethite (A-Fe3+O(OH) ICDD 01-073-0513), Magnesium Containing Calcite (ICDD 04-008-8067), Iron (ICDD 00-006-0696) and Siderite (FeCO3 ICDD 04-023-8814) from the RRUFF Database.

3.2 Premise Plumbing Pipe Loops

3.2.1 Water Chemistry

Shipments of water (Figure 3-28) received were stored in a controlled-temperature room at 4 ℃. The water quality for the baseline water and the blended water containing 25%, 50%, 75% and 100% ATW are noted in Table 3-7.

Figure 3-28. Barrel Shipment to Washington University.

Table 3-7. Water Chemistry of Baseline Water, As-Received ATW, and Blended Water with 25%, 50%, and 75% of Stabilized ATW.

		Baseline	Unstabilized ATW	Stabilized ATW	Blend 25%	Blend 50%	Blend 75%
pH	-	7.9 – 8.1	5.9 – 6.1	7.9 – 8.2	8 – 8.1	7.9 – 8.1	7.9 – 8.1
Chloramine	mg/L as Cl_2	0.2 – 0.4	0.2 – 0.4	2.3 – 2.5	2.3	2.3	2.4
Ammonia	mg/L NH_3-N	0.1 – 0.3	0.1 – 0.3	0.4 – 0.5	0.6	0.2	0.1
Chloride	mg/L	95 – 120	9.1 – 12	9.1 – 12	80 -82	58 – 62	32 – 36
Sulfate	mg/L	134- 220	0 – 0.2	0 – 0.2	146 – 150	103 – 107	48 – 52
Alkalinity	mg/L as $CaCO_3$	121 – 130	8 – 11	60 – 70	100 – 104	85 – 93	70 – 76
Pb	µg/L	ND	ND	ND	ND	ND	ND
Cu	µg/L	8 – 21	0 – 2.2	0 – 2.2	3.6	9.1	3.1
Zn	mg/L	0.3 – 0.5	0.1	0.1	0.125	0.2	0.1
Conductivity	µS/cm	1066	56	261	865	664	462

ND = Non-detect

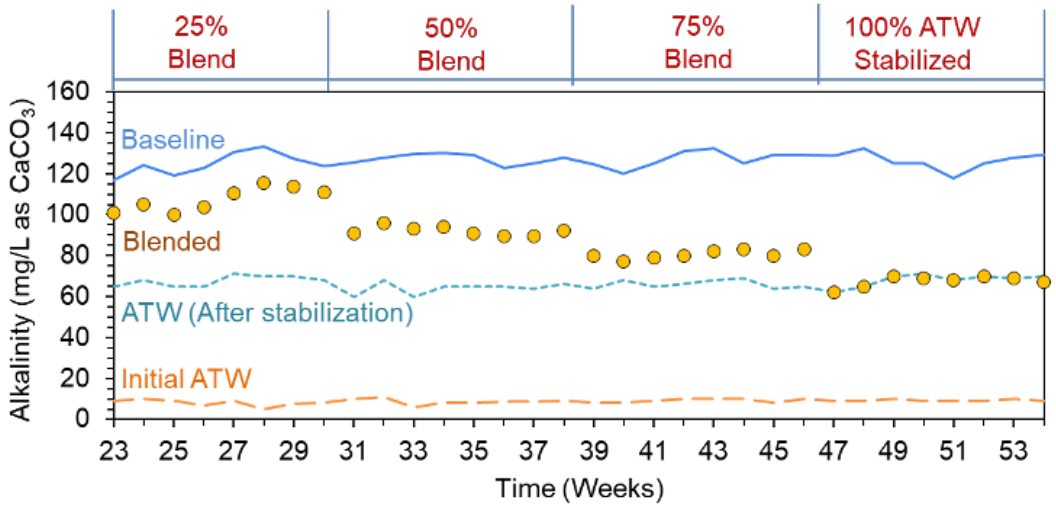

Figure 3-29. Alkalinity of Baseline, Stabilized Advanced Treated Water, Unstabilized ATW (ATW Initial) and Blended Water before Entering Pipe Loops.

The alkalinity of the baseline water was in the range of 110 to 130 mg/L as $CaCO_3$. The alkalinity of ATW was in the range of 8 to 10 mg/L as $CaCO_3$. The alkalinity of the stabilized ATW was about 65 to 70 mg/L as $CaCO_3$ after reacting with calcite. For the different stages of blending, the alkalinity of the blended water matched well with the theoretically estimated alkalinity (Figure 3-29). The alkalinity of the water did not change after recirculating in pipe loops for a week.

3.2.1.1 Water Chemistry in the Pipe Loops

Chloramine was used as the disinfectant in the baseline and advanced treated water. The chloramine dose in the baseline water was 2.5 mg/L as Cl_2. Figure 3-30 shows the residual total chlorine in the pipe loops after 24 hours of recirculation. Chloramine was readjusted each day in all the pipe loops. The inherent chlorine demand of the baseline water was1 to 1.5 mg/L based on measurements of volumes of only baseline water with added chloramine over 24 hours. The as-received ATW exerted essentially no chlorine demand over the same time duration. The total chlorine demand during the conditioning period in the copper pipes was 2.0 mg/L as Cl_2, and in the brass pipes it was 2.2 mg/L as Cl_2.

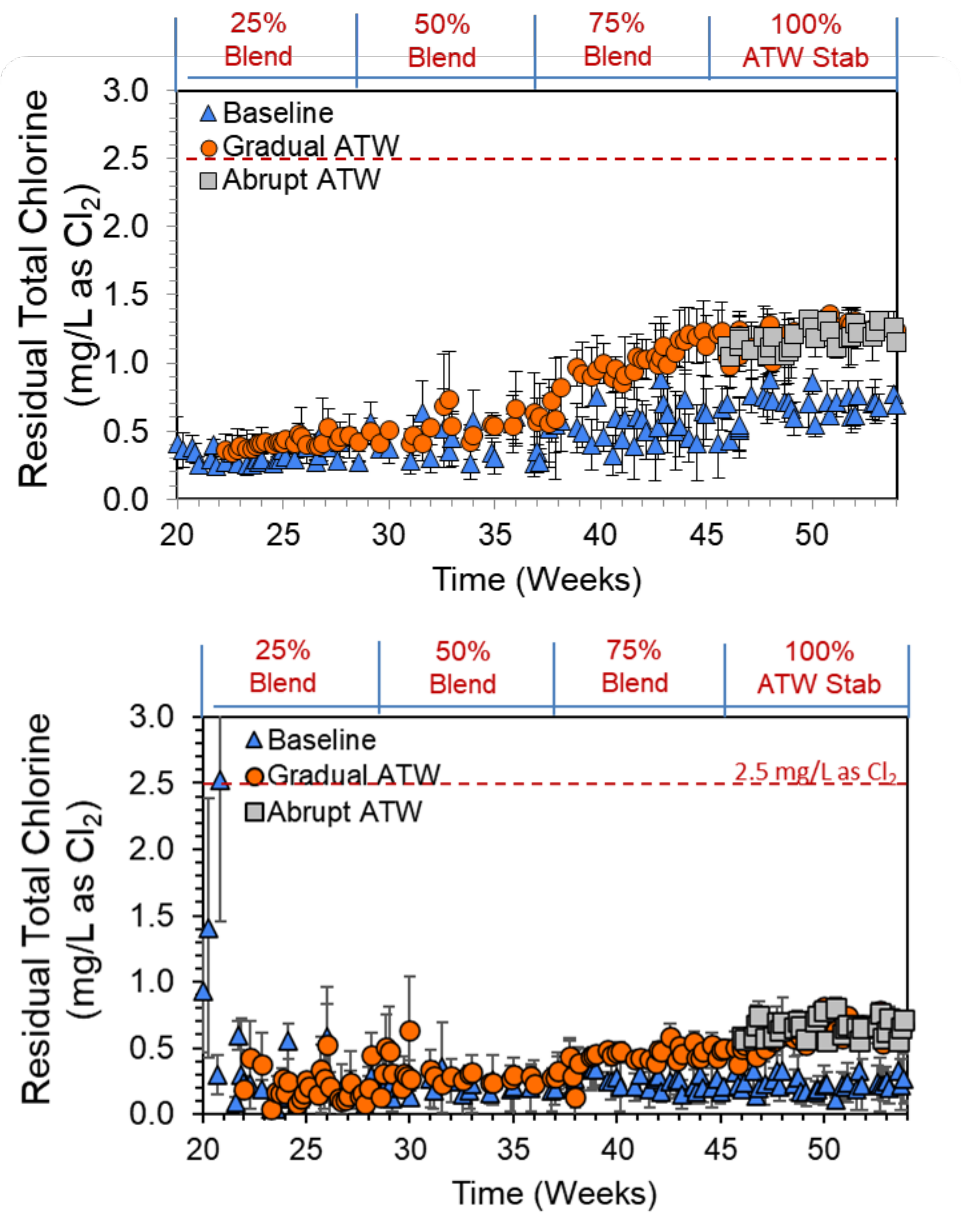

Figure 3-30. Daily Total Chlorine Residual after 24 hours for Pipe Loops Receiving Baseline Water, Gradual Introduction of ATW, and an Abrupt Switch to ATW.
Results are Shown for Copper Pipe Containing Lead Solder (top) and Brass Rods (bottom).

The total chlorine demand of blended water in the copper pipes decreased when a blend with 50% ATW was introduced to the pipe loops. The decrease in the chlorine demand was not prominent in the brass rods until a blend with 75% ATW was reached. The total chlorine demand continued to decrease in pipe loops with both materials as the percentage of blend increased to 100%. The chlorine demand in the pipe loop stabilized during the 100% ATW stage for the pipes that had gradually received blended water. The demand was similar to that seen in the pipes that had abruptly switched the water to 100% ATW. The chlorine demand in the baseline water recirculating in copper pipes and brass rod pipe assemblies decreased by 0.3 and

0.1 mg/L as Cl_2, respectively, over the full duration of the tests. Overall, the brass rods had a higher chlorine demand than the copper pipes throughout the experiment. By the end of 54 weeks of the experiment, the residual chlorine in the copper pipes was similar to the inherent chlorine demand of baseline water while that in the brass rods was still lower than the inherent chlorine demand of the baseline water. The brass may require more time to form stable corrosion products on their surface that could decrease the chlorine demand.

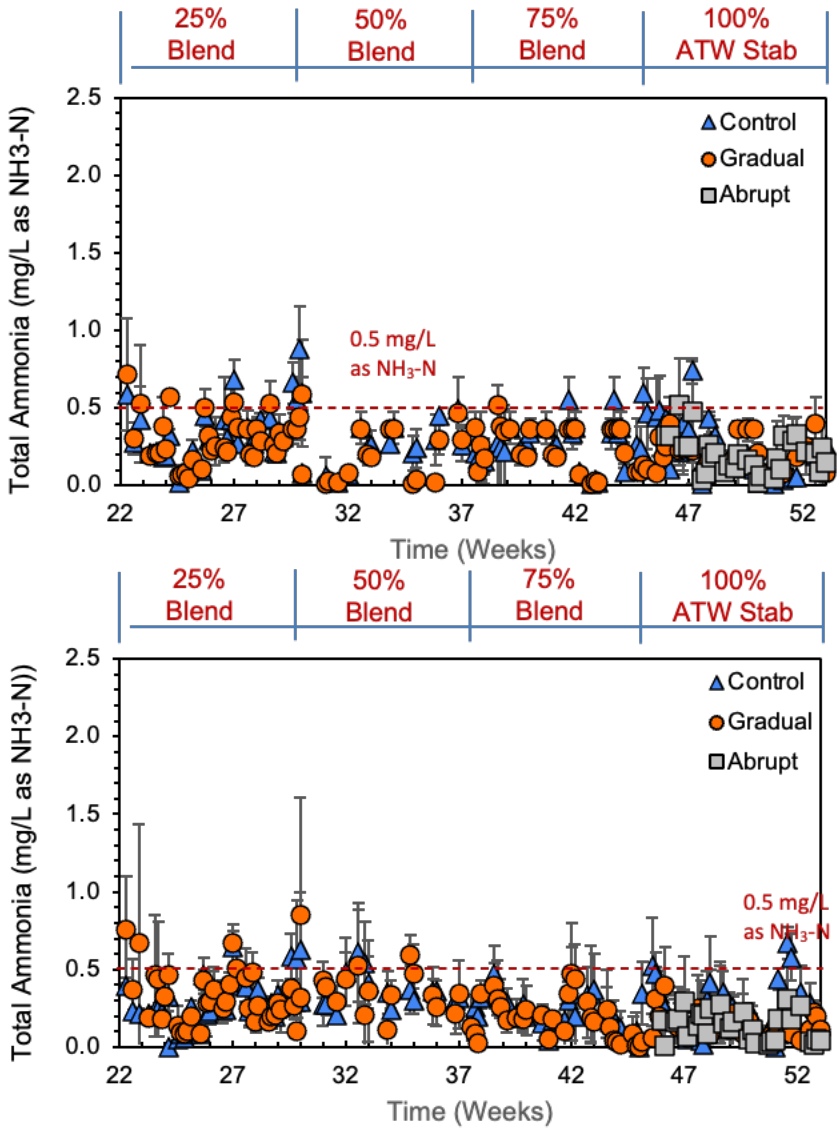

Figure 3-31. Daily Residual Total Ammonia as N after 24 hours for Pipe Loops Receiving Baseline Water, Gradual Introduction of ATW, and an Abrupt Switch to ATW.
Results are Shown for Copper Pipe Containing Lead Solder (top) and Brass Rods (bottom).

The total ammonia was targeted at 0.5 mg/L-N during the readjustment of disinfectant. The total ammonia decreased after a day of recirculation (Figure 3-31) in all pipe loops.

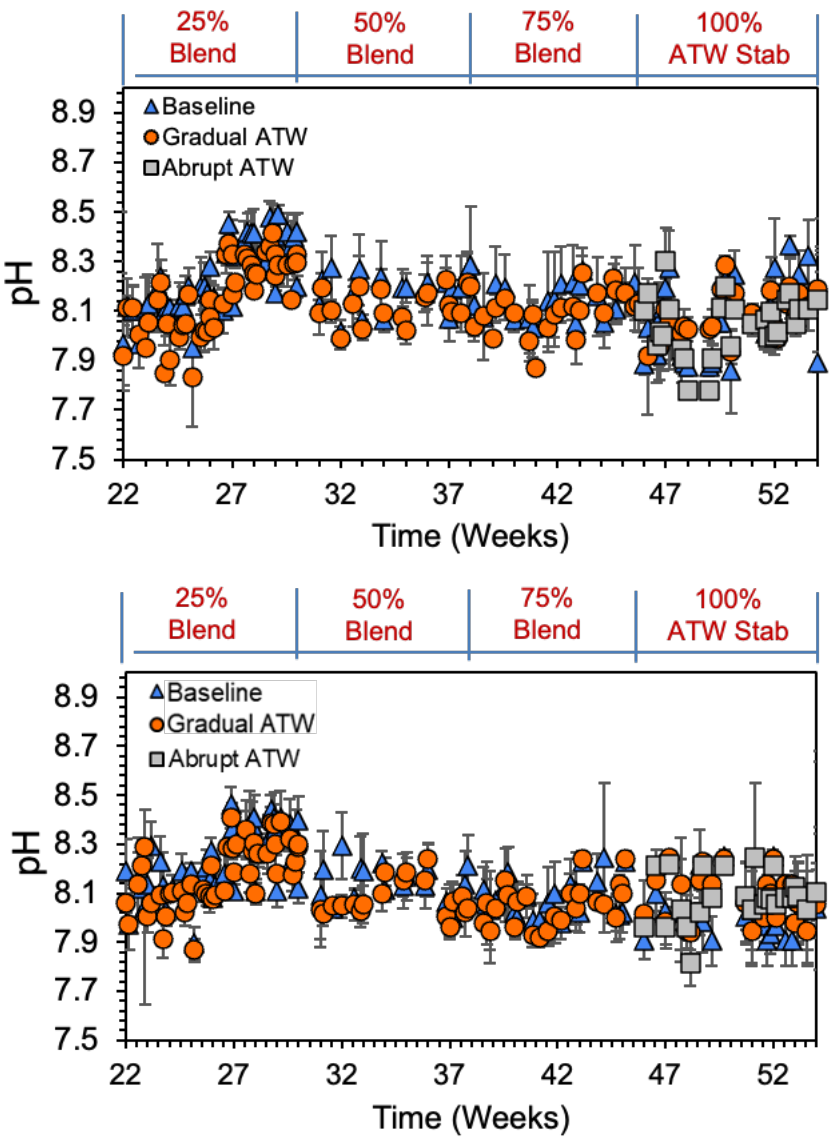

Figure 3-32. Daily pH Measurements after 24 Hours for Pipe Loops Receiving Baseline Water, Gradual Introduction of ATW, and an Abrupt Switch to ATW.
Results are Shown for Copper Pipe Containing Lead Solder (top) and Brass Rods (bottom).

The pH of the baseline water was 7.9 to 8.1. The pH drifted up to 8.3 or 8.4 over the course of each week (Figure 3-32). The pH during the recirculation with the blended water at all percentages from 25% to 100% fell in the same range as seen during conditioning. This was because the stabilized ATW had a pH of 8.1 after stabilization with calcite.

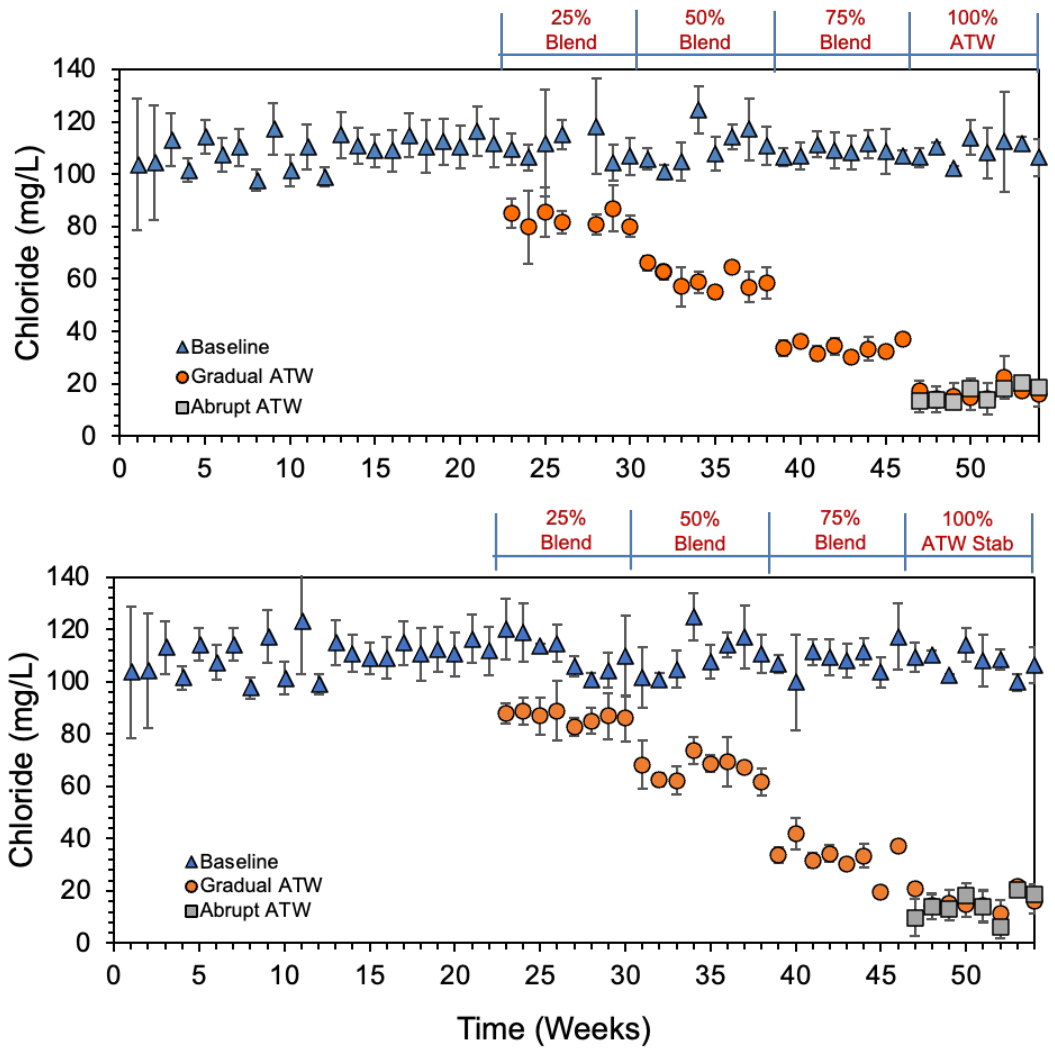

Figure 3-33. Weekly Chloride Measurements for Pipe Loops Receiving Baseline Water, Gradual Introduction of ATW, and an Abrupt Switch to ATW.
Results are Shown for Copper Pipe Containing Lead Solder (left) and Brass Rods (right).

The chloride in the baseline water varied between 95 and 120 mg/L. The ATW ranged from 9 to 12 mg/L of chloride. Figure 3-33 shows the chloride concentration in the pipe loops after a week of recirculation. The chloride in the blend with 25%, 50%, and 75% ATW was 81±1 mg/L, 60±2 mg/L, and 34±2 mg/L respectively. The measured chloride was similar to estimated concentrations based on conservative behavior upon mixing of the stabilized ATW and baseline water.

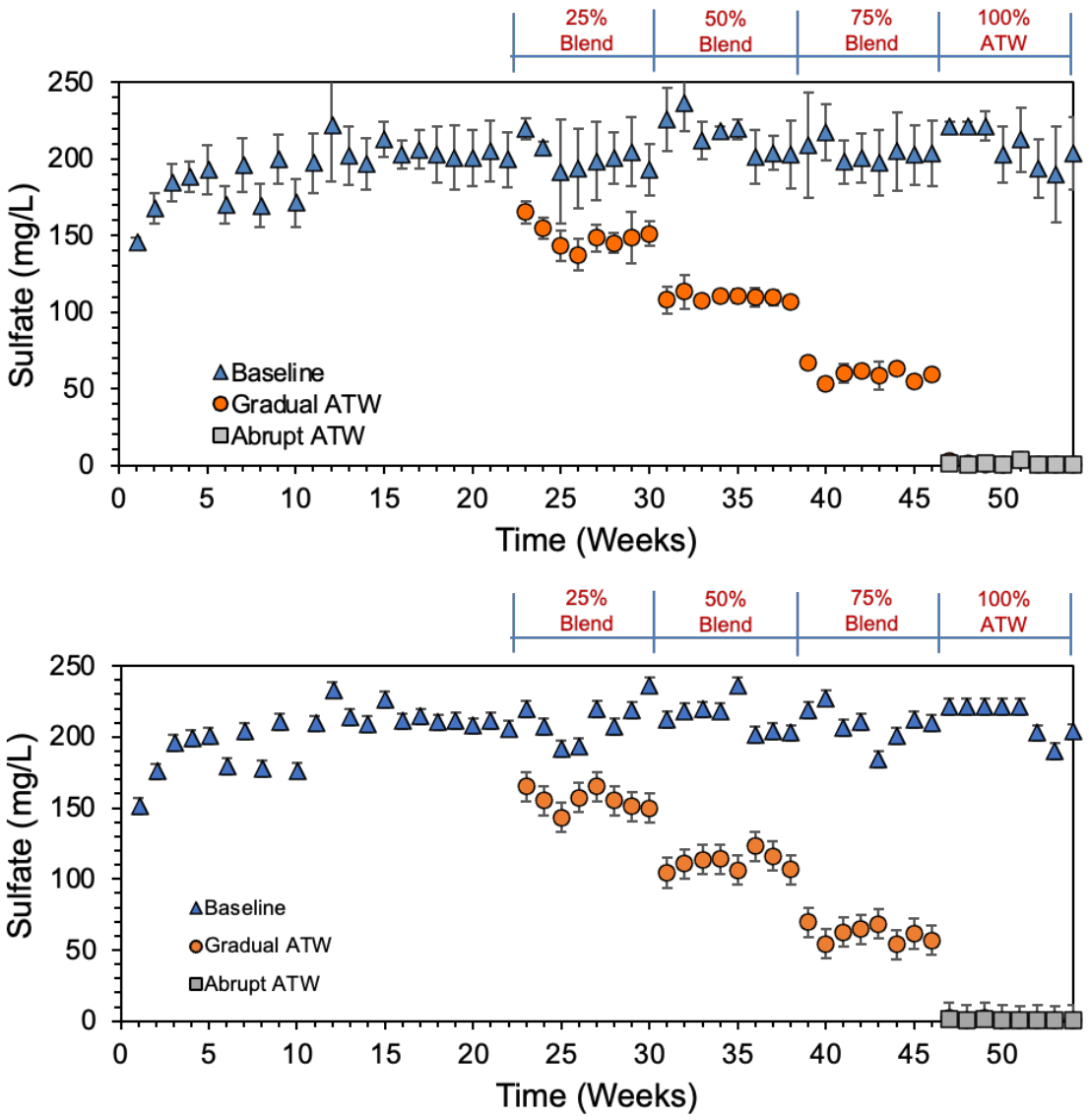

Figure 3-34. Weekly Sulfate Measurements for Gradually and Abruptly Receiving ATW and Baseline Receiving Pipe Loops with Copper Pipe Containing Lead Solder (left) and Brass Rods (right) after Recirculation.

Sulfate concentrations in the baseline water varied between 146 and 200 mg/L during the first 5 weeks (Figure 3-34). The sulfate concentration shifted to a higher range of 200 to 246 mg/L for the remainder of the testing. The ATW generally had 0.2 to 0.5 mg/L sulfate, but in some cases, the concentrations were not detectable. Sulfate in the blended water with 25%, 50%, and 75% ATW was 150±5 mg/L, 104±2 mg/L, and 50±4 mg/L, respectively.

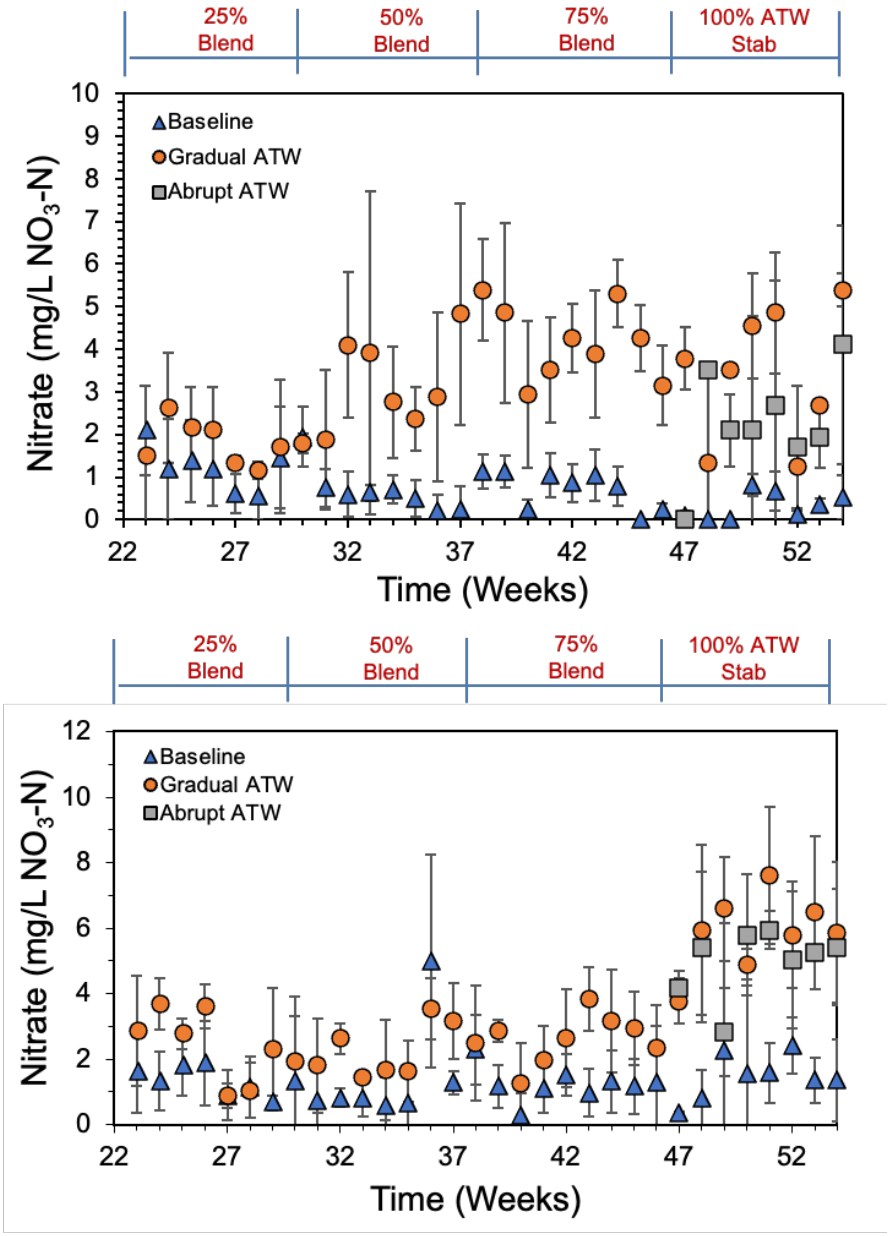

Figure 3-35. Weekly Nitrate Measurements after Recirculation of Gradual ATW, Abrupt ATW and Baseline Receiving Pipe Loops with Copper Pipe Containing Lead Solder (left) and Brass Rods (right) after Recirculation.

The nitrate concentration in the as-received ATW after recirculation (0 to 33 mg/L NO_3-N) had a larger variability than did the as-received baseline water (0 to 5 mg/L NO_3-N) (Figure 3-35). Nitrate concentrations after recirculation in the pipe loops varied from pipe to pipe. The nitrate concentrations in the gradually blended ATW for the copper pipes varied from 10 – 25 mg/L – N compared to the nitrate concentrations (5- 15 mg/L – N) in pipe loops with the brass rods between Week 30 and Week 47. The nitrate concentrations were higher (20 – 35 mg/L – N) in the brass rods pipe loops than in the pipe loops with copper pipes during Weeks 48 to 54. The reason for nitrate variability is not known at this time.

3.2.2 Impact of Blending ATW on Copper Pipes Containing Lead Solder

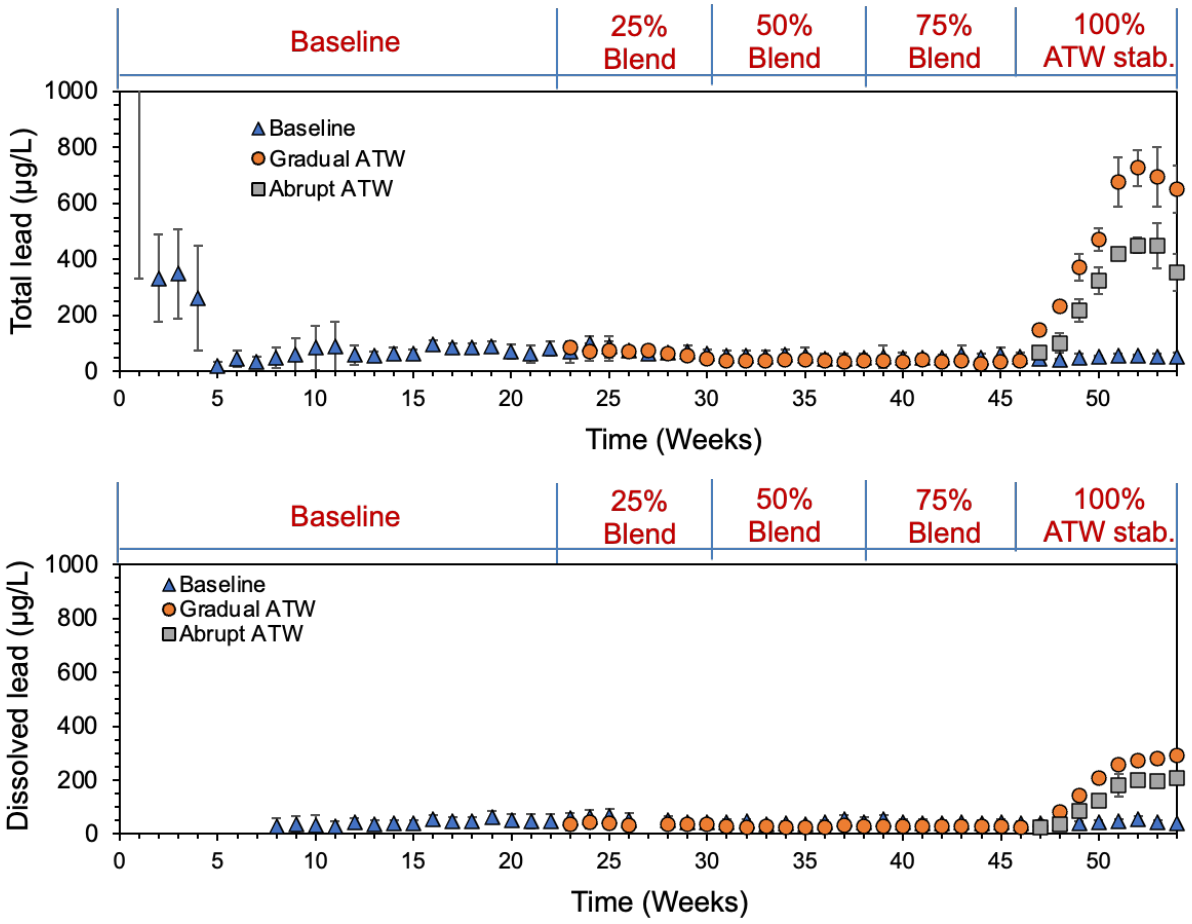

Figure 3-36. Total Lead (top) and Dissolved Lead (bottom) Release from Copper Pipes Containing Lead Solder Receiving Baseline, Gradual ATW and Abrupt ATW after Weekly Recirculation.

The copper pipes were conditioned with baseline water until the dissolved lead concentrations for all nine pipe loops varied by less than 25% for a five-week period. However, not all pipes had copper and zinc concentrations with less than 25% variability over five-week periods after that duration of conditioning.

The average total lead at the end of conditioning of all pipes (Week 22) was 82 µg/L and the average dissolved lead was 49 µg/L (Figure 3-36). However, the lead release in all pipes continued to decrease until Week 31 and then stabilized around 40 µg/L. From Week 31 onward, the lead release in the copper pipes was predominantly controlled by dissolved lead concentrations. In comparison to total lead that took 22 weeks to reach stable conditions, the average dissolved lead reached consistently low values by Week 8 in all pipe loops.

No notable effect of gradually blending ATW was observed for lead release through the stage of 75% blending. However, when 100% stabilized ATW was recirculated in the test pipes as the final stage of gradual blending to three pipe loops and as an abrupt change for three other pipe loops, the total lead dramatically increased. The concentrations increased up to 500 µg/L for pipe loops experiencing an abrupt switch to stabilized ATW and up to 750 µg/L for the pipe loops with gradual blending when those loops started receiving 100% stabilized ATW. Similarly,

the dissolved lead concentrations also started increasing when 100% ATW was introduced into pipe loops either abruptly or as the final stage of gradual blending. The dissolved lead concentrations ranged from 82 µg/L to 259 µg/L, which was only about one third of the total lead concentrations during this time.

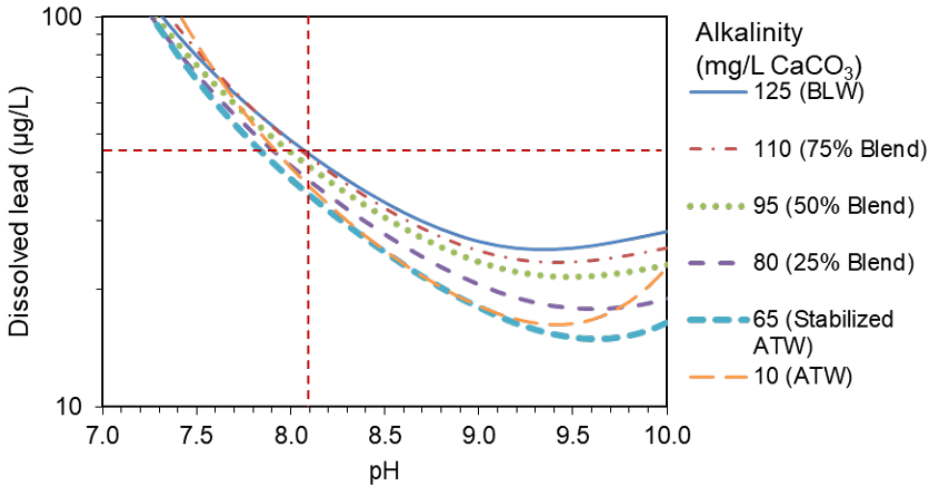

Figure 3-37. Solubility Curve for Dissolved Lead Concentrations with Hydrocerussite ($Pb_3(CO_3)_2(OH)_2$) as the Dominant Solid Controlling Lead Release.

The dominant solid at the baseline conditions of pH 8.1 and DIC of 2.51 mM was predicted to be hydrocerussite ($Pb_3(CO_3)_2(OH)_2$). The XRD results from the scale characterization showed that hydrocerussite was indeed the dominant lead solid seen on the surfaces of the copper pipes and solder, while cerussite ($PbCO_3$) was seen on lead solder only. Based on the presence of hydrocerussite, the predicted equilibrium lead concentrations for baseline, 25% ATW, 50% ATW and 75% ATW were 45, 44, 41, 38 and 35 µg/L respectively (Figure 3-37). The dissolved lead concentration observed during testing before the introduction of 100% ATW was close to the predicted equilibrium lead concentrations. The dramatic increase in the lead concentration during the recirculation with 100% ATW could not be explained by a change in the predicted equilibrium solubility; rather it is likely due to the significant decrease in the sulfate concentration as will be discussed later. Changes in the chloride and sulfate concentration can impact galvanic corrosion, which is governing the lead release in copper pipes containing lead solder.

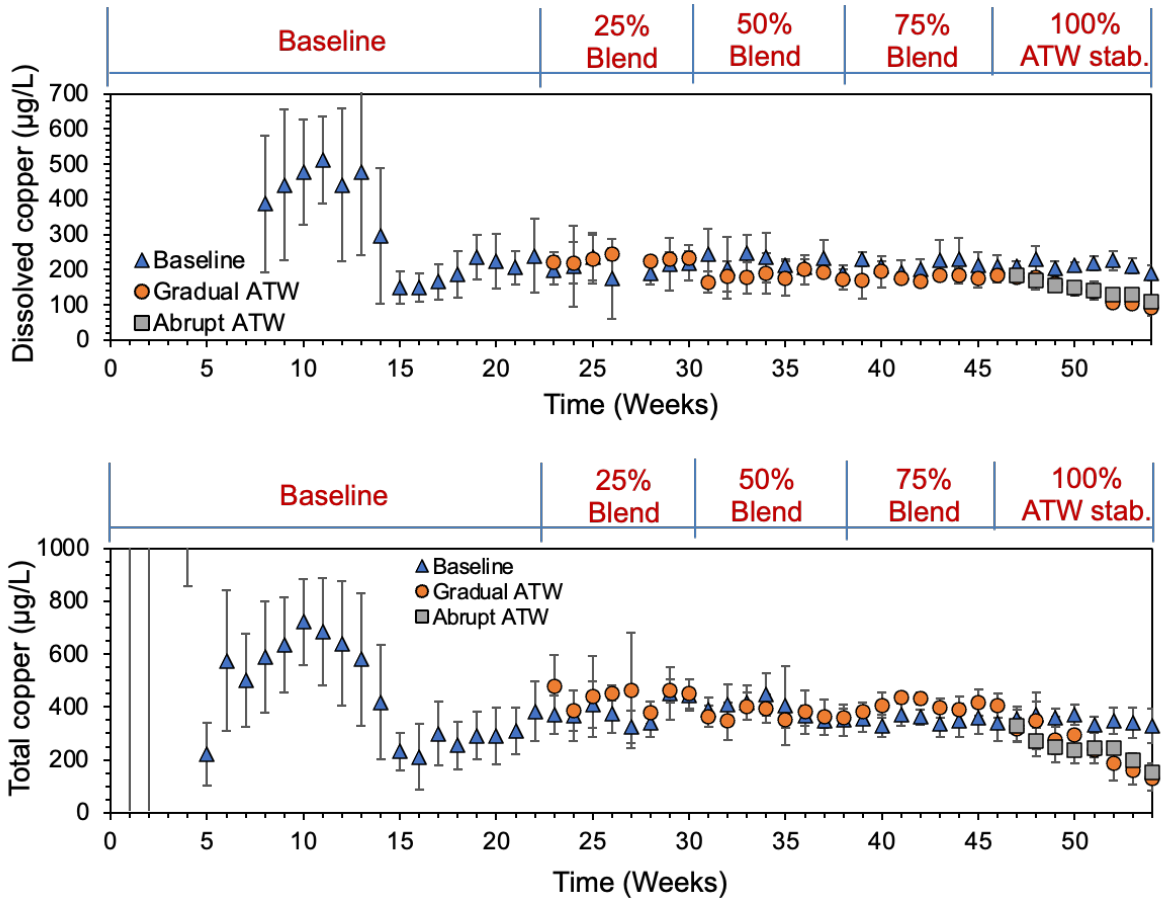

Figure 3-38. Total Copper (top) and Dissolved Copper (bottom) Release from Copper Pipes Containing Lead Solder Receiving Baseline, Gradual ATW, and Abrupt ATW after Weekly Recirculation.

The total copper (380±60 µg/L) was not significantly different for the pipes receiving baseline and blended water from Week 23 to Week 47, which was the end of the stage in which pipes with gradual blending of ATW had received 75% ATW. The dissolved copper concentrations (190±20 µg/L) remained stable throughout Week 23 to Week 46 and made up almost half of the total copper.

After the introduction of 100% ATW as both an abrupt switch and as the final stage of gradual blending (Week 48), the total copper concentrations decreased from 347 to 151 µg/L and 272 to 149 µg/L in pipes receiving 100% ATW gradually and abruptly, respectively (Figure 3-38). The concentrations of dissolved copper when pipe loops were receiving 100% gradual ATW were very similar to the dissolved copper concentrations of abrupt ATW through Week 48 to 54 (169 to 108 µg/L).

The copper-containing solid predicted to form in the baseline water in copper pipes is tenorite with a dissolved copper concentration around 10 µg/L. However, tenorite was not observed in the scale characterization nor was the observed dissolved copper close to its predicted equilibrium solubility. Instead, cuprite (Cu_2O) and copper sulfate hydroxide formed on the copper pipes (see scale analysis below in Section 3.2.4). The predicted dissolved copper concentration for copper sulfate hydrate at the chemistry of the baseline water condition is 429

µg/L, whereas for an anhydrous copper sulfate hydroxide it is 125 µg/L. Copper sulfate hydroxide solids were not observed in the pipes that had received 100% ATW at the end of the test stages.

3.2.2.1 Processes Controlling Lead and Copper Release During 100% ATW Recirculation in Copper Pipes Containing Lead Solder

The simultaneous increase in lead concentration and decrease in copper concentration that occurred during the recirculation of 100% ATW is a clear indication that galvanic corrosion influenced the release of both metals. During galvanic corrosion, copper and lead form an electrochemical cell in which copper is the protected cathode while lead is the sacrificial anode. The significant amounts of lead that were released in particulate forms are another indication that the increased lead release is associated with galvanic corrosion. During the stage with 100% ATW introduction, more than half of the total lead was present as particulate lead. Other notable observations of the changes that took place when 100% ATW was introduced are that (1) the increase in lead and decrease in copper occurred gradually over several weeks and not as an instantaneous change and (2) the solids present in scales on the inner surface of the copper pipe and lead solder at the end of testing were different for the pipes that had been switched to ATW than for the pipes that remained with baseline water over the duration of the study. Detailed information on scale analysis is presented later in Section 3.2.4, and key observations are noted below.

The Increase in lead concentrations that occurred following the switch to 100% ATW is hypothesized to be related to the dramatic decrease in in sulfate concentrations (Figure 3-34). Over the duration of the study, the sulfate concentration of the baseline water was 95-120 mg/L, and the ATW concentration was 0.2 mg/L or less. In the gradual introduction of ATW, the sulfate decreased from 56 mg/L with 75% blending to below 0.2 mg/L when 100% ATW was introduced. In the analysis of the scales on the copper pipe surfaces that were only in contact with baseline water, both copper sulfate and barium sulfate solids were observed. These sulfate solids were not observed on the pipes that had been exposed to 100% ATW, although those solids had probably been present when those pipes had been conditioned with baseline water. No lead sulfate solids were observed on the copper pipe or the lead solder surface in any of the pipes.

It is likely that the almost complete absence of sulfate at the 100% ATW condition induced the dissolution of the copper sulfate and barium sulfate solids. While there is not perfect agreement between the observed and predicted equilibrium copper concentrations in the baseline water), calculations for the saturation index of copper sulfate hydroxide ($Cu_4(SO_4)(OH)_6$), Log K_{sp} =+15.2) indicate a dramatic change from 1.04 at baseline water conditions or 1.2 at 75% blending of ATW to -1.2 in 100% ATW. A saturation index of 0 indicates that the water is in equilibrium with the solid present, and the more negative the value, the greater the driving force dissolution of the solid. Similarly, for barium sulfate present in the pipe scale, a decrease in sulfate concentration to 0.2 mg/L would promote its dissolution. Our calculations estimate that a decrease from 220 mg/L of sulfate at baseline to 0.2 mg/L sulfate would have allowed the dissolution of 470 mg of barium sulfate (275.4 mg of barium) from the scale into the volume of water recirculating in a pipe loop. In the scale analysis we measured a

barium content of 81 mg/g in the scale of the pipes receiving baseline water. For approximately 0.1 g of scales covering the copper pipe surface, only 17 mg of barium sulfate is likely to be present, which is much lower than the amount of barium sulfate that could have dissolved at 100% ATW. Consequently, the change in sulfate concentration would have been sufficient to induce the dissolution of all barium sulfate that had deposited on the pipe surfaces when baseline water was used or was part of the blend.

While previous research has observed effects of changes in chloride and sulfate concentrations on galvanic corrosion of lead, it is hypothesized that the increase in lead release in the present study was driven by the dramatic decrease in sulfate concentration and not by the change in the ratio of chloride to sulfate. In contrast to studies where CSMR increases due to higher chloride, in this case the chloride concentration substantially decreased, from 146-220 mg/L in the baseline water to 9-11 mg/L in 100% ATW. The decrease in sulfate was even more dramatic (Ng, et al. 2015).

While results indicate that the increased lead release was the result of galvanic corrosion and that the dramatic decrease in sulfate was associated with this release, an explanation for why this occurred remains a hypothesis. It is hypothesized that the much lower sulfate concentrations in the 100% ATW conditions resulted in dissolution of sulfate minerals on the copper pipe surface that had been acting as passivating layers, which limited interactions of soluble oxidants with the copper. When the sulfate-containing solids dissolved the newly exposed copper surface, the surface would then be accessible to dissolved oxidants that reacted on the copper surface and induced galvanic corrosion of the lead solder as a result of the electrical conductivity of the copper-lead connection. Because the galvanic corrosion of the lead was occurring for solder on which some lead corrosion products had already developed, the corrosion likely destabilized those corrosion products, which could explain the substantial increased in particulate lead along with the increase in dissolved lead. Similar observations have been reported in investigations of partial lead service line replacements in which new copper becomes galvanically connected to old lead pipe with pre-existing corrosion products (Wang et al., 2012; Wang et al., 2013; Triantafyllidou and Edwards 2011).

3.2.3 Impact of Blending ATW on Lead-containing Brass

The average total lead decreased in all pipes until Week 28. Around Week 30, the total concentrations were very similar to the dissolved lead concentrations, indicating a considerable decrease in particulate lead release from rods. The total lead increased upon gradual and abrupt introduction of 100% stabilized ATW. At lower amounts of ATW (25%, 50%, and 75%) during the gradual introduction of ATW, the lead concentrations were not significantly different from those in the control pipe loops that remained with baseline water. The average total lead concentrations during Week 54 in gradual (24 µg/L) and abrupt (17 µg/L) introduction of 100% ATW were four and three times higher than in the baseline pipe loops (6 µg/L), respectively (Figure 3-39).

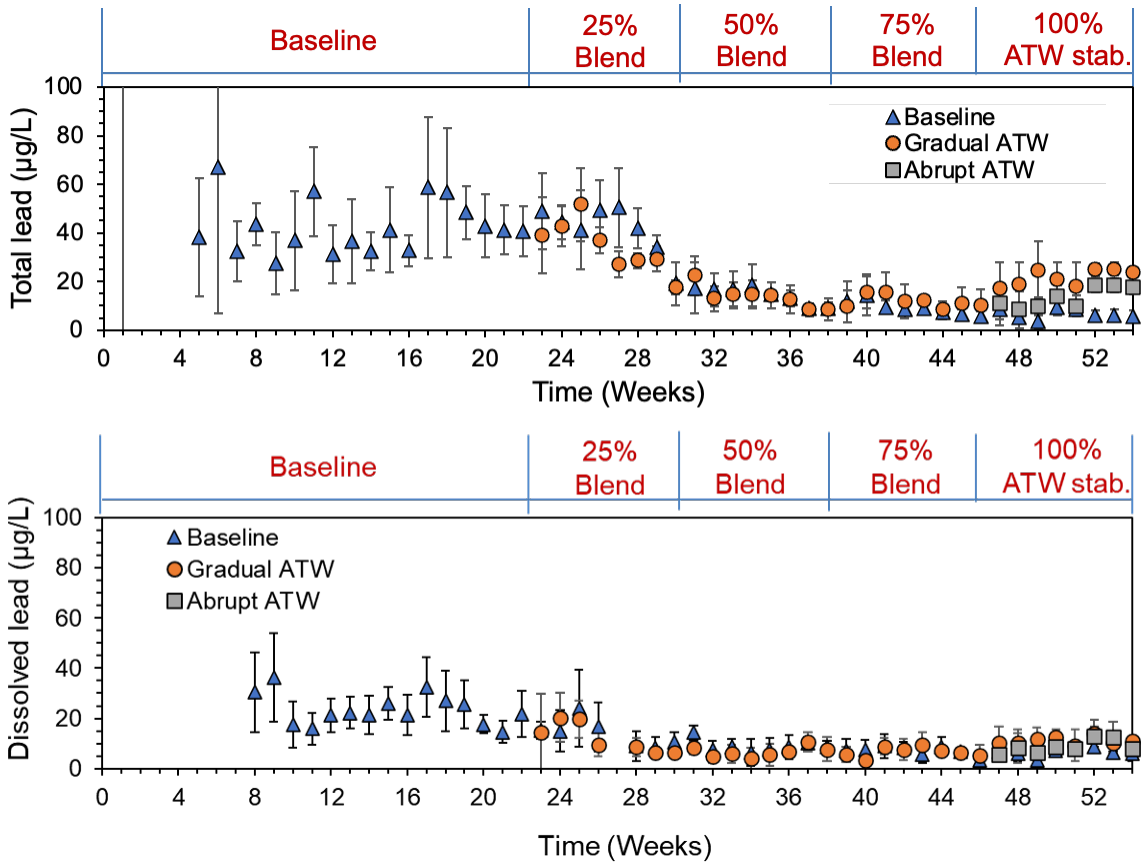

Figure 3-39. Total Lead (top) and Dissolved Lead (bottom) Release from Brass Rods Receiving Baseline, Gradual ATW and Abrupt ATW after Weekly Recirculation.

During Week 22, the average dissolved lead (22 µg/L) made up almost 50% of the total lead (41 µg/L). No differences were observed in the dissolved lead released in the presence and absence of ATW. The dissolved lead in the brass rod pipe loops was much lower than the dissolved lead in the pipe loops with copper pipes and lead solder, which is hypothesized to be due to the lower amount of lead (3%) in C360 brass than in the lead solder applied in copper pipes.

During the introduction of 100% ATW (gradually and abruptly), the total lead increased by 15 µg/L compared to that in baseline water. For this same stage of testing, no difference was observed in the dissolved lead for all the pipes. The observed lead concentrations were much lower than the predicted equilibrium solubility of a lead carbonate solid because the brass rods only contained 3% lead. No evidence was observed of a lead-based solid forming on the brass rod in baseline water or on brass rods in contact with ATW (see scale analysis discussion below in Section 3.2.4).

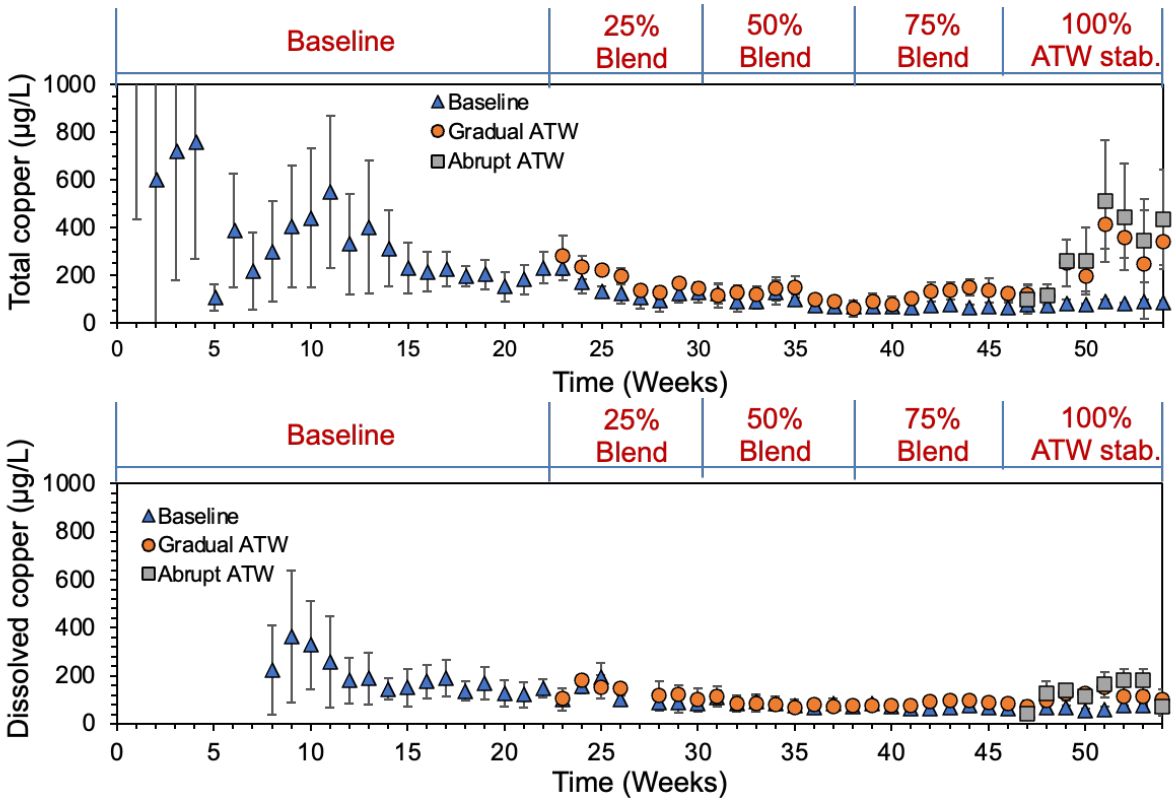

Figure 3-40. Total Copper (top) and Dissolved Copper (bottom) Release from Brass Rods Receiving Baseline, Gradual ATW and Abrupt ATW after Weekly Recirculation.

The total copper concentrations in all brass rod loops stabilized around Week 36 (Figure 3-40). The gradual introduction of ATW through the stage with 75% blending did not have a significant impact on the total copper release. A five-fold increase in total copper was observed upon introduction of 100% stabilized ATW in all test pipes either from an abrupt switch to stabilized ATW or as the final step in the gradual introduction of stabilized ATW.

The average dissolved copper concentration in pipes C1 – C9 receiving only baseline water at the end of conditioning (Week 22) was 148 µg/L. The copper increased by 100 µg/L during the recirculation of 100% ATW. Since the total copper released was significantly higher than the dissolved copper, ATW appears to have had an impact on the particulate copper release from the brass rods.

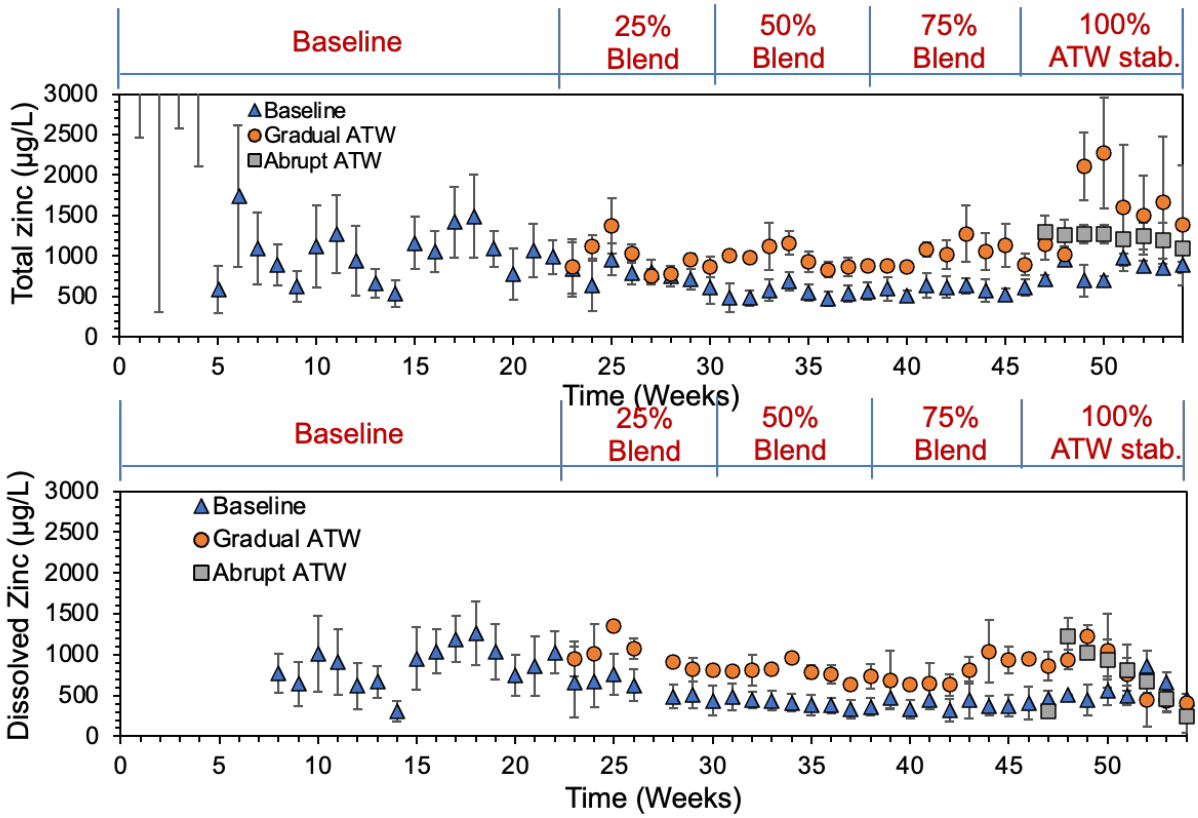

Figure 3-41. Total Zinc (top) and Dissolved Zinc (bottom) Release from Brass Rods Receiving Baseline, Gradual ATW and Abrupt ATW after Weekly Recirculation.

Zinc concentrations in the water at the end of recirculation included both zinc released from the brass rods and also zinc in the initial batches of water introduced to the pipe loops. The baseline water contained 100-200 µg/L zinc even before it came in contact with any of the pipe loop materials. One illustration of this is the data set of zinc in the copper pipes since those pipe assemblies had no source of zinc (Figure C-14).

The total zinc release in all stages of the tests never exceeded the EPA secondary maximum contaminant limit of 5 mg/L (Figure 3-41). During the last week of conditioning, the average total and dissolved zinc concentrations were around 1,000 µg/L. The zinc release was governed by the dissolved zinc. The total zinc decreased with time in all pipe loops until Week 28. After Week 28, the zinc release in the pipes receiving gradual ATW was notably higher than the baseline zinc concentrations by 400 µg/L. The zinc concentrations increased dramatically during the transition to 100% ATW from 75% ATW as the last stage of gradual ATW introduction. The pipes receiving abrupt ATW had zinc concentrations that were higher than baseline but more stable than ATW. Unlike total zinc, the dissolved zinc during gradual and abrupt introduction of 100% ATW decreased from 1,223 µg/L to 243 µg/L. The dissolved zinc at the end of testing with 100% ATW was lower than the concentrations seen at the end of 75% ATW. In contrast, the total zinc at the end of testing with 100% ATW was higher than that of 75% ATW, which indicates the ATW influenced the particulate zinc. Overall, the particulate copper to zinc ratio was 10:89, which is much lower than that of the as-received brass rods (62:35), indicating preferential release of zinc from brass.

3.2.4 Scale Analysis

3.2.4.1 Images of Scales in Copper Pipes Containing Lead Solder and Brass Rods

The scales formed on the lead solder were distinct from the scales formed on the remaining copper pipe surface in appearance and solid composition. The images of the transverse cut pipes containing lead solder were taken before scales were scraped off the surface. The halves with non-uniform coating had lead solder on them (Figure 3-42).

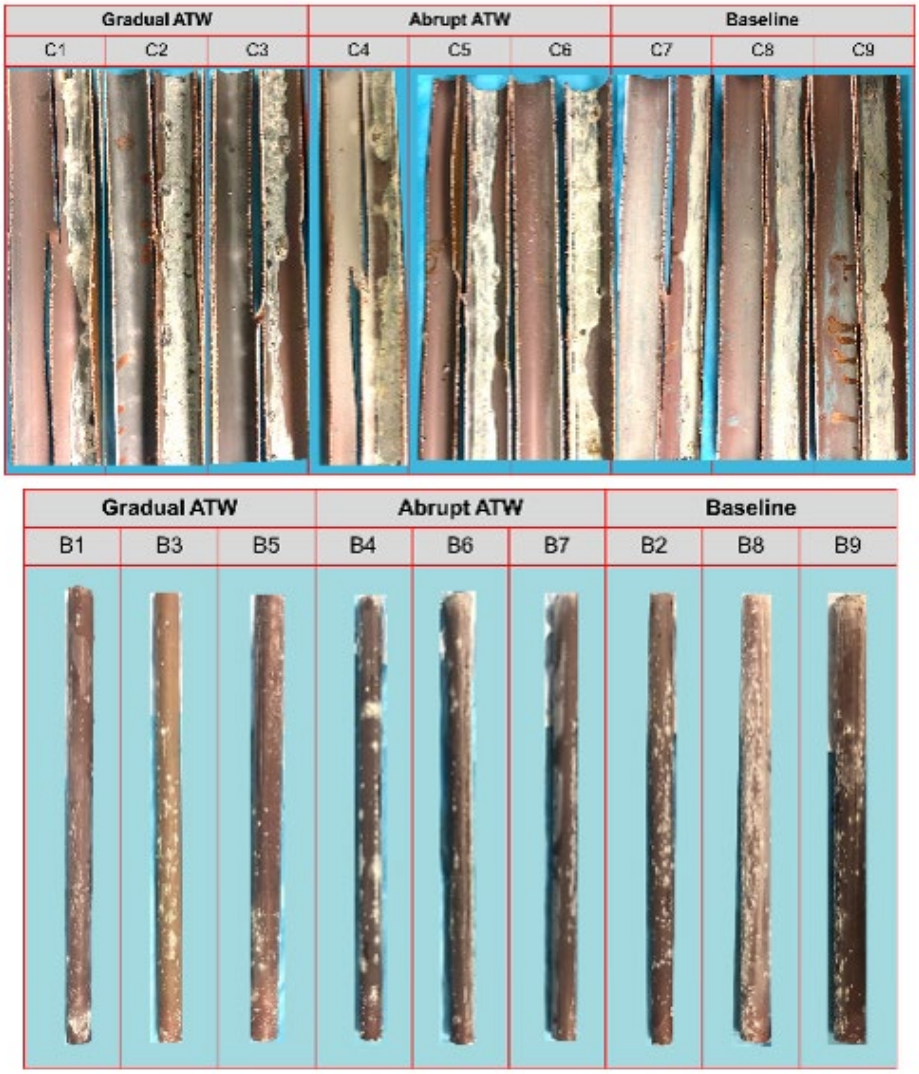

Figure 3-42. Images of Transverse Section of 8" Copper Pipes Containing Lead Solder (top) and Whole 12" Brass Rod Surface (bottom).

The solids on the solder were pale white whereas the solids on the copper pipes were dark brown and green. The corrosion products developed in the copper pipes receiving baseline water were different from those that received ATW either through blending or an abrupt switch. Sulfate-containing solids formed on the copper pipe in the presence of the baseline water, including baryte ($BaSO_4$) and copper sulfate hydroxide hydrate ($Cu_4(SO_4)(OH)_6 \cdot H_2O$) (Table 3-8). The elemental analysis also showed the presence of barium in the solids form on the pipes that had always received baseline water (Table C-1). However, barium was not

observed in the EDS analysis of the copper pipe surface, and any barium would have been below the detection limit (approximately 1% by mass) of EDS (Figure 3-43). Calcite was also seen on the baseline carrying pipes. Hydrocerussite and cuprite (Cu_2O) along with calcite were observed on the copper pipe surface of the test pipes carrying blended water with ATW except in C4 and C6. Instead, C4 and C6 had only calcite deposited on the copper pipe surface. The difference in scale composition seen for C4 and C6 versus the rest of the pipes could be due to the abrupt introduction of ATW. Prior to receiving ATW, C4, C5, C6 received only baseline water. However, C5 did not show the same scale composition as C4 and C6 (Figure 3-44).

The lead-based solids on the solder were hydrocerussite and cerussite (Table 3-8). Tin based hydroxide oxide (hydroromarchite) was also observed on the solder. In the case of solder, cerussite was more abundant than hydrocerussite and no differences were observed in the pipes receiving baseline and gradual and abrupt ATW (Figure 3-45).

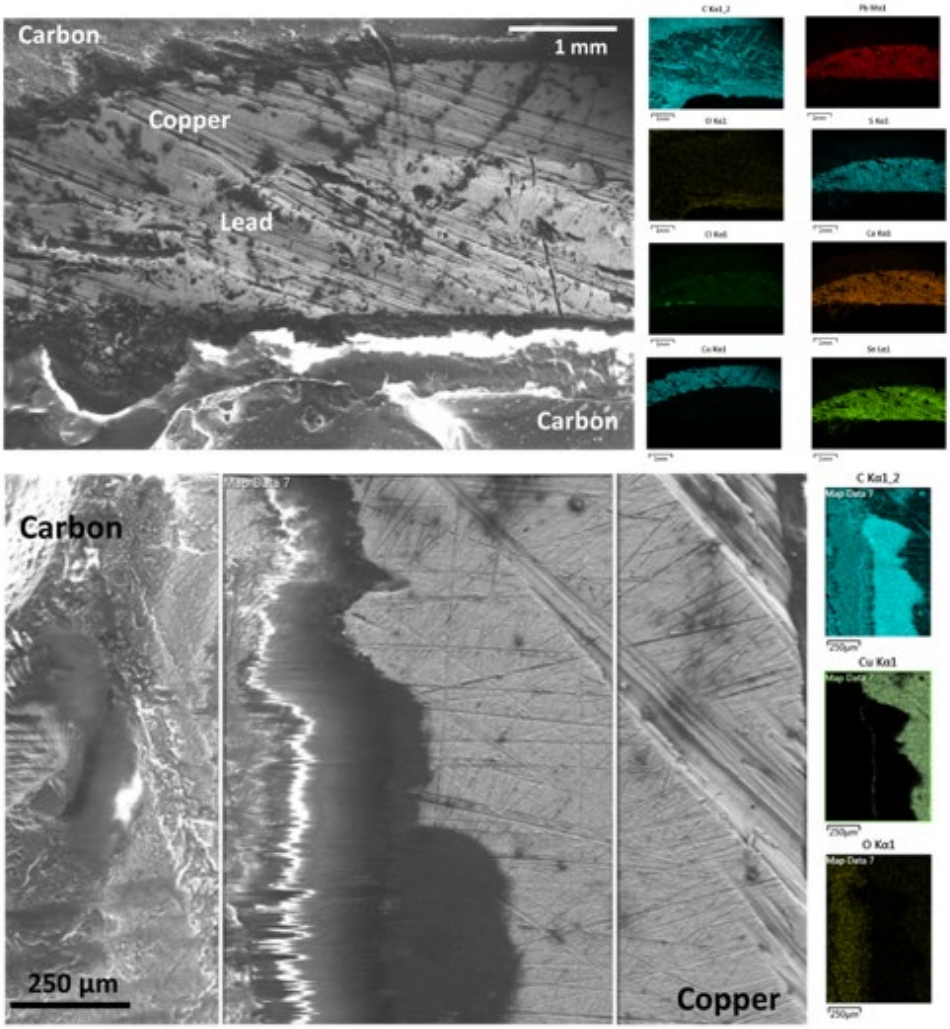

Figure 3-43. SEM and EDS Maps of Cross-sections of the Copper Pipe C7 with Lead Solder.
Top set of images represent lead solder. Bottom set of images represent a portion of the copper pipe that was not in direct contact with the lead solder. Each set of images includes the original SEM image, and EDS maps of different elements in the selected area of EDS.

Table 3-8. Solids Present on the Copper Pipe Surface That Were Identified Using XRD with Their Relative Concentration Indicated for Baseline, Gradual, and Abrupt ATW.

		Baryte	Hydro-cerussite	Mg Containing Calcite	Cerussite	Hydro-romarchite	Copper	Cuprite	Copper Sulfate Hydroxide Hydrate
Copper pipe surface									
Gradual ATW	C1		+	+			++	++	
	C2		++	+				++	
	C3		++	+	++			++	
Abrupt ATW	C4			+					
	C5		++	+			++	++	
	C6			+					
Baseline	C7	++		+					+
	C8	++		++					+
	C9	+		++					++
Solders									
Gradual ATW	C1		++		++	+			
	C2		++		++	+			
	C3		+		+				
Abrupt ATW	C4		++		+++	+			
	C5				++	+			
	C6		++		+++	+			
Baseline	C7		++		+++	+			
	C8		+		++				
	C9		+		++				

+++ indicates the relative intensity of the solids in the pipe surface

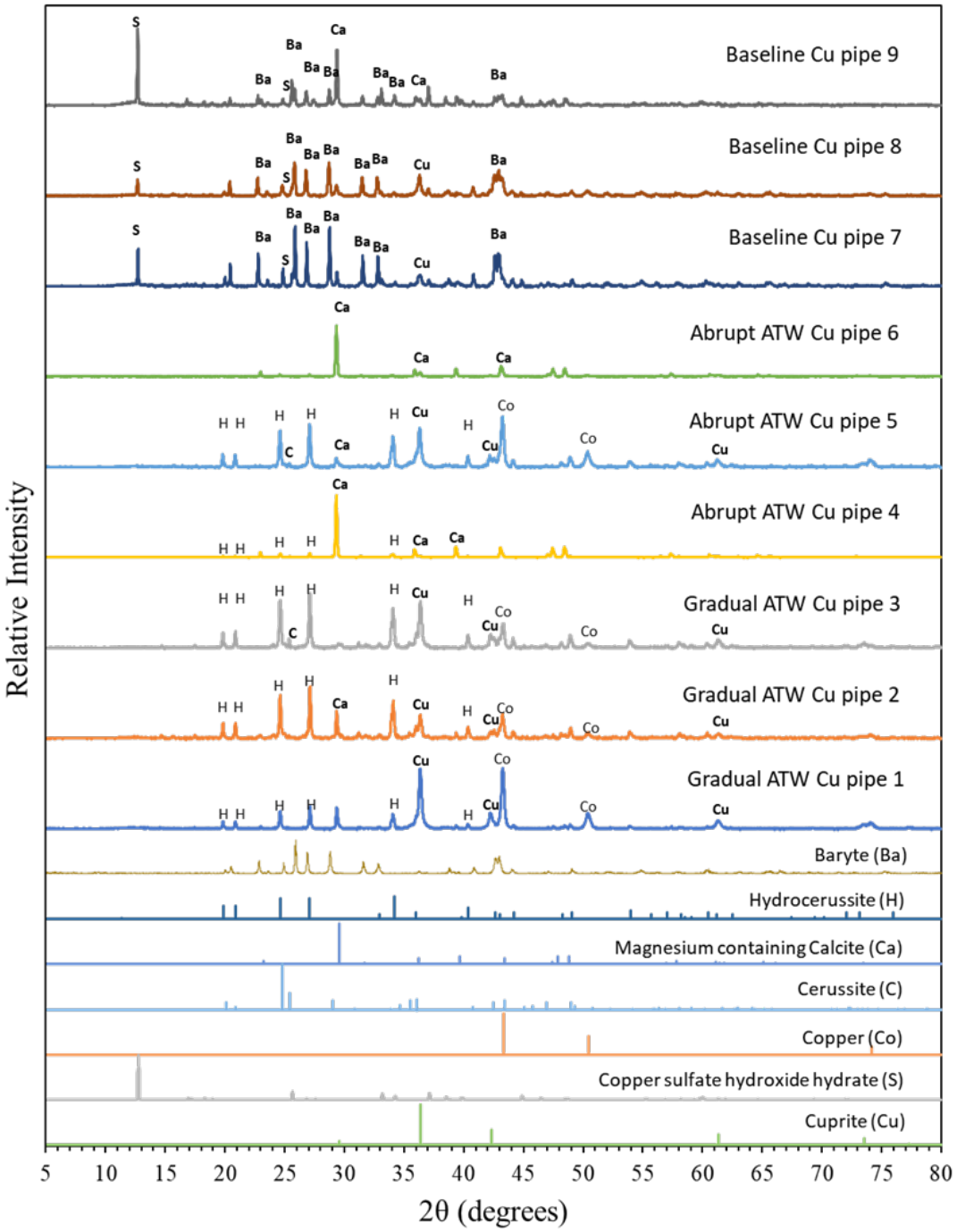

Figure 3-44. XRD Pattern of Scales Collected from the Copper Pipe Surface.
Pipes C1 – C3 Received Gradual ATW, Pipes C4–- C6 Received Abrupt ATW and Pipes C7 – C9 Received Baseline.

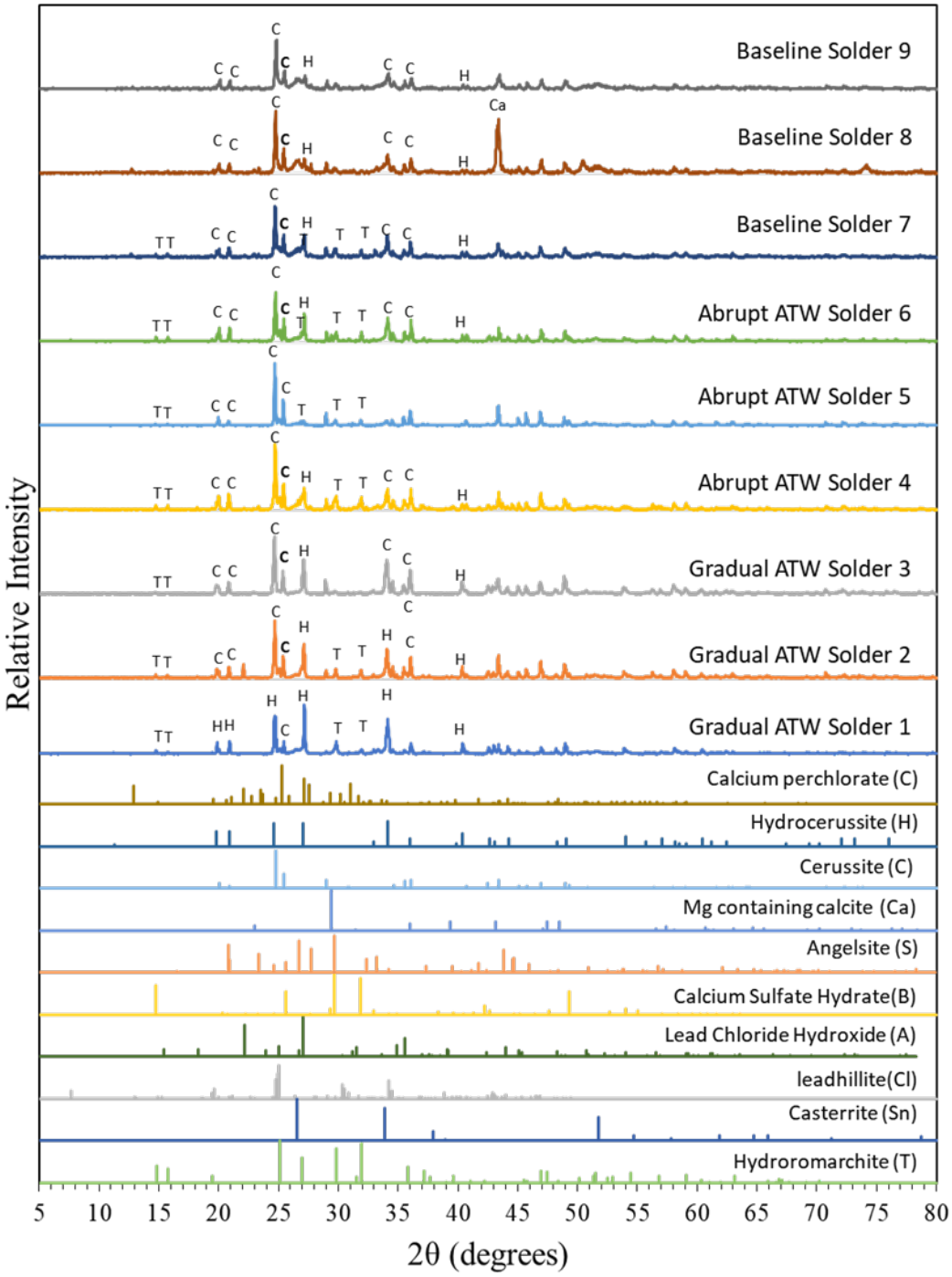

Figure 3-45. XRD Pattern of Scales Collected from the Lead Solder Region on the Copper Pipes.
Pipes C1 – C3 Received Gradual ATW, Pipes C4 – C6 Received Abrupt ATW and Pipes C7 – C9 Received Baseline.

The images of the brass rods were taken as is (Figure 3-42). The corrosion products were deposited on the outer surface of the brass rods and more deposits were formed on the edge of the brass rods. The solids formed on the brass rods were non-uniform pale white deposits with mounds scattered across the rod surface. The corrosion products on brass rods were primarily composed of zinc sulfate hydroxide, hydrozincite, and magnesium containing calcite (Table C-2, Figure C-13). The most abundant elements on the brass rods were zinc and copper

with relatively low amounts of lead and calcium (Table C-1). Figure 3-46 shows the relative amounts of copper, zinc, and lead along the red line. The line scan analysis was carried out to determine relative amounts of copper to zinc at the interface of the brass rod with the water and how it compares to that in the bulk of the brass. For the brass rod that had been used in the experiments, the lower signal of copper and zinc in the near surface region (first 100-200 µm) may be an indication of formation of a leached layer of the brass as a result the interaction of the brass with the water.

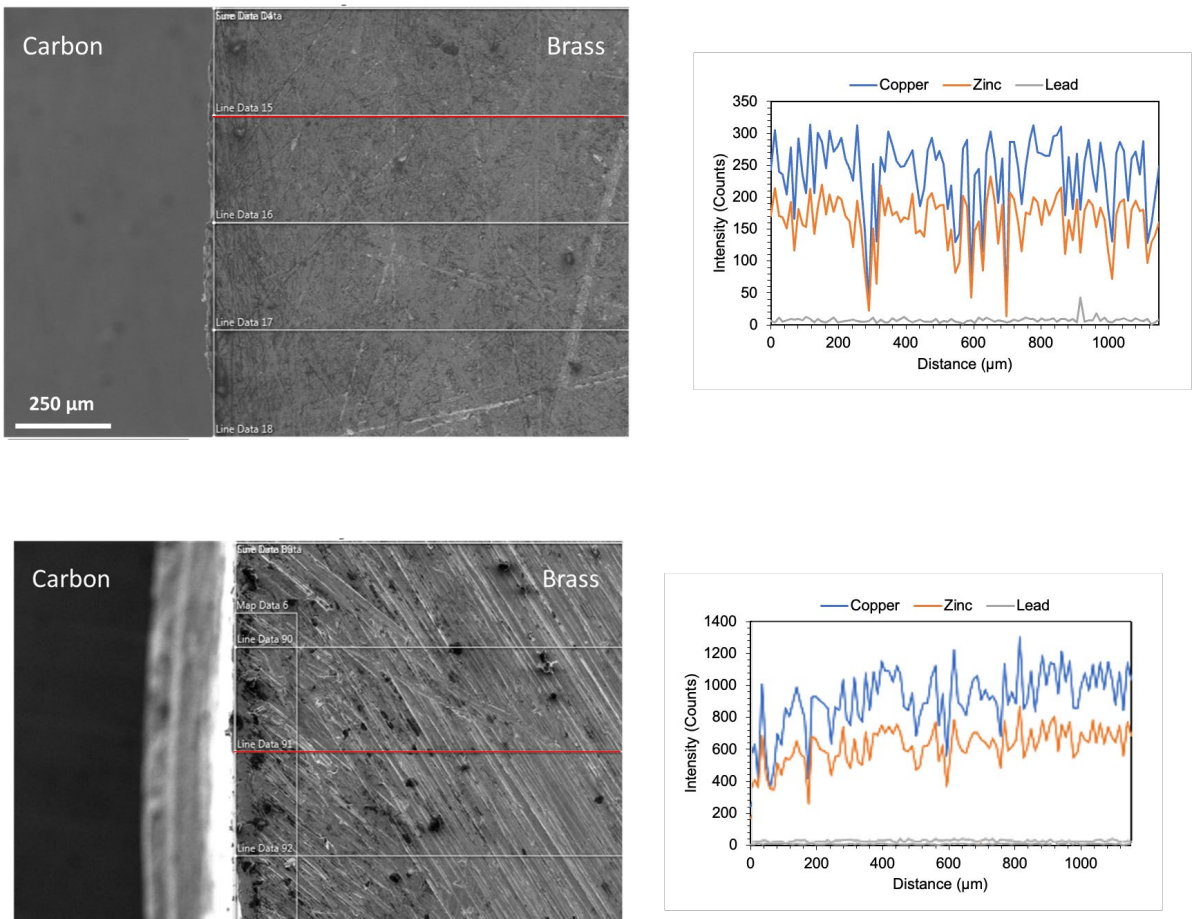

Figure 3-46. Line Scan Graphs along the Red Line Indicated on the Accompanying SEM Image Taken from the Edge of the Brass Rods As-Received (top) and Baseline Receiving Brass Rods B8 (bottom).

3.2.5 Extended Experimental Timeline

3.2.5.1 Copper Pipes Containing Lead Solder

The extended period of testing beyond the main test stages lasted 9 weeks. During weeks 55 to 58, pipe loops C1 – C6 received only unstabilized ATW and C7 – C9 received baseline water. During weeks 59 to 63, C4 – C6 were returned to baseline and C1 – C3 were returned to 100% stabilized ATW.

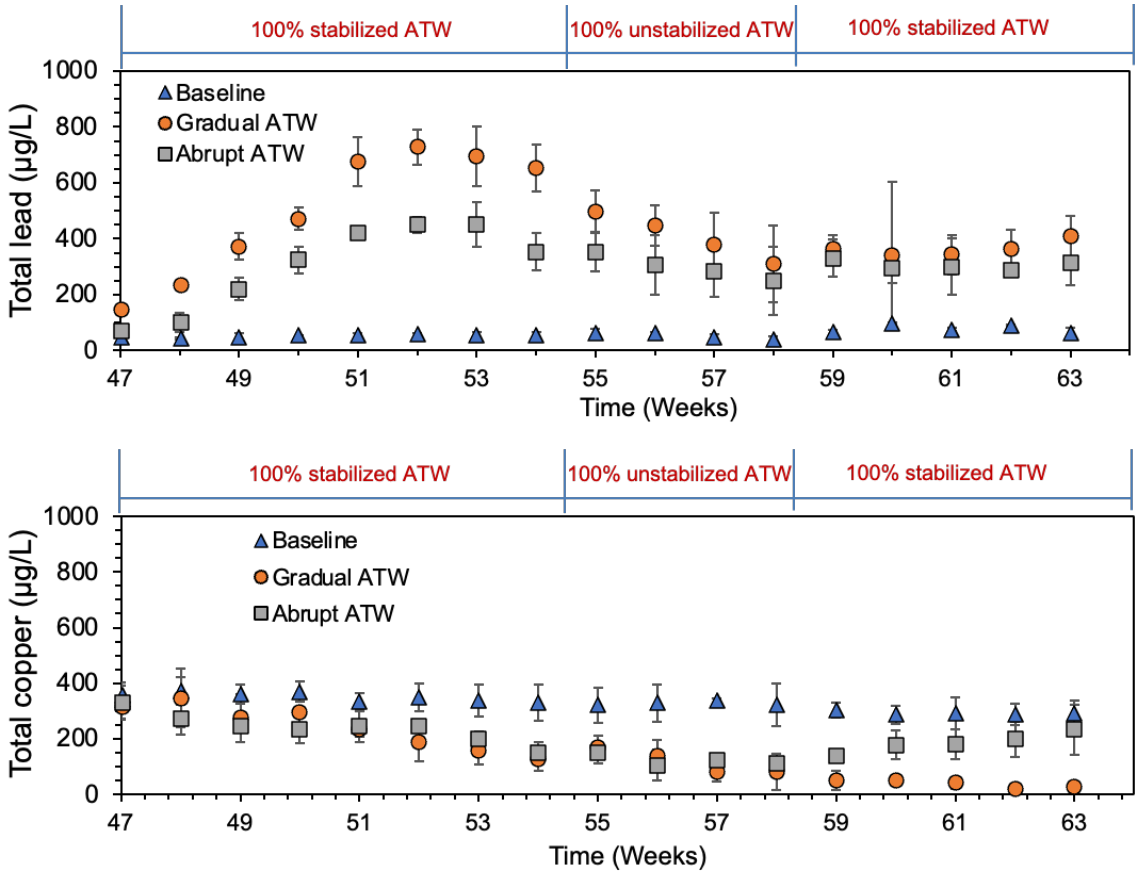

Figure 3-47. Total Lead (top) and Total Copper (bottom) Release from Copper Pipes with Lead Solder Receiving Baseline, Gradual Introduction of ATW, and an Abrupt Switch to ATW.
During Weeks 55 -58, the Gradual ATW and Abrupt ATW Pipe Loops Received Unstabilized ATW. After Week 58, the Abrupt ATW Pipe Loops Received Baseline Water, and the Gradual ATW Pipe Loops Received Stabilized ATW.

During the extended period of testing, unstabilized ATW was introduced to the pipe loops. Despite the much lower alkalinity of the unstabilized ATW, dramatic changes in the lead and copper concentrations were not observed (Figure 3-47). The lead concentrations after Week 55 decreased to a range of 400 to 500 µg/L. After the pipe loops that had experienced an abrupt switch ATW were returned to baseline water in Week 59, the lead concentrations remained elevated and did not decrease to the baseline lead concentrations. It appears that the underlying causes of the dramatic increase in lead release that first occurred when the pipe loops received 100% stabilized ATW were not resolved with a return to baseline water, at least not within five weeks.

In the case of copper release in copper pipes, the baseline copper concentrations were higher than the concentrations for gradual and abrupt ATW. When the abrupt ATW was brought back to baseline water in Week 59, the copper concentrations did gradually increase back to match the copper concentrations in the pipe loops that had always been receiving baseline water. The pipe loops that had experienced gradual introduction of stabilized ATW, a period of unstabilized ATW, and that were then reverted to stabilized ATW on Week 59 had copper concentrations that remained low.

3.2.5.2 Lead-containing Brass

The extended period was continued for 4 weeks for the pipe loops with lead-containing brass. Pipe loops B1 and B3 – B7 received only unstabilized ATW, while B2, B8, and B9 received baseline water. When the unstabilized water was recirculated in the gradual and abrupt ATW pipes, the copper and zinc concentrations decreased while the lead concentration increased (Figure 3-48).

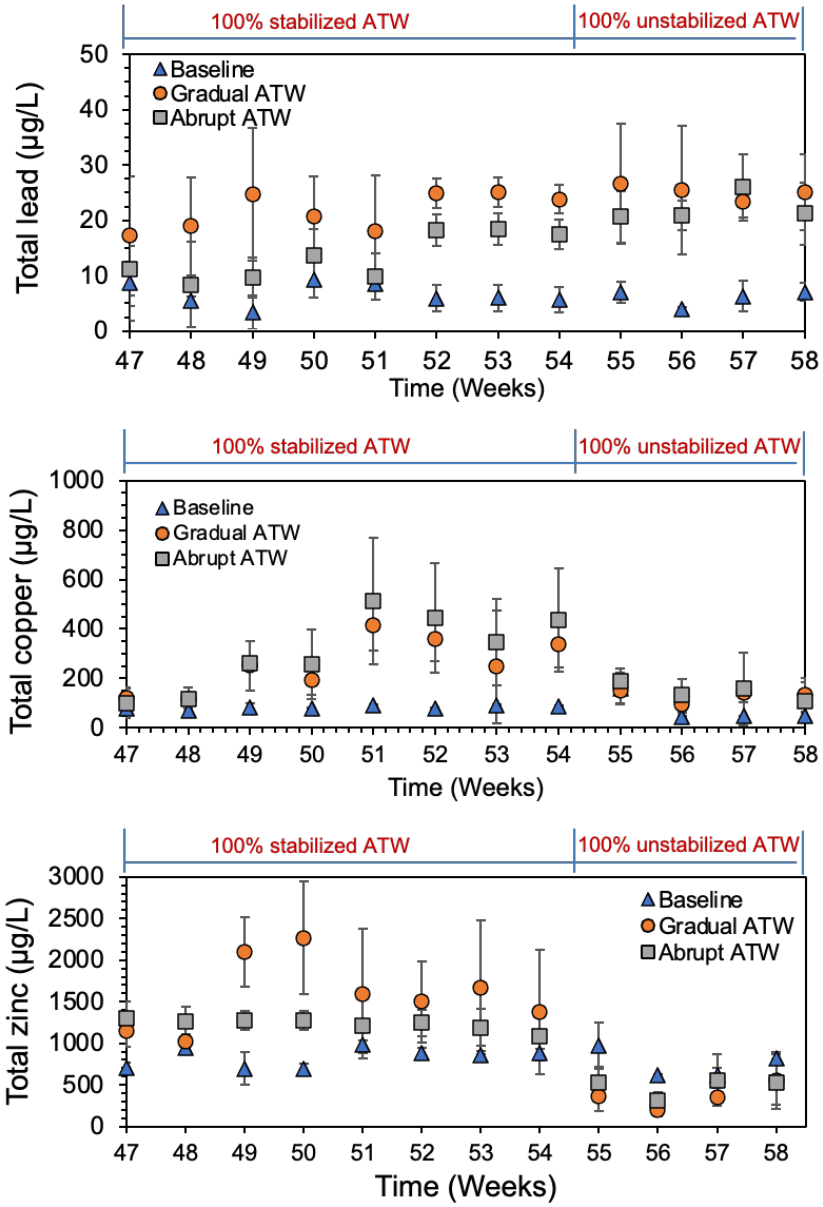

Figure 3-48. Total Lead (top) and Total Copper (bottom) Release from Brass Rods Receiving Baseline, Gradual ATW and Abrupt ATW.

During Week 55 -58, the Gradual ATW and Abrupt ATW Received Unstabilized ATW.

CHAPTER 4

Key Findings

4.1 Distribution System

After pipe harvesting and as expected, iron and manganese were released into the water during the acclimation period with BLW (baseline water) after recirculation for one week. Stabilization of ATW with calcite filters achieved the targets for alkalinity, calcium, and pH without need for additional chemical addition.

After the conditioning period, the introduction of ATW did not result in higher release of iron and manganese either for gradual addition or abrupt addition of ATW, despite the difference in water quality between ATW and BLW (i.e., groundwater). Good reproducibility was observed for the UCI pipe loops, confirming the results. The findings confirm findings of prior studies conducted for desalinated water (Blute et al., 2008; Blute et al., 2014) indicating that red water concerns can be mitigated with appropriate target water quality (pH, alkalinity, and calcium), even when changes in some parameters like sulfate and chloride occur.

Challenges were experienced in producing a stable residual disinfectant residual for the ATW, and further investigation was recommended to determine what factors influence the disinfectant residual stability in ATW water. Additional testing is summarized in Chapter 5. Similar to desalinated water, study results indicate a longer free chlorine contact time is necessary to stabilize the residuals. Significant residual loss was observed in the pipe loops during the testing and is likely due to the tuberculation and water age. Severe nitrification was not observed and no nitrification impacts on corrosion. Note that this work focused on RO-treated ATW, and studies should be conducted on non-RO ATW trains to characterize impacts to disinfectant residual.

Microbiological results showed that both *Legionella* and NTM were observed in the pipe loops; however no discernable patterns of occurrence could be ascertained. Further investigation is warranted to elucidate the importance and universality of these results.

4.2 Premise Plumbing

Introducing 100% ATW gradually and abruptly into copper pipes with lead solder dramatically increased the lead concentrations and simultaneously decreased copper concentrations. The simultaneous increase in lead concentration and decrease in copper concentration that occurred during the recirculation of 100% ATW is a clear indication that galvanic corrosion influenced the release of both metals.

Similarly, the gradual and abrupt addition of 100% ATW in brass rods containing lead increased particulate lead concentrations, total copper concentrations, and particulate zinc concentrations. Water quality was variably impacted in recirculated water. Alkalinity, chloride, and sulfate concentrations of the 25%, 50%, 75%, and 100% blended water did not change after recirculating in the pipe. However, nitrate concentrations in the ATW after recirculation were

higher and had a larger variability than the as-received baseline water. Nitrate concentrations after recirculation in the pipe loops varied from pipe to pipe to a greater degree than could be explained by nitrification.

The corrosion products developed in the copper pipes receiving baseline water were different from those that received ATW either through blending or an abrupt switch. The solids on the pipes receiving gradual ATW were different from two out of three pipes receiving abrupt ATW. The copper pipe surface of the pipes receiving baseline water had baryte, copper sulfate hydroxide hydrate and calcite deposition. The copper pipe surface of pipes receiving gradual blend had hydrocerussite, cuprite and calcite. In the case of the pipes receiving abrupt ATW, only calcite was seen except in one pipe that had solid composition similar to those receiving gradual ATW.

In the case of solder, cerussite, hydrocerussite and hydroromarchite were observed and no differences were observed in the copper pipes receiving baseline and gradual and abrupt ATW. Similarly, no differences in the scale composition were observed for the brass rods receiving baseline water, gradual ATW, and abrupt ATW. The corrosion products on brass rods were primarily composed of zinc sulfate hydroxide, hydrozincite, and magnesium containing calcite.

4.3 Overall

Pipe loop testing can be useful for water agencies by allowing for an examination of specific materials that comprise an individual distribution system and customer premise plumbing. This study provides useful information about pipe loop testing design and operation for utilities.

Results of the study demonstrated that effective stabilization of ATW minimized impacts to the water quality from cast iron pipes. Impacts on premise plumbing were minor except for introduction of 100% ATW into the pipes. For copper pipe with lead solder, 100% ATW dramatically increased lead and decreased copper concentrations in the water, consistent with a mechanism of galvanic corrosion. The solids present in scales on the inner surface of the copper pipe and lead solder at the end of testing were different for the pipes that had been switched to ATW than for the pipes that remained with baseline water over the duration of the study, indicating that dissolution of sulfate minerals may occur with much lower sulfate water quality. This testing highlighted that water quality stability for one type of material does not provide effective corrosion for all.

CHAPTER 5

WRF 5193 Add-On: Disinfection Residual Formation in Stabilized Advanced Treated Water

5.1 Objectives

This work is an add-on to the previous study that was conducted (WRF 4953 Chapters 1 through 4). The primary objective of this Add-On project (WRF 5193) was to further evaluate the observation that chlorine residuals can significantly decrease in stabilized advanced treated water.

In the WRF 4953 chapters, pipe loop testing is described that evaluated the impacts of alternative water supplies (potable reuse) on distribution system water quality. Advanced treated water (ATW) from the MWD Regional Recycled Water Facility was stabilized through a calcite filter prior to introduction into pipe loops. Free chlorine then ammonia were added to the stabilized advanced treated water to form chloramines. Despite the lack of organic matter in the ATW, significant loss of total chlorine residual was observed that appeared to be a function of time (i.e., water held overnight had more constant residuals).

The chlorine residual issue is an important topic to pursue, as little research has been conducted on disinfectant residual stability in ATW and the results could drive design approaches for all different kinds of applications at full-scale. A similar phenomenon has been observed in desalinated water, with elevated bromide concentrations suspected of forming bromamine and resulting in a rapid loss of chlorine residual. The mechanism is uncertain for ATW, as bromide concentrations are not expected to be elevated in ATW. This research (WRF 5193) was undertaken to determine the potential impact that chlorine loss can have in ATW.

5.2 Testing Approach and Sampling Procedure

The WRF 5193 project used the existing configuration at MWD's PureWater demonstration facility, which included either of these trains depending on the sampling date:

- May 2021 – Nitrification-Denitrification tertiary membrane bioreactor (NdN tMBR) followed by single-pass RO then UV/Cl_2 AOP (chlorine dose of 3.5 mg/L free chlorine before AOP)
- November 2022 – Nitrification tertiary membrane bioreactor (N-only tMBR) followed by double-pass RO then UV/Cl_2 AOP (chlorine dose of 1.4 mg/L free chlorine before AOP)

Stabilized ATW was produced by running the PureWater demonstration facility treated water, initially stored in the ATW tank, through a calcite bed and cartridge filter and into the stabilization tank, as depicted in Figure 5-1.

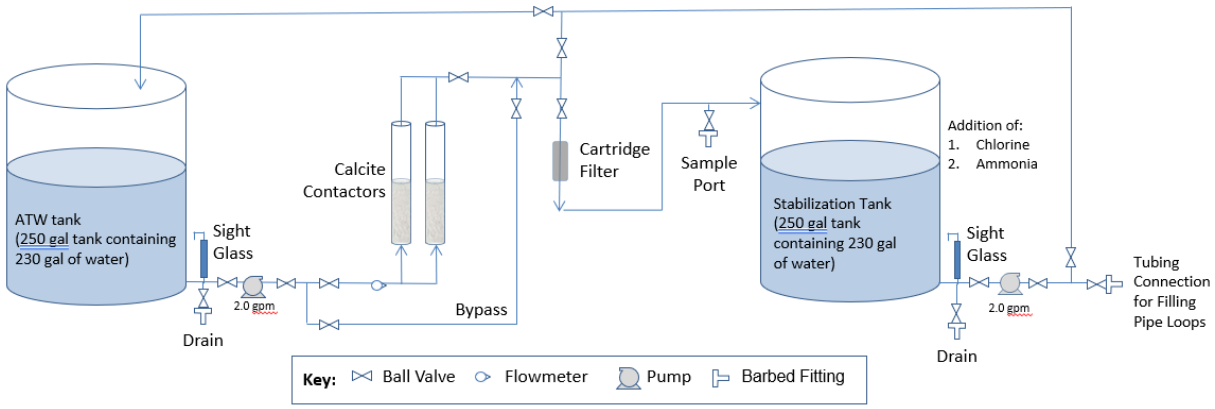

Figure 5-1. Advanced Treated Water Stabilization Process.

Testing consisted of three sets of samples:

1. Chlorine stability in ATW without calcite stabilization
2. Chlorine stability in ATW with calcite stabilization
3. Chloramine stability in ATW with calcite stabilization

For these tests, stabilized water quality was characterized by an alkalinity of 74 mg/L as $CaCO_3$ and calcium of 72 mg/L $CaCO_3$, pH of 7.8, and calcium carbonate precipitation potential (CCPP) of -0.9 mg/L as $CaCO_3$ and Langelier Saturation Index (LSI) of -0.09. Testing from the previous phase (WRF 4953) found variability of CCPP from approximately -3 to +8; results during this additional testing phase were within the envelope of the water quality previously tested.

5.2.1 Test 1: Chlorine Stability in ATW Without Calcite Stabilization

ATW water was collected from the MWD PureWater demonstration facility in the ATW tank. Before calcite stabilization was conducted on the ATW, 6 L of ATW water was sampled from the tank. The unstabilized ATW was measured in the field for alkalinity, calcium, pH, temperature, total chlorine, and total ammonia. In addition, chloride, sulfate, bromide, iodide, and TOC samples were collected, as these parameters may have an impact on chlorine demand or residual stability.

Chlorine stock solution was tested using distilled water to determine the stock solution strength. A dose equivalent to 4.0 mg/L chlorine (without demand) was added to the unstabilized ATW and sampled at intervals of 5 minutes, 15 minutes, 30 minutes, 2 hours, 4 hours, 6 hours, and 8 hours. Three water batches were dosed and sampled at each time interval to provide a triplicate analysis. Table 5-1 depicts the samples collected as a function of time from initial chlorine dosing.

Table 5-1. Test 1 Chlorine Addition before Calcite Stabilization.

Bottle #	5 min	15 min	30 min	2 hrs	4 hrs	6 hrs	8 hrs
1	X	X	X	X	X	X	X
2	X	X	X	X	X	X	X
3	X	X	X	X	X	X	X

5.2.2 Test 2: Chlorine Addition after Calcite Stabilization

For the second test, ATW water was passed through the calcite contactor and cartridge filter at a flow rate of 1 gpm. Approximately 6 L of stabilized ATW water was collected for Test 2. The stabilized ATW was measured in the field for alkalinity, calcium, pH, temperature, total chlorine, and total ammonia. In addition, chloride, sulfate, bromide, iodide, and TOC samples were collected for laboratory analysis.

A dose equivalent to 4.0 mg/L chlorine (without demand) was added to the stabilized ATW and sampled at intervals of 5 minutes, 15 minutes, 30 minutes, 2 hours, 4 hours, 6 hours, and 8 hours. Three water batches were dosed and sampled at each time interval to provide a triplicate analysis. Table 5-2 depicts the samples collected as a function of time from initial chlorine dosing.

Table 5-2. Test 2 Chlorine Addition after Calcite Stabilization.

Bottle #	5 min	15 min	30 min	2 hrs	4 hrs	6 hrs	8 hrs
1	X	X	X	X	X	X	X
2	X	X	X	X	X	X	X
3	X	X	X	X	X	X	X

5.2.3 Test 3: Chlorine and Ammonia Addition after Calcite Stabilization

For the third test, ATW water was passed through the calcite contactor and cartridge filter at a flow rate of 1 gpm. Approximately 6 L of stabilized ATW water was collected for Test 3. The stabilized ATW was measured in the field for alkalinity, calcium, pH, temperature, total chlorine, and total ammonia. In addition, chloride, sulfate, bromide, iodide, and TOC samples were collected for laboratory analysis.

A dose equivalent to 4.0 mg/L chlorine (without demand) was added to the stabilized ATW. Next, 0.5 mg/L ammonia (as nitrogen) was added to achieve a 5:1 chlorine:ammonia-N ratio (following initial chlorine degradation as observed in Test 2). The chloraminated water was sampled at intervals of 5 minutes, 15 minutes, 30 minutes, 2 hours, 4 hours, 6 hours, and 8 hours. Three water batches were dosed and sampled at each time interval to provide a triplicate analysis. Table 5-3 depicts the samples collected as a function of time from initial chlorine dosing.

Table 5-3. Test 3 Chloramine Addition after Calcite Stabilization.

Bottle #	5 min	15 min	30 min	2 hrs	4 hrs	6 hrs	8 hrs
1	X	X	X	X	X	X	X
2	X	X	X	X	X	X	X
3	X	X	X	X	X	X	X

5.3 Analytical Methods

Tables 5-4 and 5-5 summarize the field and lab analytical methods, including sample volumes, method reporting level (MRL), minimum detection level (MDL), and required preservatives used for this testing.

Table 5-4. Field Analytical Methods

Analyte	Analytical Method/ Instrument	Sample Volume Required (mL)	Method Reporting Limit
Alkalinity, Total	Hach 8203 (Digital Titration)	100	10 mg/L as $CaCO_3$
Calcium	Hach 8204 (Digital Titration)	100	10 mg/L as $CaCO_3$
pH/Temperature	SM 2550 (Thermometric)/ SM 4500H-B (Electrometric)	30	N/A
Chlorine, Total	Hach 8167 (DPD Method)	10	0.02 mg/L
Ammonia, Total	Hach 8155 (Salicylate Method)	10	0.02 mg/L as N

Table 5-5. Laboratory Analytical Methods.

Analyte	Analytical Method	Method Reporting Limit	Method Detection Limit	California MCL	California SMCL (or Notification Level*)
Chloride	EPA 300.0	0.5 mg/L	0.19 mg/L	N/A	250 mg/L*
Sulfate	EPA 300.0	0.5 mg/L	0.24 mg/L	N/A	250 mg/L*
Bromide	EPA 300.0	0.5 mg/L	0.012 mg/L	N/A	N/A
Iodide	EPA 332.0	1.0 mg/L	0.45 mg/L	N/A	
TOC	SM 5310B	0.30 mg/L	0.019 mg/L	N/A	N/A

5.4 Results

This section presents the results for the pipe loops for the disinfectant stability testing. Results reported include field data and laboratory data.

Prior to dosing, an initial sample of ATW was tested using the stock solution to determine the approximate dose that should be added to yield 2.5 to 3.0 mg/L chlorine residual at the 5-minute time point. A dose of 4 mg/L Cl_2 was found to provide this range of residual.

Figure 5-2 shows the time series data for Test 1 (unstabilized ATW with chlorine), Test 2 (stabilized ATW with chlorine) and Test 3 (stabilized ATW with chloramines). Good reproducibility among the triplicate samples for each time point was observed, shown as the standard deviation on each data point. Results of the testing revealed that the most significant decreases occurred in the first 5 minutes after dosing (approximately 1.0 to 1.5 mg/L) and for stabilized ATW with chlorine after 4 hours of contact time after which the residual reached a plateau. Chloramine yielded less total chlorine residual loss compared with chlorine for stabilized ATW, indicating that chlorine reactivity with stabilized ATW was less than with chloramine. From these results, it appears that stabilization with calcite results in greater chlorine loss for free chlorine but not chloramine, which might be either due to addition of constituents or the final water quality.

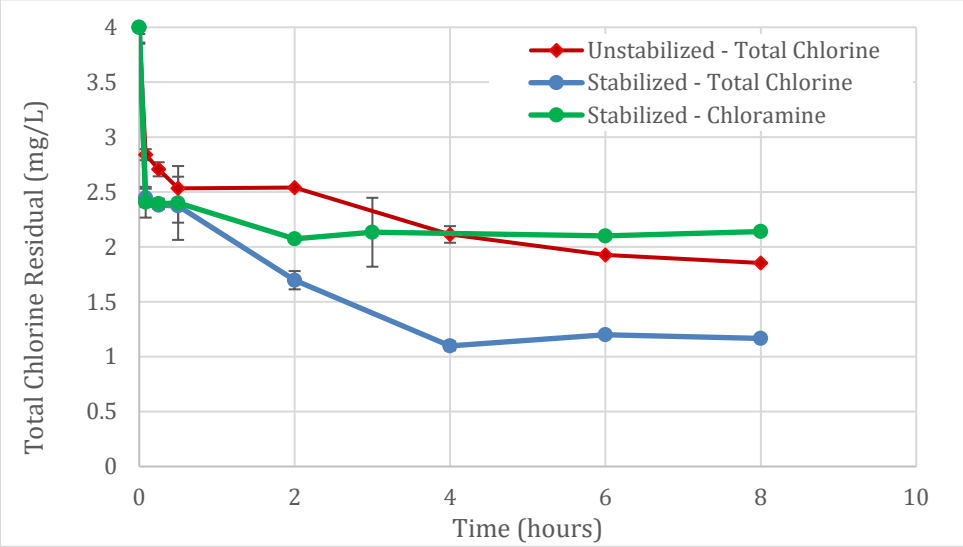

Figure 5-2. Chlorine Residuals after Initial Dosing.

Laboratory results confirmed low concentrations of anions and TOC, as expected for ATW produced from a treatment train including reverse osmosis (Table 5-6). An increase was observed in TOC, however, which may at least partly account for higher demand in stabilized ATW.

Similar chlorine residual losses were observed for testing conducted on desalinated water from a West Basin Municipal Water District (West Basin) (Figure 5-3). In the West Basin study, the role of bromide (present at 0.26 mg/L) was hypothesized to cause the chlorine residual loss. However, the ATW tested from the MWD PureWater demonstration facility had non-detect concentrations of bromide (Table 5-6). The cause for the initial chlorine residual loss remains unclear; however, both this study and the West Basin study showed that a period of approximately 4 hours is sufficient to reach a plateau on chlorine residual loss.

Table 5-6. Laboratory Results for Stabilized ATW.

Analyte	ATW Stabilized Result	ATW Stabilized Result	Method Reporting Limit	Method Detection Limit
Chloride	11	11	0.5 mg/L	0.19 mg/L
Sulfate	0.39	0.84	0.5 mg/L	0.24 mg/L
Bromide	<0.012	<0.012	0.5 mg/L	0.012 mg/L
Iodide	<0.45	<0.45	1.0 mg/L	0.45 mg/L
TOC	0.19	0.43	0.30 mg/L	0.019 mg/L

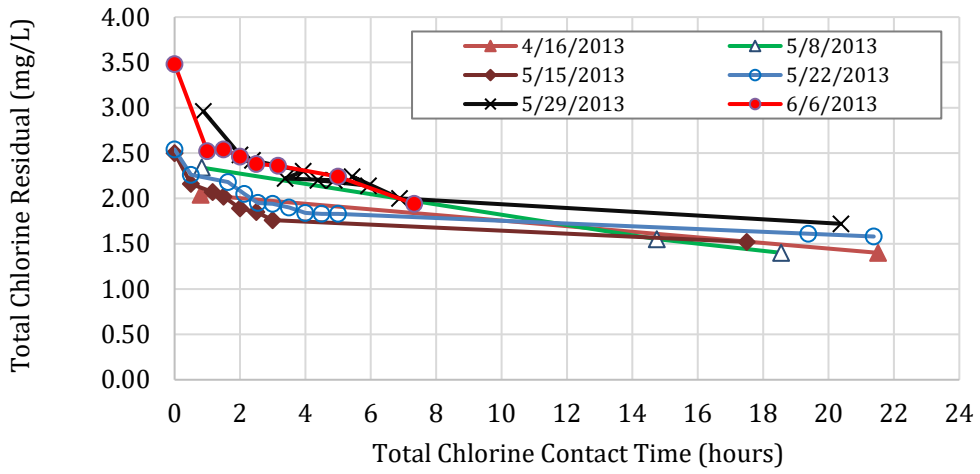

Figure 5-3. Chlorine Residuals in Stabilized Desalinated Water for West Basin.
(Adapted from Hazen and Sawyer 2014).

Of note, the testing conducted in WRF 5193 did not show as significant or rapid a residual loss compared with the results obtained in the WRF 4953 testing a year prior. One difference in the dates was the use of different ATW unit processes as described previously.

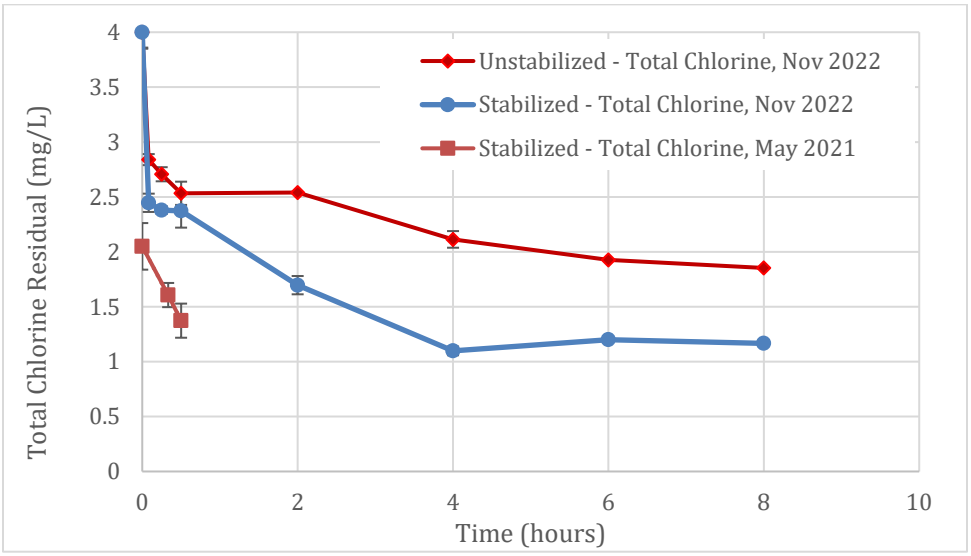

Figure 5-4. Chlorine Residuals for Tests Conducted in May 2021 and November 2022.

5.5 Conclusions

Disinfectant residual stability in finished water produced by advanced water treatment of wastewater has shown significant chlorine residual loss, particularly for free chlorinated water. The loss is most significant over the initial period, reaching a plateau at about four hours after initial dosing. Losses are similar in magnitude to those observed for a desalinated study, although it is not likely that bromide plays a significant role in the losses for ATW since concentrations were non-detect for ATW (which was proposed as a cause of the desalinated water disinfectant losses).

Additional study is needed to further determine how the ATW treatment train and fluctuations in water quality impact chlorine residual stability. Variation has been observed in this project for the two dates tested, continuing to pose the question of the mechanism and the magnitude of residual losses for which accommodations should be planned.

APPENDIX A

Pipe Harvesting Plan

A.1 Plan Objectives

The objective of the Pipe Harvesting Plan was to outline the procedures for extracting and transporting pipe to the study site at the Metropolitan Water District of Southern California's (MWD) Regional Recycled Water Advanced Purification Center (RRWAPC) in Carson, CA. This pipe harvesting plan included the sources of pipe samples; pipe handling and transportation requirements; and a schedule for pipe harvesting and pipe loop construction. Pipe harvesting was be performed by one of the participating utilities. Currently, Los Angeles Department of Water and Power (LADWP), Golden State Water Company (GSWC), and the City of Pasadena are evaluating pipeline replacement projects to identify appropriate pipe segments.

A.2 Identification of Materials for Testing

Prior testing has shown the value of harvesting unlined cast iron (UCI) tuberculated pipe, including both the complex precipitates and biofilms associated with the tubercles. Tuberculated UCI pipe is susceptible to causing colored water if water is corrosive. Newly installed ductile iron pipe is lined, making it unrepresentative of the precipitates and biofilms present in distribution systems. Therefore, representative materials must be harvested from the distribution system. Pipe loop testing of distribution system materials will focus on UCI pipe to test the stability of the deposits with blends of ATW.

A.3 Sources of Pipe

Specific piping types and size were selected by balancing the study objectives with study testing site constraints and project budget. A pipe diameter of four to six inches was selected for pipe loop testing because it is representative of typical system components while still being compatible with site size constraints. Using information gained from a prior pipe loop study[1], lengths of pipe sections were chosen to simultaneously (1) provide sufficient pipe surface area to water volume to be able to observe build-up constituents representing corrosion occurrence (e.g., iron and from UCI), (2) provide sufficient surface area so that the impact of variability from pipe surfaces is minimized, and (3) enable testing on the available space at the pilot site for the number of pipe loops desired.

Hazen and Sawyer confirmed that the utility/contractor had available couplings needed to cap and connect the harvested pipe to the pipe loops and keep the inside of the pipe wet during transport to the site. The steps for harvesting the pipe are outlined in the Harvesting Procedures section.

A.4 Preparation for Pipe Harvesting

Several steps were taken in preparation for the pipe harvesting. Prior to the pipe harvesting, Hazen and Sawyer began constructing the pipe loops (except for the harvested materials) to allow for quick installation of the UCI following the pipe harvesting. The loops were prepared so

that the pipe remained without water for as short of a time as possible to minimize disruption to the existing scale.

A.5 Harvesting Procedures

The following procedure was used to extract existing pipe segments for the purpose of a pipe loop study through pilot-scale testing:

- Four 4-foot segments of 4-inch or 6-inch UCI pipe were harvested from the distribution system, with advance testing to ensure that the pipe is unlined. The pipe was visually inspected to ensure that pipe was fairly uniform in appearance with respect to tuberculation and was not leaking. Photographs were taken of all phases of the pipe harvesting work.
- Any shock or disturbances to the pipe sections were prevented or mitigated during the excavation process to ensure that existing scale build-up within the pipe was kept intact. Hand shovels were used when clearing soil in the surrounding area of the pipe sections to minimize these impacts.
- The pipe order, orientation (e.g., up, down) and flow direction were labeled on the pipe prior to pipe excavation. The outer crust of the pipe was carefully scraped off, which will allow duct tape to adhere onto the pipe surface.
- The harvested pipe was drained and cut into four 4-foot-long segments on the site. Each section was handled with care to prevent any bending or flexing during transport to the pilot testing site.
- After cutting, the contractor immediately capped pipe segments on both ends to maintain humid conditions within the pipe to keep the scale damp. Layers of scale will slough off if the scale dries out, which is to be avoided.
- While harvesting the UCI pipe, the pipeline interior was visibly inspected to determine if scale formation or corrosion was present.
- The pipes were placed onto a flatbed truck/trailer and transported to the pilot testing site. Caution was taken to limit any vibration on the pipes by securing each segment down. Water was completely drained from the pipes to prevent potential sloshing of residual water that could have destroyed the scale structure.
- Upon arrival at the pilot testing site, the pipes were immediately assembled to minimize the time without water flowing through them.

A.6 Harvesting Schedule

To maintain the overall project schedule, the harvesting was planned for November or December 2020. Hazen and Sawyer worked with utilities to coordinate pipe harvesting work with ongoing CIP water main replacement projects.

APPENDIX B

Calcite Contactor Media Specifications

COLUMBIA RIVER CARBONATES
P.O. Box 2350 – 300 North Pekin Road
Woodland, Washington 98674
TEL: (360) 225 – 6505
FAX: (360) 225 – 5082
WATTS: (800) 735 – 6690

Puri-Cal ™

Puri-Cal ™

Typical Physical Characteristics

Mean Particle Size (µm)	550
Moisture (%)	< 0.2
Specific Gravity	2.7
Bulk Density (lb/cu. ft.)	89

Typical Chemical Analysis

$CaCO_3$ (%)	> 95
$MgCO_3$ (%)	< 3
Acid Insoluble (%)	< 2

CAS# 1317-65-3

NSF®
Certified to NSF/ANSI 60
MUL 400 gm/L

Typical Size Distribution

0.1% Plus 16 mesh (U.S. Standard)
10% Minus 40 mesh (U.S. Standard)

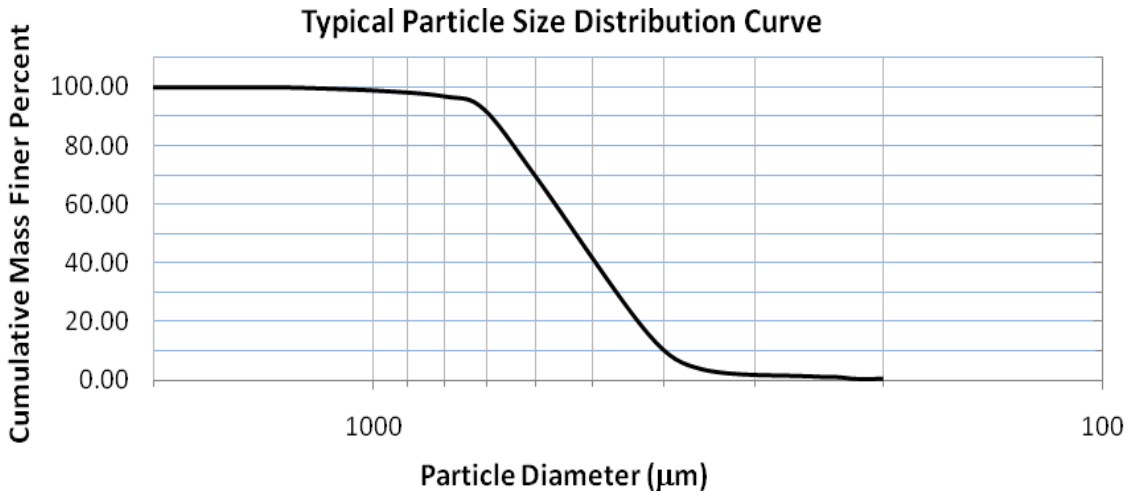

DATA SHEET

Revised by Leif Backstrom
November 2010

APPENDIX C

Scale Analysis

C.1 Elemental Composition of the Scales

Table C-1. Elemental Composition Reported in Mg/G of Scales Collected from Pipes. C1 – C3, C1 Solder – C3 Solder and B1-B3-B5 Received 100% ATW as a Gradual Blend. C4-C6, C4 Solder – C6 Solder, B4-B6-B7 Received 100% ATW Abruptly and C7- C9 and B2-B8-B9 Received Baseline Water.

		Al	Ca	Fe	Cu	Zn	Sn	Ba	Pb
Gradual ATW	**C1**	10			698	6	22	4	65
	C2	18	22		411	9	65	6	100
	C3	14	18		469	10	84	5	178
Abrupt ATW	**C4**	10			156	5	38	3	67
	C5	10	39		718	5	33	3	68
	C6	13	20		244	8	27	5	45
Baseline	**C7**	21	19		321	23	23	81	73
	C8	29	31		371	14	67	86	23
	C9	20	54		592	11	15	19	8
Gradual ATW	**cSolder1**	3	15		36	2	315	2	301
	cSolder2	6	33		93	5	146	3	425
	cSolder3	4	18		19	3	332	2	538
Abrupt ATW	**cSolder4**	3	11		25	2	446	1	449
	cSolder5	9	35		31	5	288	4	230
	cSolder6	4	13		32	5	328	2	513
Baseline	**cSolder7**	9	34		74	17	313	4	510
	cSolder8	6	22		383	6	159	2	324
	cSolder9	5	16		128	5	228	2	523
Gradual ATW	**B1**	12	14	3	41	664	1	2	15
	B3	11	13	10	315	491	8	3	48
	B5	11	10	9	55	556	2	3	10
Abrupt ATW	**B4**	12	27		153	619	2	2	18
	B6	12	9	8	40	673	2	2	51
	B7	14	18	4	23	718	1	2	16
Baseline	**B2**	25	6	11	81	627	2	3	14
	B8	18	19		28	740	1	2	11
	B9	16	19	4	44	608	1	2	33

DL: 0.5 mg/g for 0.1 g of solid digested (for all elements except Ca and Fe)
DL: 2.5 mg/g for 0.1 g of solid digested (for Ca and Fe)

C.1.1 EDS Line Scans of a Cross-Section of a Brass Rod

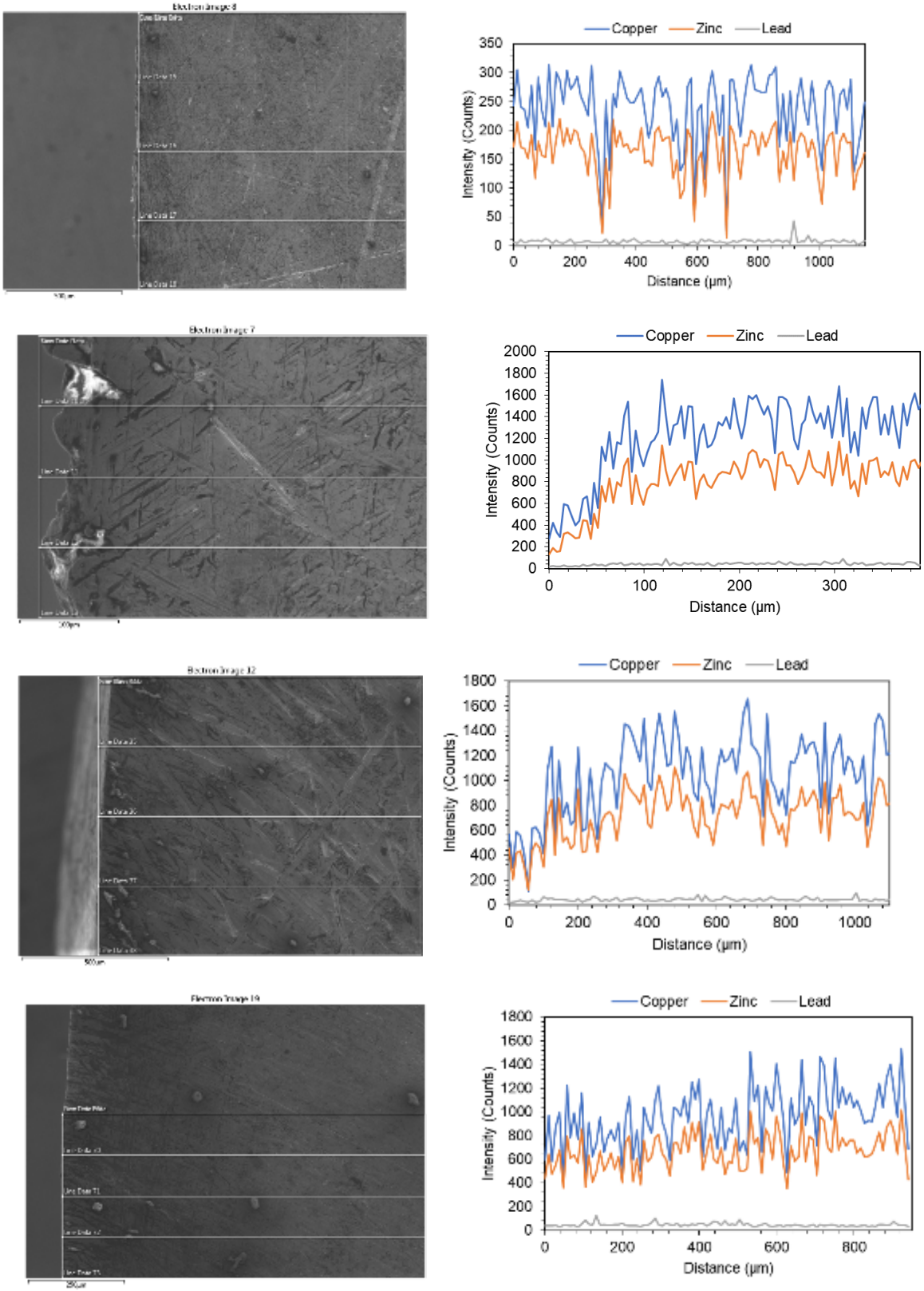

Figure C-1. Line Scan Images Accompanying the SEM Image of the Edge of the Brass Rods Receiving Gradual ATW (As-Received Brass Rod, B1, B3, B5).

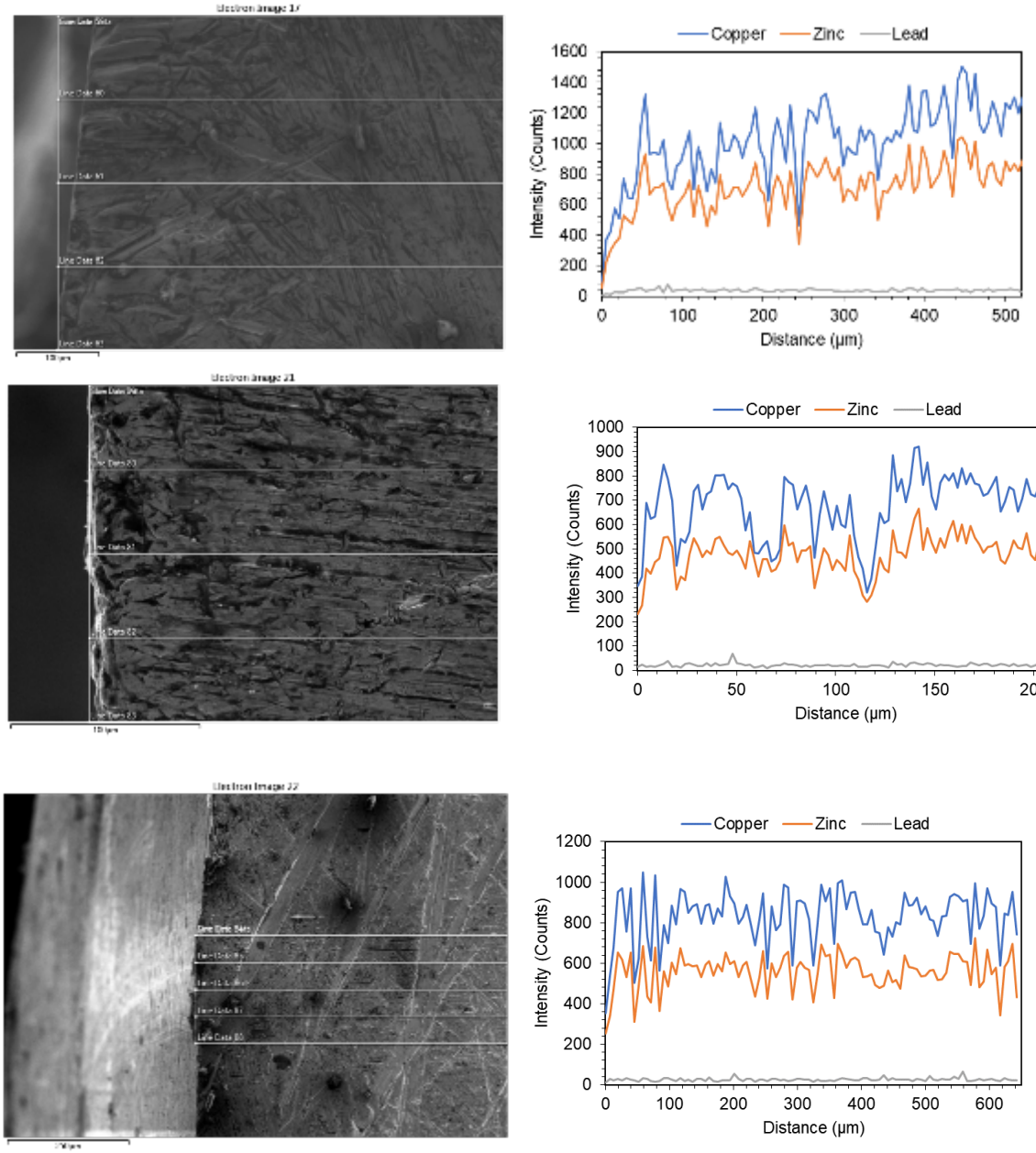

Figure C-2. Line Scan Images Accompanying the SEM Image of the Edge of the Brass Rods Receiving Gradual ATW (B4, B6, B7).

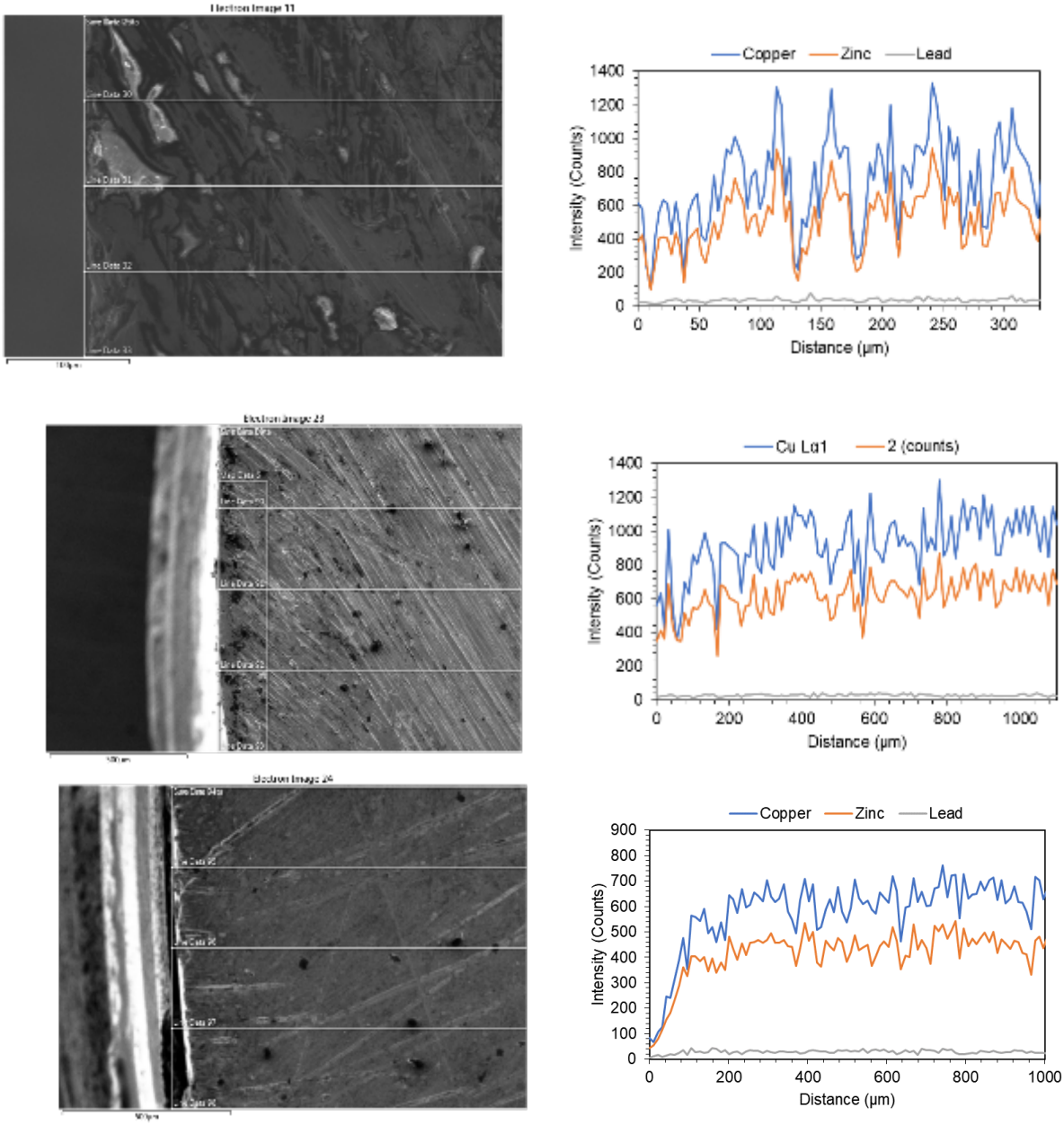

Figure C-3. Line Scan Images Accompanying the SEM Image of the Edge of the Brass Rods Receiving Gradual ATW (B2, B8, B9).

C.2 SEM Images of the Cross-Section of the Copper Pipes Containing Lead Solder

C.2.1 Pipes Receiving Gradual ATW (C1, C2 and C3)

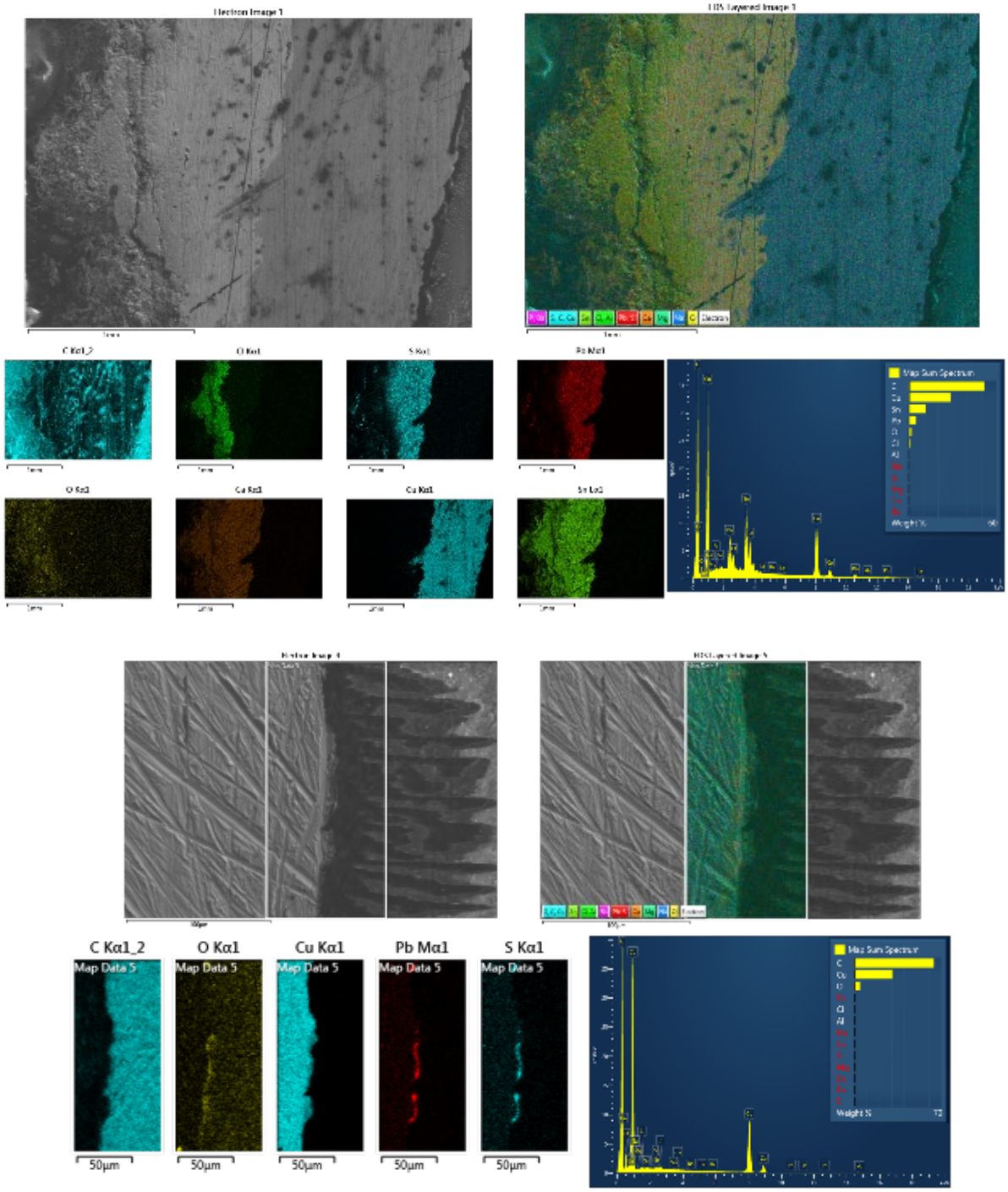

Figure C-4. SEM and EDS Maps of the Cross-Section of the Copper Pipe C1 with Lead Solder (top) Followed by a Copper Pipe Area Away from Lead (bottom) Consisting of SEM Image, SEM Image with a Multielement Overlay, EDS Maps of Different Elements and Semi-quantitative Elemental Composition in the Selected Area of EDS.

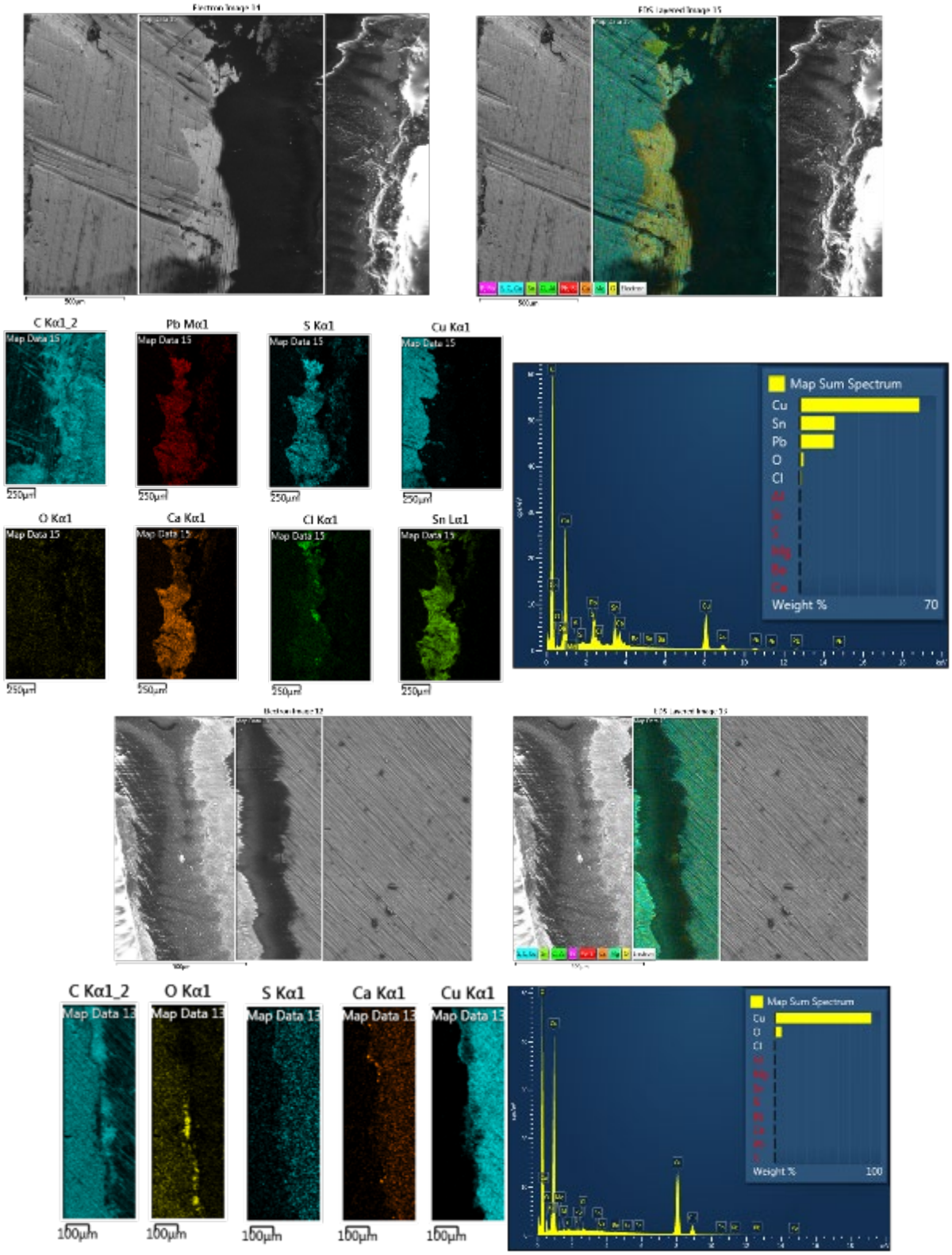

Figure C-5. SEM and EDS Maps of the Cross-Section of the Copper Pipe C2 with Lead Solder (top) Followed by a Copper Pipe Area Away from Lead (bottom) Consisting of SEM Image, SEM Image with a Multielement Overlay, EDS Maps of Different Elements and Semi-quantitative Elemental Composition in the Selected Area of EDS.

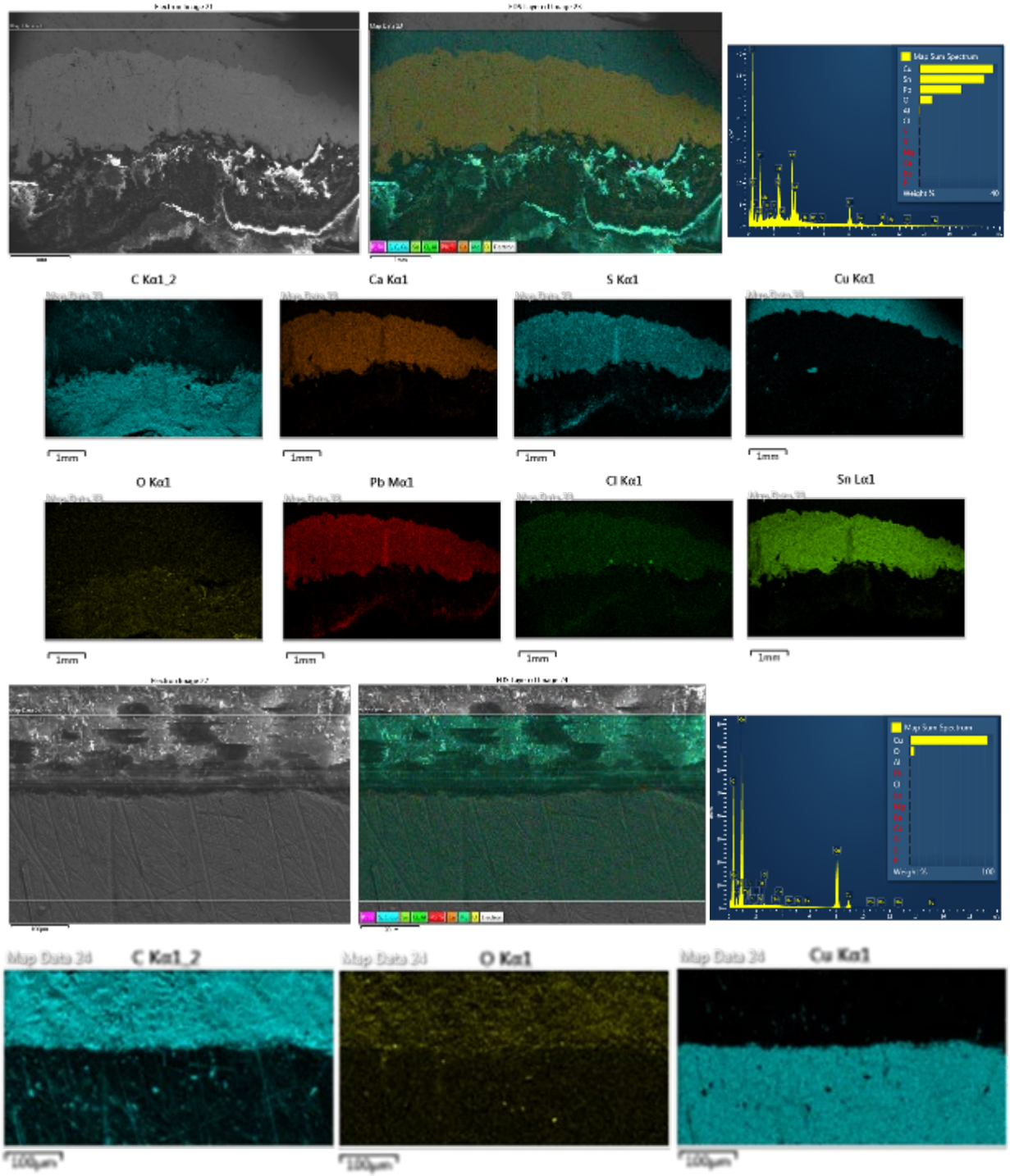

Figure C-6. SEM and EDS Maps of the Cross-Section of the Copper Pipe C3 with Lead Solder (top) Followed by a Copper Pipe Area Away from Lead (bottom) Consisting of SEM Image, SEM Image with a Multielement Overlay, EDS Maps of Different Elements and Semi-quantitative Elemental Composition in the Selected Area of EDS.

C.2.2 Pipes Receiving Abrupt ATW

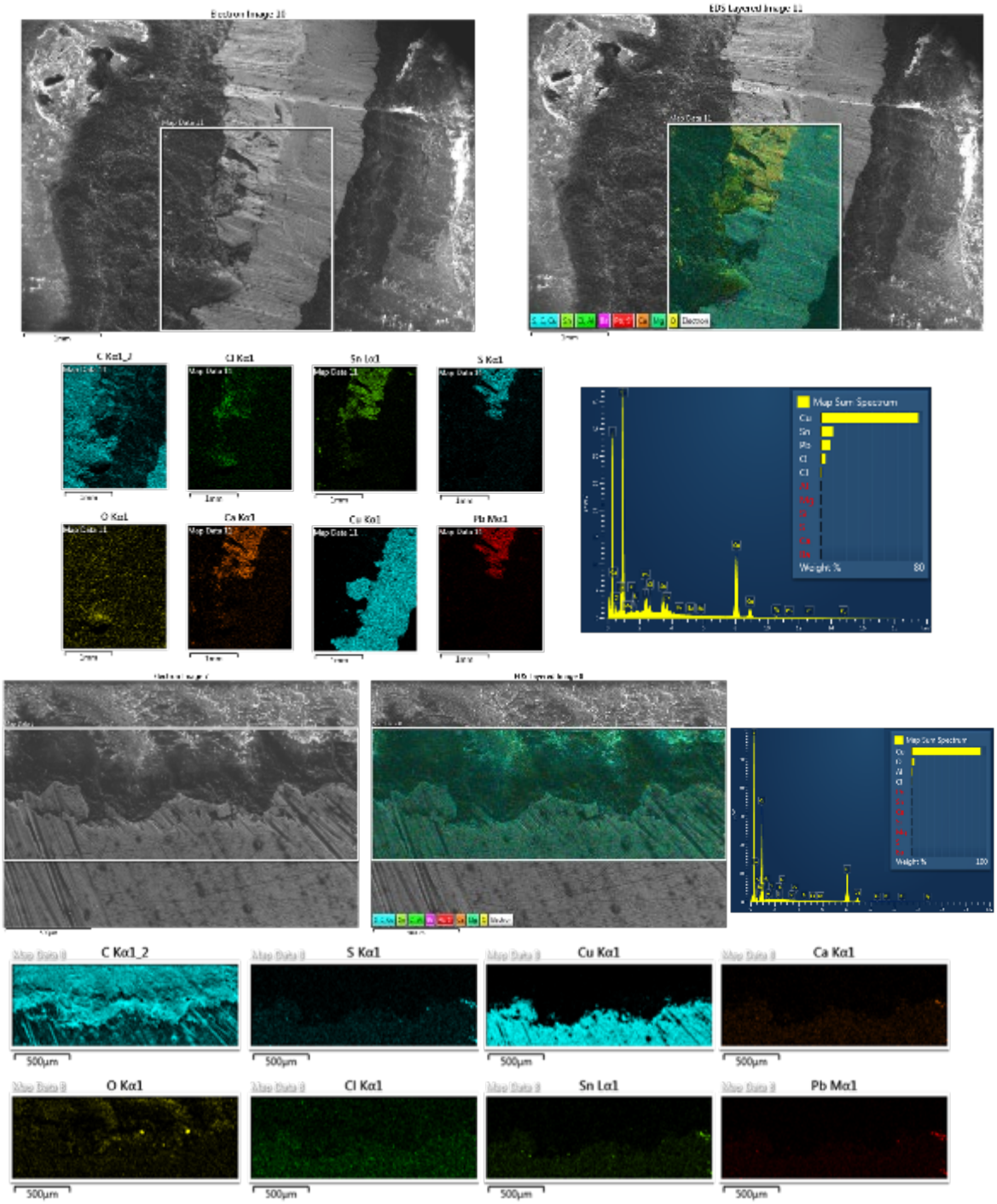

Figure C-7. SEM and EDS Maps of the Cross-Section of the Copper Pipe C4 with Lead Solder (top) Followed by a Copper Pipe Area Away from Lead (bottom) Consisting of SEM Image, SEM Image with a Multielement Overlay, EDS Maps of Different Elements and Semi-quantitative Elemental Composition in the Selected Area of EDS.

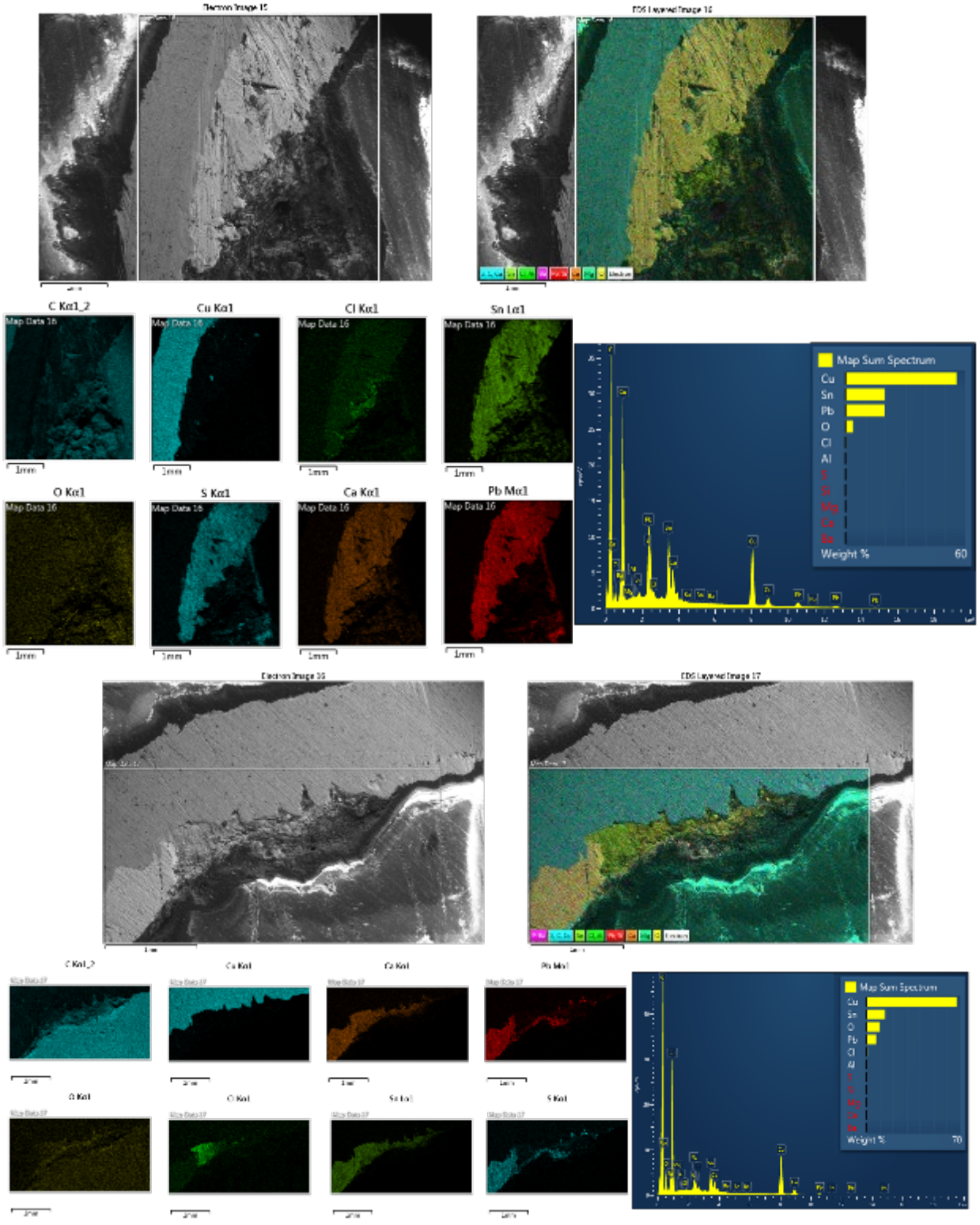
C Kα1_2
Cu Kα1
Cl Kα1
Sn Lα1
O Kα1
S Kα1
Ca Kα1
Pb Mα1
Map Sum Spectrum
Cu
Sn
Pb
O
Cl
Al
Weight %
60
70

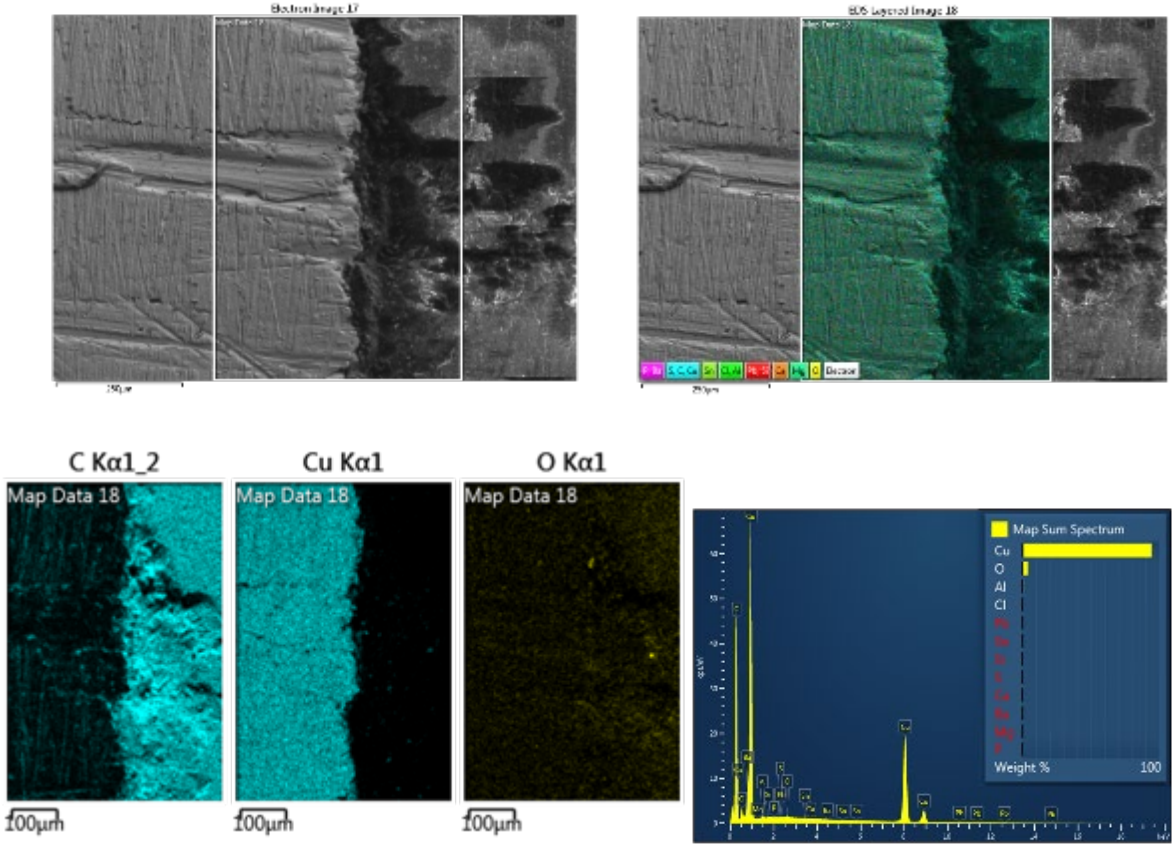

Figure C-8. SEM and EDS Maps of the Cross-Section of the Copper Pipe C5 with Lead Solder (top) Followed by a Copper Pipe Area Away from Lead (bottom) Consisting of SEM Image, SEM Image with a Multielement Overlay, EDS Maps of Different Elements and Semi-quantitative Elemental Composition in the Selected Area of EDS.

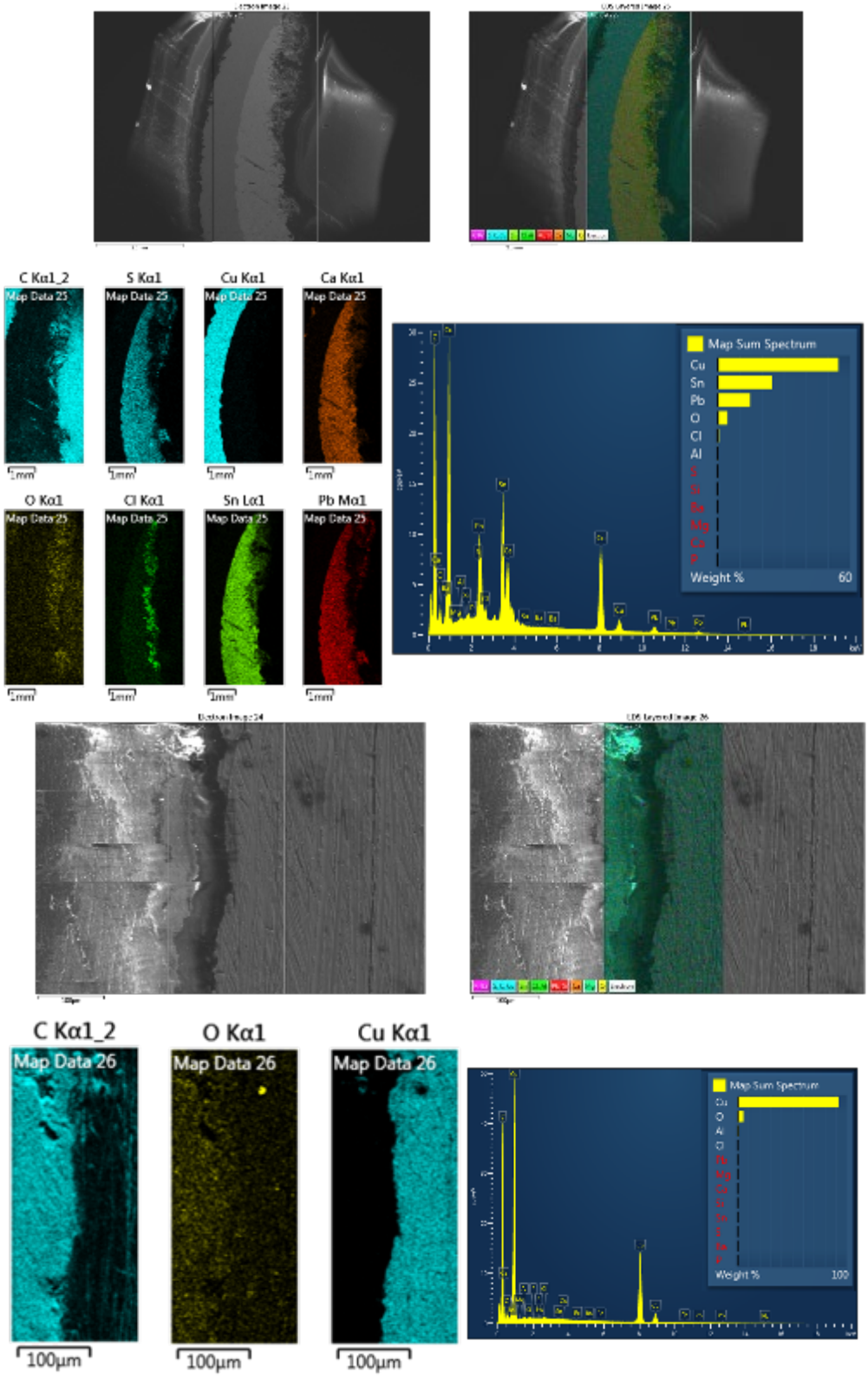

Figure C-9. SEM and EDS Maps of the Cross-Section of the Copper Pipe C6 with Lead Solder (top) Followed by a Copper Pipe Area Away from Lead (bottom) Consisting of SEM Image, SEM Image with a Multielement Overlay, EDS Maps of Different Elements and Semi-quantitative Elemental Composition in the Selected Area of EDS.

C.2.3 Pipes Receiving Baseline

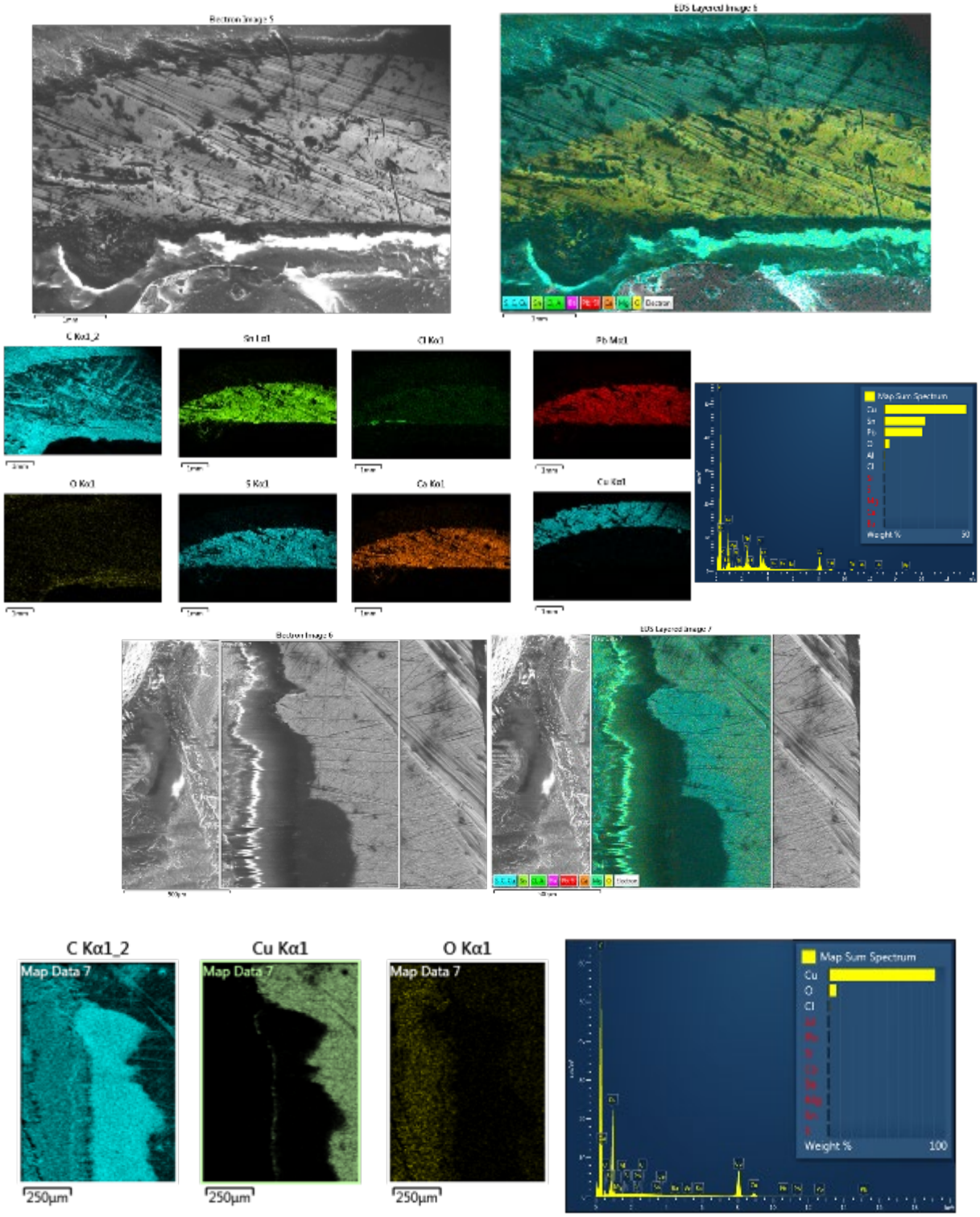

Figure C-10. SEM and EDS Maps of the Cross-Section of the Copper Pipe C7 with Lead Solder (top) Followed by a Copper Pipe Area Away from Lead (bottom) Consisting of SEM Image, SEM Image with a Multielement Overlay, EDS Maps of Different Elements and Semi-quantitative Elemental Composition in the Selected Area of EDS.

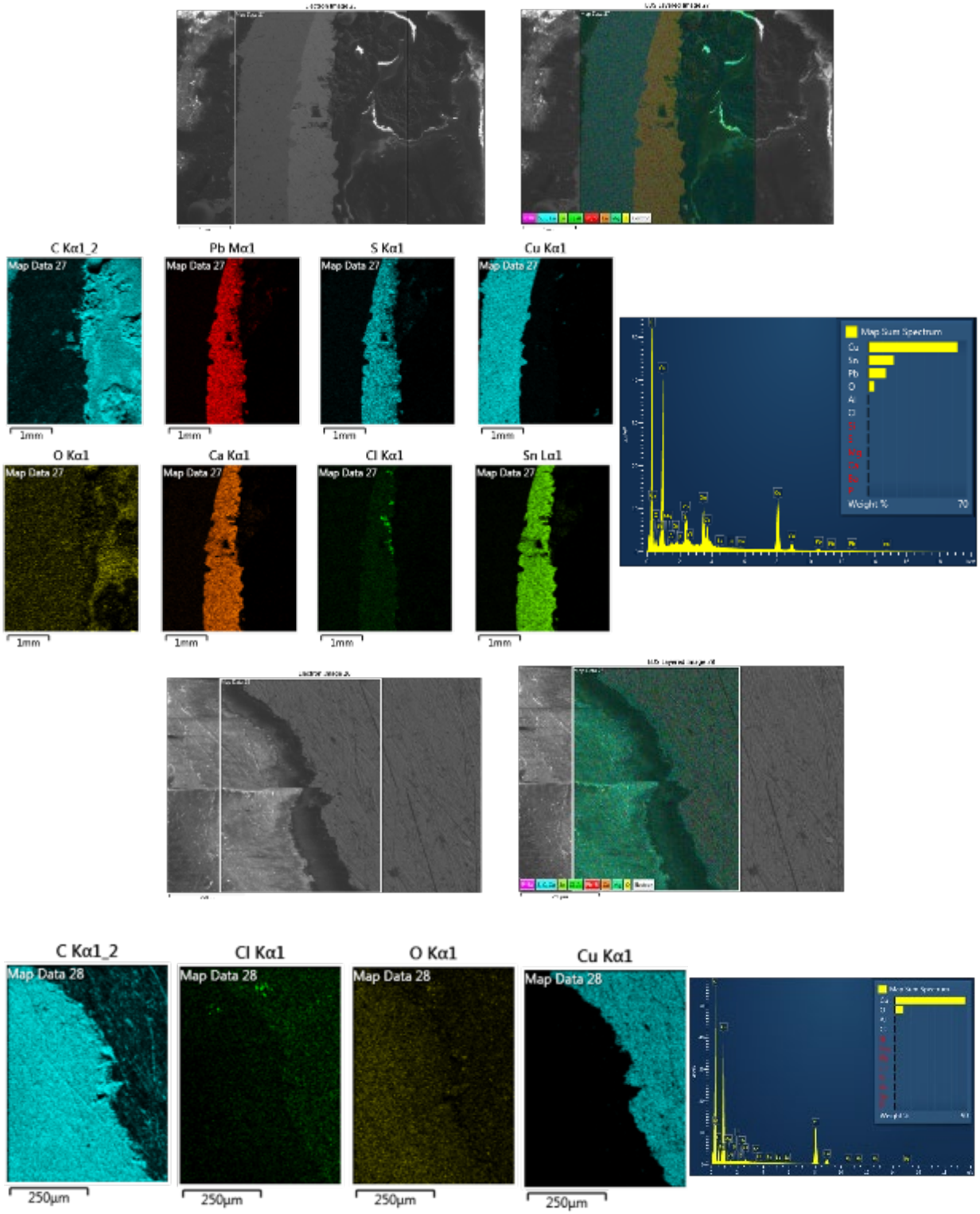

Figure C-11. SEM and EDS Maps of the Cross-Section of the Copper Pipe C8 with Lead Solder (top) Followed by a Copper Pipe Area Away from Lead (bottom) Consisting of SEM Image, SEM Image with a Multielement Overlay, EDS Maps of Different Elements and Semi-quantitative Elemental Composition in the Selected Area of EDS.

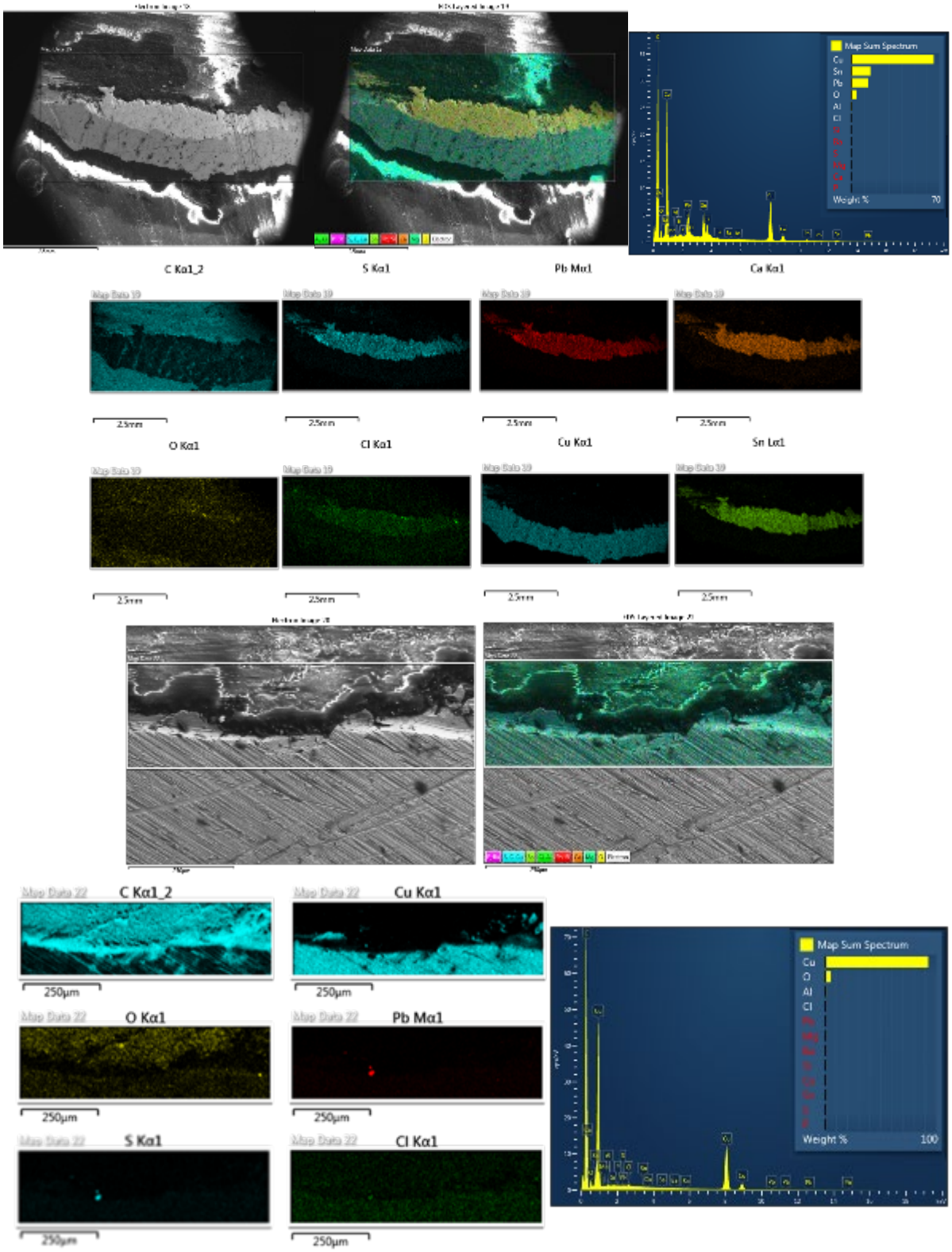

Figure C-12. SEM and EDS Maps of the Cross-Section of the Copper Pipe C9 with Lead Solder (top) Followed by a Copper Pipe Area Away from Lead (bottom) Consisting of SEM Image, SEM Image with a Multielement Overlay, EDS Maps of Different Elements and Semi-quantitative Elemental Composition in the Selected Area of EDS.

C.3 XRD of Scales Collected from the Copper Pipes Containing Lead Solder and Brass Rods

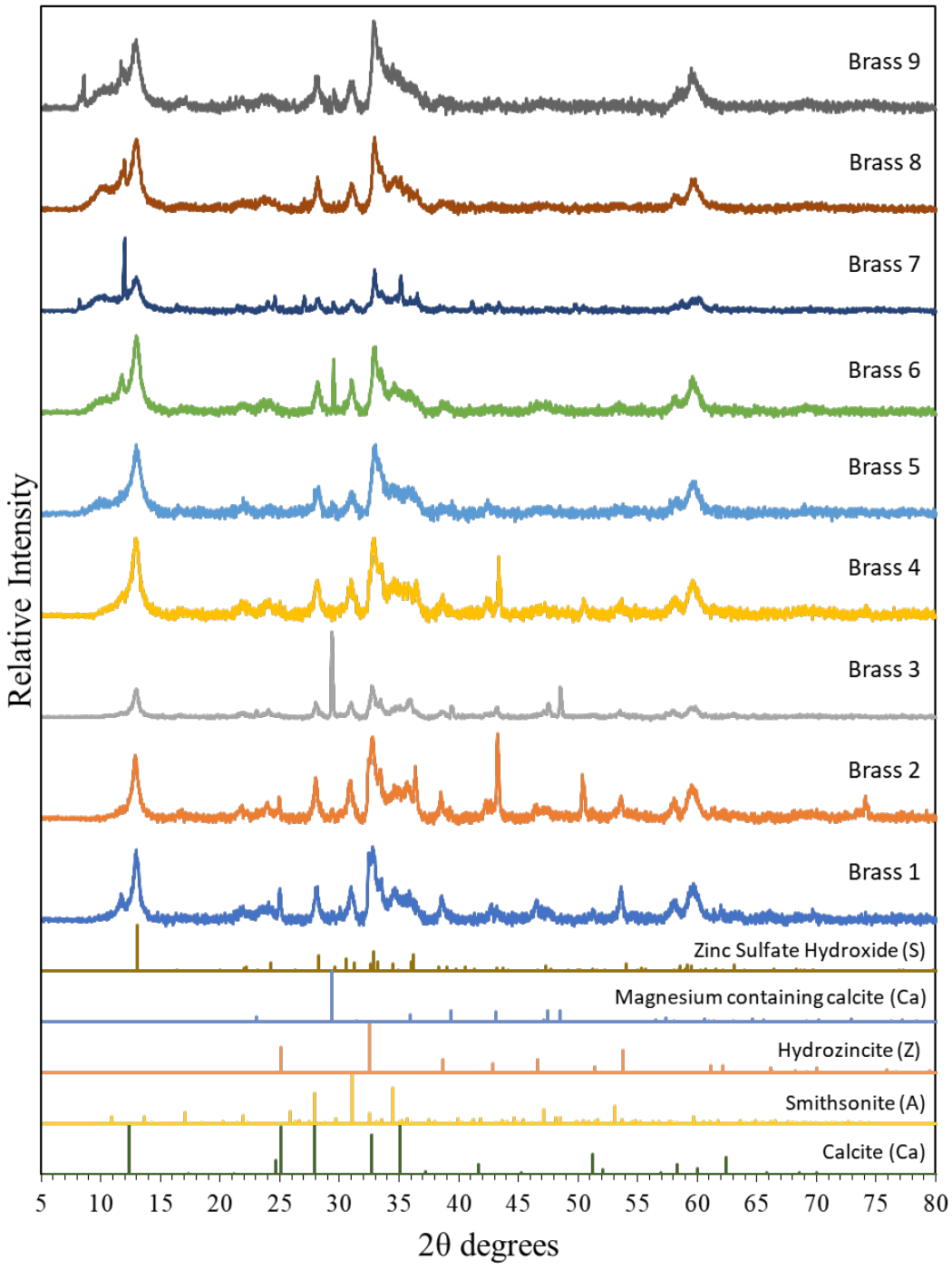

Figure C-13. XRD Pattern of Scales Collected from the Brass Rod Surface. Pipes B1, B3 and B5 Received Gradual ATW, Pipes B4, B6 and B7 Received Abrupt ATW and Pipes B2, B8 and B9 Received Baseline.

Table C-2. Solids Present on the Copper Pipe Surface That Were Identified Using XRD with Their Relative Concentration Indicated for Baseline, Gradual and Abrupt ATW.

	Zinc Sulfate Hydroxide	Hydrozincite	Mg Containing Calcite
B1	+	+	
B2	+	+	
B3	+		+
B4	+		
B5	+		
B6	+		+
B7	+		
B8	+		
B9	+		

+++ indicates the relative intensity of the solids in the pipe surface

C.4 Zinc Concentrations in Copper Pipes with Lead Solder

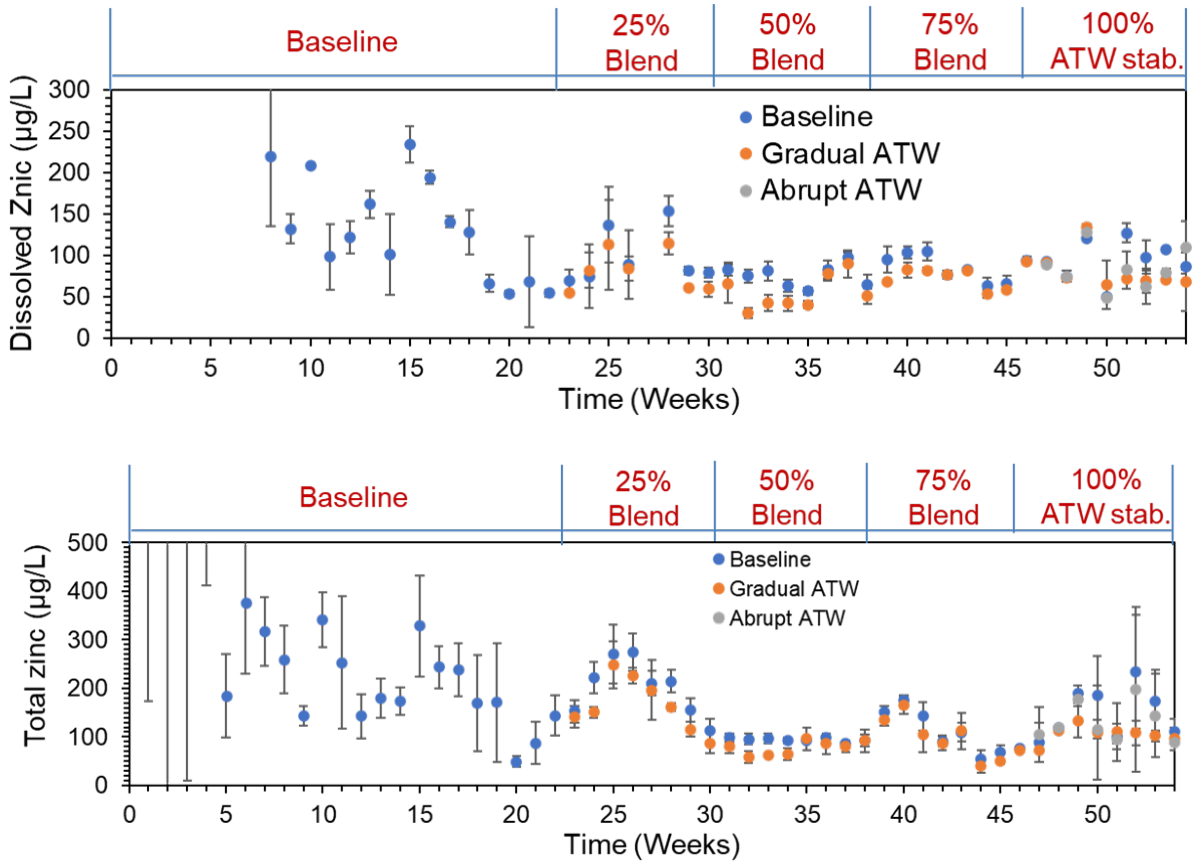

Figure C-14. Total Zinc (top) and Dissolved Zinc (bottom) Release from Copper Pipes Containing Lead Solder Receiving Baseline, Gradual ATW and Abrupt ATW.

References

Aghasadeghi, K., B. Trueman, S. Peldszus, A. Jakovljevic, P. Beaulieu, G. Gagnon, and P. Huck. 2019. "Revisiting Sodium Silicates as a Corrosion Control Treatment for Lead: A Pilot Study." In *Proc. of the Annual AWWA Water Quality Technology Conference*. Dallas, TX: AWWA.

Arnold, R., M. Raetz, and M. Edwards. 2011."Effects of Alkalinity, NOM, and Orthophosphate on Galvanic Corrosion." In *Proc. of the Annual AWWA Conference*. Washington, DC: AWWA.

Arnold, R. B. Jr. 2011. "New Insights into Lead and Copper Corrosion: Impacts of Galvanic Corrosion, Flow Pattern, Potential Reversal, and Natural Organic Matter." Master's Thesis, Virginia Polytechnic Institute and State University. etd-05132011-163933_Arnold_RB_T_2011.pdf (vt.edu)

Arnold, R. B., A. Griffin, and M. Edwards. 2012. "Controlling Copper Corrosion in New Construction by Organic Matter Removal." *Journal American Water Works Association* 104 (5): E310-317.

Arnold, R. B., A. E. Keithley, A. Cherry, K. Coffey, and J. Macauley. 2021. "Know the Benefits of Effective Manganese Management Strategies." *Opflow* 47 (8): 10-15.

Arnold, R. B., B. Rosenfeldt, J. Rhoades, C. Owen, and W. Becker. 2020. "Evolving Utility Practices and Experiences With Corrosion Control." *Journal American Water Works Association*, 112 (7): 26-40.

AwwaRF (American Water Works Association Research Foundation) and DVGW-Technologiezentrum Wasser. 1996. Internal Corrosion of Water Distribution Systems. 2nd edition. Project #725. Denver, CO: AwwaRF.

Bae, Y., J. D. Pasteris, and D. E. Giammar. 2020.""Impact of Orthophosphate on Lead Release from Pipe Scale in High pH, Low Alkalinity Water." *Water Research* 177: 115764.

Benjamin, M. M., H. Sontheimer, and P. Leroy. 1996. "Chapter 2: Corrosion of Iron and Steel." In *Internal Corrosion of Water Distribution Systems* (2nd Edition), edited by the American Water Works Association Research Foundation and DVGW-Technologiezentrum Wasser. Denver, CO: AwwaRF.

Blute, N. K., M. J. McGuire, N. West, N. Voutchkov, P. Maclaggan, and K. Reich. 2008. "Integration of Desalinated Seawater into a Distribution System: A Corrosion Pilot Study" *Journal American Water Works Association*, 100 (9): 117-131.

Blute, N., J. Pickard, Y. Wu, K. Chau, and L. Grijalva. 2014. "Ocean Desalination Water Quality Integration Study at West Basin MWD." In *Proc. of the Annual AWWA ACE Conference*. Boston, MA: AWWA.

Cantor, A. F., D. Denig-Chakroff, R. Vela, M. Oleinik, and D. Lynch. 2000. "Use of Polyphosphate in Corrosion Control." *Journal American Water Works Association* 92 (2): 95-102.

Camara, E., K. Montreuil, A. Knowles, and G. Gagnon. 2013. "Role of the Water Main in Lead Service Line Replacement: A Utility Case Study." *Journal American Water Works Association* 105 (8): E423-E431.

Cartier, C., E. Dore, L. Laroche, S. Nour, M. Edwards, and M. Prevost. 2013. "Impact of Treatment on Pb Release from Full and Partially Replaced Harvested Lead Service Lines (LSLs)." *Water Research* 47 (2): 661-671.

Chiodini, R. A. 1998. “Use of Sodium Silicate for the Control of Lead and Copper.” *J. New England American Water Works Association*, 112 (2): 147-152.

Choi, J., B. G. Choi, and S. Hong. 2015. “Effects of NF Treated Water on Corrosion of Pipe Distribution System and its Implications to Blending with Conventionally Treated Water.” *Desalination* 360: 138-145.

Desantis, M. K., S. Triantafyllidou, M. R. Schock, and D. A. Lytle. 2018. “Mineralogical Evidence of Galvanic Corrosion in Drinking Water Lead Pipe Joints.” *Environmental Science & Technology* 52 (6): 3365-3374.

Deshommes, E., L. Laroche, S. Nour, C. Cartier, and M. Prévost. 2010. “Source and Occurrence of Particulate Lead in Tap Water.” *Water Research* 44 (12): 3734-3744.

Dodrill, D. M., and M. Edwards. 1995. “Corrosion Control on the Basis of Utility Experience.” *Journal American Water Works Association* 87 (7): 74-85.

Doré, E., E. Deshommes, L. Laroche, S. Nour, and M. Prevost. 2019. “Study of the Long-Term Impacts of Treatments on Lead Release from Full and Partially Replaced Harvested Lead Service Lines.” *Water Research* 149: 566-577.

Doré, E., E. Deshommes, L. Laroche, S. Nour, and M. Prévost. 2019. “Lead and Copper Release from Full and Partially Replaced Harvested Lead Service Lines: Impact of Stagnation Time Prior to Sampling and Water Quality.” *Water Research* 150: 380-391.

Dryer, D. J., and G. V. Korshin. 2007. “Investigation of the Reduction of Lead Dioxide by Natural Organic Matter.” *Environmental Science and Technology* 41 (15): 5510-5514.

Dudi, A. 2004. “Reconsidering Lead Corrosion in Drinking Water: Product Testing, Direct Chloramine Attack and Galvanic Corrosion.” Master’s thesis, Virginia Polytechnic Inst. and State Univ., Blacksburg, Va.

Edwards, M., J. Ferguson, and S. Reiber. 1994. “The Pitting Corrosion of Copper.” *Journal American Water Works Association* 86 (7): 74-90.

Edwards, M., M. Schock, and T. E. Meyer. 1996. “Alkalinity, pH, and Copper Corrosion By-product Release.” *Journal American Water Works Association* 88 (3): 81-94.

Edwards, M., and N. Sprague. 2001. “Organic Matter and Copper Corrosion By-product Release: A Mechanistic Study.” *Corrosion Science* 43 (1): 1-18.

Edwards, M., L. Hidmi, and D. Gladwell. 2002. “Phosphate Inhibition of Soluble Copper Corrosion Byproduct Release.” *Corrosion Science* 44 (5): 1057.

Edwards, M., and A. Dudi. 2004. “Role of Chlorine and Chloramine in Corrosion of Lead-Bearing Plumbing Materials.” *Journal American Water Works Association* 96 (10): 69-81.

Edwards, M. A., and S. Triantafyllidou. 2007. “Chloride-to-Sulfate Mass Ratio and Lead Leaching to Water.” *Journal American Water Works Association* 99 (7): 96-109.

Elfland, C., P. Scardina, and M. Edwards. 2010. “Lead-Contaminated Water from Brass Plumbing Devices in New Buildings.” *Journal American Water Works Association* 102 (11): 66-76.

Frenkel, A. I., and G. V. Korshin. 1999. “EXAFS Studies of the Chemical State of Lead and Copper in Corrosion Products Formed on the Brass Surface in Potable Water.” *Journal of Synchrotron Radiation* 6: 653-655.

Gerke, T. L., J. B. Maynard, M. R. Schock, and D. L. Lytle. 2008. “Physiochemical Characterization of Five Iron Tubercles from a Single Drinking Water Distribution System: Possible New Insights on Their Formation and Growth.” *Corrosion Science* 50 (7): 2030-2039.

Hazen and Sawyer. 2014. “Water Quality Integration Report.” Report to West Basin Municipal Water District.

Hill, A. S., and F. Lemieux. 2022. “Beware of Legacy Manganese Issues in Distribution Systems.” *Opflow* 48 (1): 16-21.

Hu, J., H. Dong, Q. Xu, W. Ling, J. Qu, and Z. Qiang. 2018. “Impacts of Water Quality on the Corrosion of Cast Iron Pipes for Water Distribution and Proposed Source Water Switch Strategy.” *Water Research* 129: 428-435.

Imran, S. A., J. D. Dietz, G. Mutoti, W. Xiao, J. S. Taylor, and V. Desai. 2006. “Optimizing Source Water Blends for Corrosion and Residual Control in Distribution Systems.” *Journal American Water Works Association* 98 (5): 107-115.

Kim, E. J., and J. E. Herrera. 2010. “Characteristics of Lead Corrosion Scales Formed During Drinking Water Distribution and their Potential Influence on the Release of Lead and Other Contaminants.” *Environmental Science and Technology* 44 (16): 6054-6061.

Kim, E. J., J. E. Herrera, D. Huggins, J. Braam, and S. Koshowski. 2011.“Effect of pH on the Concentrations of Lead and Trace Contaminants in Drinking Water: A Combined Batch, Pipe Loop and Sentinel Home Study.” *Water Research* 45 (9): 2763-2774.

Korshin, G. V., J. F. Ferguson, and A. N. Lancaster. 2000. “Influence of Natural Organic Matter on the Corrosion of Leaded Brass in Potable Water.” *Corrosion Science* 42 (1): 53-66.

Korshin, G. V., J. F. Ferguson, and A. N. Lancaster. 2005. “Influence of Natural Organic Matter on the Morphology of Corroding Lead Surfaces and Behavior of Lead-Containing Particles.” *Water Research* 39 (5): 811-818.

LeChevallier, M. W., C. Norton, A. K. Camper, P. Morin, B. Ellis, W. Jones, A. Rompe, M. Prevost, J. Coallier, P. Servais, D. Holt, A. Delanoue, and J. Colbourne. 1998. *Microbial Impact of Biological Filtration*. Project 917. Denver, CO: AWWA Research Foundation.

Lei, I.-L., D.-Q. Ng, S. S. Sable, and Y.-P. Lin. 2018. “Evaluation of Lead Release Potential of New Premise Plumbing Materials.” *Environmental Science and Pollution Research* 25 (28): 27971-27981.

Li, S., L. Ni, C. Sun, and L. Wang. 2004. “Influence of Organic Matter on Orthophosphate Corrosion Inhibition for Copper Pipe in Soft Water.” *Corrosion Science* 46 (1): 137-145.

Li, X., H. Wang, Y. Zhang, C. Hu, and M. Yang. 2014. “Characterization of the Bacterial Communities and Iron Corrosion Scales in Drinking Groundwater Distribution Systems with Chlorine/Chloramine.” *International Biodeterioration & Biodegradation* 96: 71-79.

Li, X., H. Wang, X. Hu, C. Hu, and L. Liao. 2016. “Characteristics of Corrosion Scales and Biofilm in Aged Pipe Distribution Systems with Switching Water Source.” *Engineering Failure Analysis* 60: 166-175.

Li, B., B. F. Trueman, E. Dore, and G. A. Gagnon. 2021. “Effectiveness of Sodium Silicates for Lead Corrosion Control: A Critical Review of Current Data.” *Environmental Science & Technology Letters* 8 (11): 932-939.

Lin, N. H., A. Torrents, A. P. Davis, M. Zeinali, and F. A. Taylor. 1997. “Lead Corrosion Control from Lead, Copper‐Lead Solder, and Brass Coupons in Drinking Water Employing Free and Combined Chlorine.” *Journal of Environmental Science & Health Part A,* 32 (4): 865-884.

Lin, Y.-P., and R. L. Valentine. 2008. “The Release of Lead from the Reduction of Lead Oxide (PbO_2) by Natural Organic Matter.” *Environmental Science and Technology* 42 (3): 760-765.

Lin, Y.-P., and R. L. Valentine. 2009. “Reduction of Lead Oxide (PbO_2) and Release of Pb(II) in Mixtures of Natural Organic Matter, Free Chlorine and Monochloramine.” *Environmental Science and Technology* 43 (10): 3872-3877.

Lin, Y.-P., and R. L. Valentine. 2010. “Reductive Dissolution of Lead Dioxide (PbO_2) in Acidic Bromide Solution.” *Environmental Science & Technology* 44 (10): 3895-3900.

Lintereur, P. A., S. J. Duranceau, J. S. Taylor, and E. D. Stone. 2012. “Sodium Silicate Impacts on Lead Release in a Blended Potable Water Distribution System.” *Desalination and Water Treatment* 16 (1-3): 427-438.

Liu, H., K. D. Schonberger, G. V. Korshin, J. F. Ferguson, P. Meyerhofer, E. Desormeaux, and H. Luckenbach. 2010.“Effects of Blending of Desalinated Water with Treated Surface Drinking Water on Copper and Lead Release.” *Water Research* 44 (14): 4057-4066.

Lytle, D., M. Schock, and T. Sorg. 1996. “Controlling Lead Corrosion in the Drinking Water of a Building by Orthophosphate and Silicate Treatment.” *Journal of New England Water Works Association* 110 (3): 202-217.

Lytle, D. A., and M. R. Schock. 2000. “Impact of Stagnation Time on Metal Dissolution from Plumbing Materials in Drinking Water.” *Journal of Water Supply: Research and Technology-AQUA* 49 (5): 243-257.

Lytle, D., P. Sarin, and V. L. Snoeyink. 2005. “The Effect of Chloride and Orthophosphate on the Release of Iron from a Cast Iron Pipe Section.” *Journal of Water Supply: Research and Technology – AQUA* 54 (5): 267-281.

Lytle, D., and M. R. Schock. 2008. “Pitting Corrosion of Copper in Waters with High pH and Low Alkalinity.” *Journal American Water Works Association* 100 (3): 115-129.

Lytle, D., and M. Nadagouda. 2010. “A Comprehensive Investigation of Copper Pitting Corrosion in a Drinking Water System.” *Corrosion Science* 52 (6): 1927-1938.

Lytle, D. A. 2017. “Corrosion of Distribution System Materials in Low Dissolved Inorganic Carbon (Alkalinity) Waters.” Presentation at the Metropolitan Water District of Southern California Expert Workshop, October 2017.

Lytle, D. A., M. Tang, A. T. Francis, A. J. O’Donnell, and J. L. Newton. 2020. “The Effect of Chloride, Sulfate, and Dissolved Inorganic Carbon on Iron Release from Cast Iron.” *Water Research*, 183: 116037.

Marshall, B. 2004. “Initiation, Propagation, and Mitigation of Aluminum and Chlorine-Induced Pitting Corrosion.” Master’s thesis, Virginia Polytechnic Inst. and State Univ., Blacksburg, Va.

Masters, S., and M. Edwards. 2015.“Increased Lead in Water Associated with Iron Corrosion.” *Environmental Engineering Science* 32 (5): 361-369.

Masters, S., J. Parks, A. Atassi, and M. A. Edwards. 2015. “Distribution System Water Age Can Create Premise Plumbing Corrosion Hotspots.” *Environmental Monitoring and Assessment* 187 (9): 559.

McNeill, L., and M. Edwards. 2001. “Iron Pipe Corrosion in Distribution Systems.” *Journal American Water Works Association* 93 (7): 88-100.

McNeill, L. S., and M. Edwards. 2002. “Phosphate Inhibitor Use at US Utilities.” *Journal American Water Works Association* 94 (7): 57-63.

Mishrra, A., Z. Wang, V. Sidorkiewicz, and D. E. Giammar. 2021. “Effect of Sodium Silicate on Lead Release from Lead Service Lines.” *Water Research* 188: 116485.

Ng, D. Q., and Y. P. Lin. 2015. “Effects of pH Value, Chloride and Sulfate Concentrations on Galvanic Corrosion Between Lead and Copper in Drinking Water.” *Environmental Chemistry* 13 (4): 602-610.

Nguyen, C. K., K. R. Stone, A. Dudi, and M. A. Edwards. 2010. “Corrosive Microenvironments at Lead Solder Surfaces Arising from Galvanic Corrosion with Copper Pipe.” *Environmental Science and Technology* 44 (18): 7076-7081.

Nguyen, C. K., K. R. Stone, and M. A. Edwards. 2011. “Chloride-to-Sulfate Mass Ratio: Practical Studies in Galvanic Corrosion of Lead Solder.” *Journal American Water Works Association* 103 (1): 81-92.

Peng, C. Y., G. V. Korshin, R. L. Valentine, A. S. Hill, M. J. Friedman, and S. H. Reiber. 2010. “Characterization of Elemental and Structural Composition of Corrosion Scales and Deposits Formed in Drinking Water Distribution Systems.” *Water Research* 44 (15): 4570-4580.

Rushing, J. C., and M. Edwards. 2004. “Effect of Aluminum Solids and Chlorine on Cold Water Pitting of Copper.” *Corrosion Science* 46 (12): 3069.

Salveson, A., J. Sutherland, E. Garvey, E. Charbonnet, E. Steinle-Darling, and M. Edwards. 2018. *Blending Requirements for Water From Direct Potable Reuse Treatment Facilities*. Project 4536. Denver, CO: The Water Research Foundation.

Sandvig, A., P. Kwan, G. Kirmeyer, B. Maynard, R. Mast, and R. Rhodes. 2008. *Contribution of Service Line and Plumbing Fixtures to Lead and Copper Rule Compliance Issues*. Report 91229. Denver, CO: AwwaRF.

Sarin, P., J. Clement, V. Snoeyink, and W. Kriven. 2003. “Iron Release from Corroded Unlined Cast-Iron Pipe.” *Journal American Water Works Association* 95 (11): 85-96.

Sarin, P., V. L. Snoeyink, J. Bebee, K. K. Jim, M. A. Beckett, W. M. Kriven, and J. A. Clement. 2004a. “Iron Release from Corroded Iron Pipes in Drinking Water Distribution Systems: Effect of Dissolved Oxygen.” *Water Research* 38 (5): 1259-1269.

Sarin, P., V. L. Snoeyink, D. A. Lytle, and W. M. Kriven. 2004b. “Iron Corrosion Scales: Model for Scale Growth, Iron Release and Colored Water Formation.” *Journal Environmental Engineering* 130 (4): 364-373.

Sarver, E., K. Dodson, R. P. Scardina, R. Lattyak, M. Edwards, and C. Nguyen. 2011. “Copper Pitting in Chlorinated High-pH Potable Water.” *Journal American Water Works Association* 103 (3): 86-98.

Sarver, E., and M. Edwards. 2012. “Inhibition of Copper Pitting Corrosion in Aggressive Potable Waters.” *International Journal of Corrosion,* Vol. 2012, Article ID 857823.

Schock, M., and D. Lytle. 2010.“Internal Corrosion and Deposition Control.” In *Water Quality and Treatment: A Handbook of Community Water Supplies*, edited by J.K Edzwald, 6th ed. New York: McGraw-Hill.

Shuldener, H. L., and S. Sussman. 1960. “Silicate as a Corrosion Inhibitor in Water Systems.” *Corrosion* 16 (7): 354t-358t.

Stericker, W. 1938. “Sodium Silicates in Water to Prevent Corrosion.” *Industrial & Engineering Chemistry* 30 (3): 348-351.

Sun, H., B. Shi, D. A. Lytle, Y. Bai, and D. Wang. 2014. “Formation and Release Behavior of Iron Corrosion Products under the Influence of Bacterial Communities in a Simulated Water Distribution System.” *Environmental Science: Processes & Impacts* 16 (3): 576-585.

Sun, H., B. Shi, F. Yang, and D. Wang. 2017. “Effects of Sulfate on Heavy Metal Release from Iron Corrosion Scales in Drinking Water Distribution System.” *Water Research* 114: 69-77.

Tam, Y. S., and P. Elefsiniotis. 2009. “Corrosion Control in Water Supply Systems: Effect of pH, Alkalinity, and Orthophosphate on Lead and Copper Leaching from Brass Plumbing.” *J Environ Sci Health A Tox Hazard Subst Environ Eng* 44 (12): 1251-1260.

Tang, Z., S. Hong, W. Xiao, and J. Taylor. 2006. “Impacts of Blending Ground, Surface, and Saline Waters on Lead Release in Drinking Water Distribution Systems.” *Water Research* 40 (5): 943-950.

Tang, M., V. Nystrom, K. Pieper, J. Parks, B. Little, R. Guilliams, T. Esqueda, and M. Edwards. 2018. “The Relationship between Discolored Water from Corrosion of Old Iron Pipe and Source Water Conditions.” *Environmental Engineering Science* 35 (9): 943-952.

Taylor, J., J. Dietz, A. Randall, and S. Hong. 2005. “Impact of RO-Desalted Water on Distribution Water Qualities.” *Water Science and Technology* 51 (6-7): 285-291.

Thompson, J., B. Scheetz, M. Schock, D. Lytle, and P. Delaney. 1997. “Sodium Silicate Corrosion Inhibitors: Issues of Effectiveness and Mechanism.” Reprinted from Proc. AWWA Water Quality Technology Conference.

Triantafyllidou, S. 2006. “Addressing and Assessing Lead Threats in Drinking Water: Non-Leaded Brass, Product Testing, Particulate Lead Occurrence and Effects of the Chloride to Sulfate Mass Ratio on Corrosion.” Master’s thesis, Virginia Polytechnic Inst. and State Univ., Blacksburg, Va.

Triantafyllidou, S., and M. Edwards. 2011. “Galvanic Corrosion After Simulated Small-Scale Partial Lead Service Line Replacements.” *Journal American Water Works Association* 103 (9): 85-99

Trueman, B., and G. Gagnon. 2016. “Understanding the Role of Particulate Iron in Lead Release to Drinking Water.” *Environmental Science and Technology* 50 (17): 9053-9060.

U.S. EPA. 2004. "Desktop Corrosion Control Study." Prepared by the Washington Aqueduct and CH2M Hill, Philadelphia, PA. https://archive.epa.gov/region03/dclead/web/pdf/corrosioncontrol.pdf.

Volk, C. J., and M. W. LeChevallier. 1999. "Impacts of the Reduction of Nutrient Levels on Bacterial Water Quality in Distribution Systems." *Applied and Environmental Microbiology* 65 (11): 4957-4966.

Wang, Y., H. Jing, V. Mehta, G. J. Welter, and D. E. Giammar. 2012. "Impact of Galvanic Corrosion on Lead Release from Aged Lead Service Lines." *Water Research* 46 (16): 5049-5060.

Wang, H., C. Hu, L. Zhang, X. Li, Y. Zhang, and M. Yang. 2014. "Effects of Microbial Redox Cycling of Iron on Cast Iron Pipe Corrosion in Drinking Water Distribution Systems." *Water Research* 65: 362-370.

Wang, Y., V. Mehta, G. J. Welter, and D. E. Giammar. 2013. "Effect of Connection Methods on Lead Release From Galvanic Corrosion." *Journal American Water Works Association* 105 (7): E337-E351.

Wehle, V. 1982. "Influence of Phosphates and/or Silicates on the Corrosion Behaviour of Drinking Water Towards Installation Materials." The Institute of Water Engineers and Scientists, Scientific Section Symposium on the Internal Corrosion of Iron Mains and Copper Services. The Chameleon Press Ltd. 54: London.

Willison, H., and T. H. Boyer. 2012. "Secondary Effects of Anion Exchange on Chloride, Sulfate, and Lead Release: Systems Approach to Corrosion Control." *Water Research* 46 (7): 2385-2394.

Xie, Y., Y. Wang, V. Singhal, and D. E. Giammar. 2010. "Effects of pH and Carbonate Concentration on Dissolution Rates of the Lead Corrosion Product PbO_2." *Environmental Science and Technology* 44 (3): 1093-1099.

Yang, F., B. Shi, J. Gu, D. Wang, and M. Yang. 2012. "Morphological and Physicochemical Characteristics of Iron Corrosion Scales Formed under Different Water Source Histories in a Drinking Water Distribution System." *Water Research* 46 (16): 5423-5433.

Yang, F., B. Shi, Y. Bai, H. Sun, D. A. Lytle, and D. Wang. 2014. "Effect of Sulfate on the Transformation of Corrosion Scale Composition and Bacterial Community in Cast Iron Water Distribution Pipes." *Water Research* 59: 46-57.

Zhang, Y., A. Griffin, and M. Edwards. 2008. "Nitrification in Premise Plumbing: Role of Phosphate, pH and Pipe Corrosion." *Environmental Science and Technology* 42 (12): 4280-4284.

Zhang, Y., A. Griffin, M. Rahman, A. Camper, H. Baribeau, and M. Edwards. 2009. "Lead Contamination of Potable Water Due to Nitrification." *Environmental Science & Technology* 43 (6): 1890-1895.

Zhang, Y., A. Griffin, and M. Edwards. 2010. "Effect of Nitrification on Corrosion of Galvanized Iron, Copper, and Concrete." *Journal American Water Works Association* 102 (4): 83-93.